AD-A189 730 CETANE SCALE EVALUATION AND POSSIBLE MODIFICATION(U) 1/2
WAYNE STATE UNIV DETROIT MI CENTER FOR AUTOMOTIVE
RESEARCH N A HENEIN 23 DEC 87 ARO-21397.2-EG
UNCLASSIFIED DAAG29-84-K-0164 F/G 21/4 NL

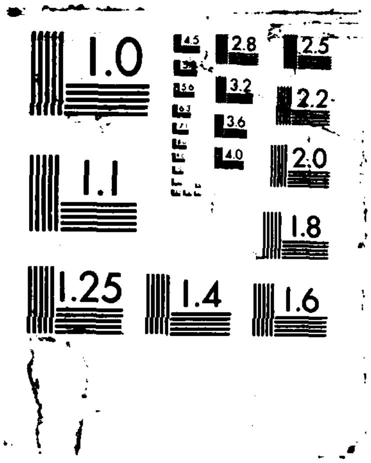
1.0
4.5
5.0
5.6
6.3
7.1
8.0
2.8
3.2
3.6
4.0
2.5
2.2
2.0
1.1
1.8
1.25
1.4
1.6

ARO 21397.2-EG ②

CETANE SCALE EVALUATION AND POSSIBLE MODIFICATION

FINAL REPORT

N.A. HENEIN
PROFESSOR OF MECHANICAL ENGINEERING
DIRECTOR, CENTER FOR AUTOMOTIVE RESEARCH
WAYNE STATE UNIVERSITY
DETROIT, MI

23 DECEMBER 1987

U.S. ARMY RESEARCH OFFICE

CONTRACT NO. DAAG 29-84-K-0164

WAYNE STATE UNIVERSITY
COLLEGE OF ENGINEERING
CENTER FOR AUTOMOTIVE RESEARCH
DETROIT, MI 48202

APPROVED FOR PUBLIC RELEASE;
DISTRIBUTION UNLIMITED

CETANE SCALE EVALUATION AND POSSIBLE MODIFICATION

FINAL REPORT

N.A. HENEIN
PROFESSOR OF MECHANICAL ENGINEERING
DIRECTOR, CENTER FOR AUTOMOTIVE RESEARCH
WAYNE STATE UNIVERSITY
DETROIT, MI

23 DECEMBER 1987

U.S. ARMY RESEARCH OFFICE

CONTRACT NO. DAAG 29-84-K-0164

WAYNE STATE UNIVERSITY
COLLEGE OF ENGINEERING
CENTER FOR AUTOMOTIVE RESEARCH
DETROIT, MI 48202

APPROVED FOR PUBLIC RELEASE;
DISTRIBUTION UNLIMITED

UNCLASSIFIED
SECURITY CLASSIFICATION OF THIS PAGE

REPORT DOCUMENTATION PAGE

1a. REPORT SECURITY CLASSIFICATION Unclassified

1b. RESTRICTIVE MARKINGS

2a. SECURITY CLASSIFICATION AUTHORITY

2b. DECLASSIFICATION / DOWNGRADING SCHEDULE

3. DISTRIBUTION / AVAILABILITY OF REPORT
Approved for public release;
distribution unlimited.

4. PERFORMING ORGANIZATION REPORT NUMBER(S)
Final

5. MONITORING ORGANIZATION REPORT NUMBER(S)

6a. NAME OF PERFORMING ORGANIZATION
Wayne State University
College of Engineering

6b. OFFICE SYMBOL *(If applicable)*
Final

7a. NAME OF MONITORING ORGANIZATION
U. S. Army Research Office

6c. ADDRESS *(City, State, and ZIP Code)*
Detroit, MI 48202

7b. ADDRESS *(City, State, and ZIP Code)*
P. O. Box 12211
Research Triangle Park, NC 27709-2211

8a. NAME OF FUNDING / SPONSORING ORGANIZATION
U. S. Army Research Office

8b. OFFICE SYMBOL *(If applicable)*

9. PROCUREMENT INSTRUMENT IDENTIFICATION NUMBER

8c. ADDRESS *(City, State, and ZIP Code)*
P. O. Box 12211
Research Triangle Park, NC 27709-2211

10. SOURCE OF FUNDING NUMBERS

PROGRAM ELEMENT NO.	PROJECT NO.	TASK NO.	WORK UNIT ACCESSION NO.

11. TITLE *(Include Security Classification)*
CETANE SCALE EVALUATION AND POSSIBLE MODIFICATIONS

12. PERSONAL AUTHOR(S)
Henein, Naeim A.

13a. TYPE OF REPORT Final

13b. TIME COVERED FROM 9-1-84 TO 8-31-87

14. DATE OF REPORT *(Year, Month, Day)* 1987, November 23

15. PAGE COUNT 108

16. SUPPLEMENTARY NOTATION The view, opinions and/or findings contained in this report are those of the author(s) and should not be construed as an official Department of the Army position, policy, or decision, unless so designated by other documentation.

17. COSATI CODES

FIELD	GROUP	SUB-GROUP

18. SUBJECT TERMS *(Continue on reverse if necessary and identify by block number)*
Cetane number, diesel fuels, ignition delay, cold starting.

19. ABSTRACT *(Continue on reverse if necessary and identify by block number)*

An evaluation is made of the validity and accuracy of the Cetane Scale in rating fuels used in diesel engines. Six problems have been identified, analyzed and possible solutions have been proposed. Three of the problems are intrinsic to the scale and are related to its inability to rate low ignition quality fuels, instability of the ignition delay meter and the inconformity of the CFR combustion system with actual diesel systems. The other three problems are related to fuels and engines. These are the invalidity of C.N. in correlating the ignition delay data, its inaccuracy in ranking overall engine performance and emissions and its inability in rating the cold startability of engines on different fuels. The cold startability problem is investigated in two engines, under steady and actual starting conditions in a cold room. Also, a mathematical model is developed to predict the startability of the engine. These investigations indicate

cont'd

20. DISTRIBUTION / AVAILABILITY OF ABSTRACT
☐ UNCLASSIFIED/UNLIMITED ☐ SAME AS RPT. ☐ DTIC USERS

21. ABSTRACT SECURITY CLASSIFICATION
Unclassified

22a. NAME OF RESPONSIBLE INDIVIDUAL

22b. TELEPHONE *(Include Area Code)*

22c. OFFICE SYMBOL

DD FORM 1473, 84 MAR

83 APR edition may be used until exhausted.
All other editions are obsolete.

SECURITY CLASSIFICATION OF THIS PAGE
UNCLASSIFIED

very clearly that the cetane rating is a hot engine, high temperature test and is unable to rate the cold startability of diesel engines.

Keywords: Cetane number; Diesel fuels.

TABLE OF CONTENTS

LIST OF FIGURES

Figure Title Page

Section 2: Cetane Scale: Function, Problems and Possible Solutions.

Section 3: C.N. Rating of Cold Startability of Diesel Engines on Different Fuels.

Section 4: Effect of Fuel Volatility on Autoignition and Combustion at Low Ambient Temperatures.

SECTION 1

EXECUTIVE SUMMARY

Many problems are experienced by the military and industry in using the Cetane Scale to rate the fuels for diesel engines. The main objectives of this program are:

1. To evaluate the validity and accuracy of the Cetane Scale in rating fuels used in diesel engines.
2. Identify the problems.
3. Propose solutions.
4. Investigate the C.N. as a cold startability indicator.

To meet the first three objectives the function of the Cetane Scale is identified and six problems are examined and solutions proposed. These problems are:

1. Inability of the ASTM D-613 Method to Rate Low Ignition Quality Fuels.
2. Instability of the Ignition Delay Meter in Rating Low Ignition Quality Fuels.
3. Inconformity of the CFR Combustion System with actual Diesel Systems.
4. Invalidity of C.N. in Correlating the I.D. for Different Fuels, Engines and Operating Conditions.
5. Inaccuracy of C.N. in Ranking the Overall Performance and Emission Behaviour of Fuels in Diesel Engines.
6. Inability of C.N. in Rating the Cold Startability of Diesel Engines on Different fuels.

A possible solutions for these problems are proposed in this report.

To meet the fourth objective experimental investigations supported by a mathematical model have been conducted. Experiments were conducted at low ambient temperatures in a cold room at steady operating conditions and under actual starting conditions. The tests covered ambient temperatures ranging from 25°C to - 45°C or till the engine failed to fire or start.

The steady state experiements were conducted on a single cylinder TACOM engine on a variety of fuels. The ignition delay and the misfiring temperature were measured for each fuel. The results showed that the ignition delay of the high volatility fuels is shorter than the ignition delay for the low volatility fuels having the same Cetane number. Also, the misfiring temperature was found to decrease as the volatility of the fuel increases. These results indicate that the fuel volatility plays a major role in the combustion process of the diesel engine at low ambient temperatures.

The starting tests were conducted on air cooled, direct injection diesel engine in the cold room. The results indicated that the Cetane number is not capable of rating the startability of the engine on different fuels. A low Cetane fuel which is volatile was able to start the engine while a high Cetane less volatile fuel failed to start the engine.

The above investigations indicate very clearly that the C.N. is a hot engine, high temperature test and is unable to rate the cold startability of diesel engines.

It is recommended that an investigation be made to find the necessary modifications in the scale to make it of value in the rating of the cold starting of the diesel engines on different fuels.

SECTION 2

CETANE SCALE: FUNCTION, PROBLEMS AND POSSIBLE SOLUTIONS

2.1 BACKGROUND

Many efforts have been made during the last 60 years to rate the behaviour of different fuels in diesel engines. Combustion noise was one of the performance parameters, of concern to researchers. As early as 1931 LeMesurier and Stansfield [1] proved, from experiments on several compression-ignition engines, that the combustion knock was broadly related to the delay which occurred between the moment of injection and the beginning of rapid pressure rise. They reported that different engines seemed to have only slightly different relative effects on the fuels tested. Subsequent investigators such as Boerlage and Broeze 1931 [2], Pope and Murdock 1932 [3], Schweitzer et al 1933-1937 [4,5,6] used the ignition delay as the criteria to rate the behaviour of the different fuels in diesel engines.

The reference fuel of the highest rating of 100, on the scale has been n-hexadecane, $C_{16}H_{34}$, known as n-Cetane. The reference fuel of the lowest rating of zero on the scale had been alpha-methyl-naphthalene, $C_{11}H_{10}$, from 1932 to 1962. The C.N. according to this scale is

$$\text{C.N.} = \%\ \text{n-Cetane} \qquad (1)$$

In 1962 ASTM [7] replaced alpha-methyl-naphthalene (αMN) with a new low-cetane number reference fuel, hepta methylnonane (HMN). The cetane rating for heptamethylnonane is 15.

The definition of the ASTM C.N. [7] is the whole nomber nearest to the value determined by calculation from the percentage by volume of normal cetane in a blend with HMN which matches the ignition quality of the test fuel when compared by the D-613 ASTM Cetane Method. The matching blend percentages to the first decimal are inserted in the following equation to obtain the C.N.

$$C.N. = \%\ n\text{-cetane} + 0.15\ (\%\ HMN) \tag{2}$$

The single cylinder engine used in the fuel rating is known as CFR (Cooperative Fuels Research) engine, manufactured by Waukesha Company. The engine specifications are given in Appendix A, and the operating conditions for the ASTM D-613 test procedure are given in Appendix B.

There has been growing concern during the last two decade over many problems associated with the Cetane number determined by the ASTM D-613 method, particularly for alternate fuels which have been considered as replacements of the regular diesel fuel or as fuel extenders [8]. Additional concern is over the use of C.N. to rate the performance, gaseous emmissions, exhaust solid particulates, white smoke and the cold startability of diesel engines.

The purpose of this section is to identify the original function of the Cetane rating of the fuel by using the ASTM D-613 method, and to examine the different problems of concern to the technical community.

This section examines six problems and introduces possible solutions or recommends actions to reach solutions. These problems are:

1. Inability of the ASTM D-613 Method to Rate Low Ignition Quality Fuels.
2. Instability of the Ignition Delay Meter in Rating Low Ignition Quality Fuels.
3. Inconformity of the CFR Combution System with Actual Diesel Systems.

4. Invalidity of C.N. in Correlationg the I.D. for Different Fuels, Engines and Operating Conditions.
5. Inaccuracy of C.N. in Ranking the Overall Performance and Emission Behaviour of Fuels in Diesel Engines.
6. Inability of C.N. in Rationg the Cold Startability of Diesel Engine on Different Fuels.

2.2 FUNCTION OF C.N.

The basic function of the C.N. is to rate the autoignition properties of fuels in diesel engines. The details of the autoignition chemical processes are not known because they are very complex, fast and involve many unstable combustion radicals which are not easy to trace. The autoignition chemical processes are preceeded by physical processes which are dependent on the fuel physical properties and the design of the injection system and the combustion chamber of the engine. In the ASTM D-613 the measurement of the autoignition delay of the fuel is done by measuring the ignition delay in the standard engine under standard operating conditions, and adjusting the compression ratio C.R. such that the I.D. is 2.41 m sec., or 13° CA at 900 RPM. The start of injection is at 13° CA before TDC and the pressure rise due to combustion (or the end of I.D.) should take place at TDC.

No other combustion or engine performance parameter is measured during the rating test.

2.3 PROBLEMS AND POSSIBLE SOLUTIONS

In this section six problems are examined

The first three are intrinsic problems associated with ASTM D-613 procedure or the CFR engine design. The last three are fuel/engine problems related to the behaviour of fuels in actual diesel engine.

2.3.1 Problem 1: Inability of ASTM D-613 Method to Rate Low Ignition Quality Fuels:

Very high compression ratios are needed to rate alternate fuels, haveing low cetane numbers. Figure 1 shows the relationship between the compression ratio and C.N. according the ASTM D-613 and equation (2) in which HMN is used as the bottom of the scale at 15 C.N. The same figure shows the same relationship with αMN as the zero C.N. fuel according to equation (1). It is clear that the relationship is close to linear for fuels haveing C.N. between 100 and 50. At C.N. less than 50 the slope of the curve increases at a high rate as the C.N. decreases. Figure 1 shows that a C.R. of about 29.5 is needed for rationg a fuel having C.N. = 10. Higher compression ratios are needed for rating lower C.N. fuels.

The very high compression ratios needed for rating low C.N. fuels has been the concern of many investigators [9]. Urban and Gray 1968 [10] of the U.S. Army Fuels and Lubricants Research Laboratory reported the results of a comprehensive study on the feasiblity of three alternate methods to solve this problem and rate low ignition quality fuels. The first method was to blend n-cetane fuel with the sample and then calculate the sample C.N. from the C.N. of the blend. This method was found to be unsatisfactory. More recently, Hardenberg and Ehnert 1981 [11] reported dissatisfaction with this method in determining the C.N. of alcohols. The second method reported by Urban and Gray [10] is to correlate the C.N. and Octane number of the sample. They reported that the C.N. estimated by this method was less raliable than C.N. directly

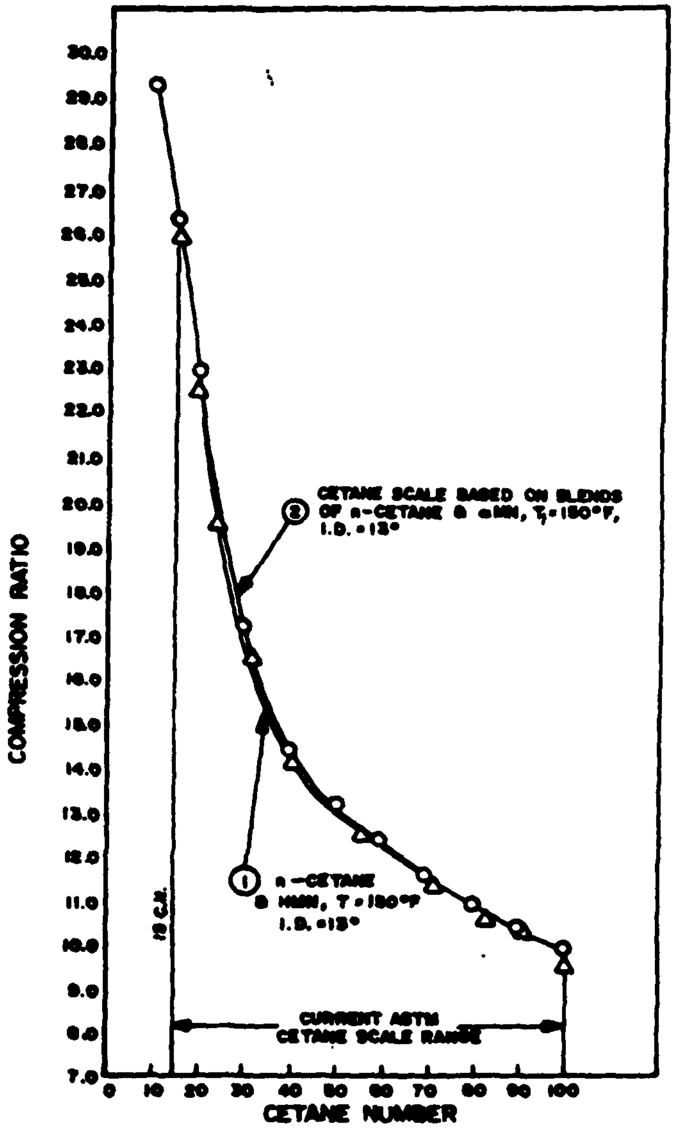

Fig. (1): Relationship between C.N. and C.R. in the Cetane Rating.

determined. The third method is to modify the ASTM-D613 procedure by using longer I.D. than the standard delay of 13° C.A. at 900 RPM. Figure 2 shows the results obtained for the present program and indicate a small reduction in the C.R. as a result of using an I.D. of 17° C.A. instead of the standard 13° C.A. Similar results were reproted by Bowder [12].

Another method to solve this problem, proposed by the French Army [13] to Waukesha Motor Company, is to use a compression plug which has a notch cut deeply into one side to clear the transfer port between the two chambers in order to increase the highest C.R. of the standard CFR engine. This proposal was not favored by Waukesha Motor Company because of the tendency of this plug to create a different flow pattern and turbulence in the prechamber of the standard CFR engine and the different machining operations required for the tapered shape of the slot. Waukesha proposed back to the French Army the use of a modified high compression ratio plug which has a symmetrical truncated conical end, to reach C.R. higher than 31:1. Figure 3 shows such a plug. No tests were reported on the effectiveness of this plug in rating the low ignition quality fuels.

An analysis of the parameters which affect the autoignition process of the fuels in any diesel engine [14] indicated that the I.D. is most sensitive to the air temperature and molecular structure of the fuel, in addition to the air pressure according to

$$I.D._p = \frac{A \quad e^{\frac{E}{\bar{R}T}}}{p^n} \qquad (3)$$

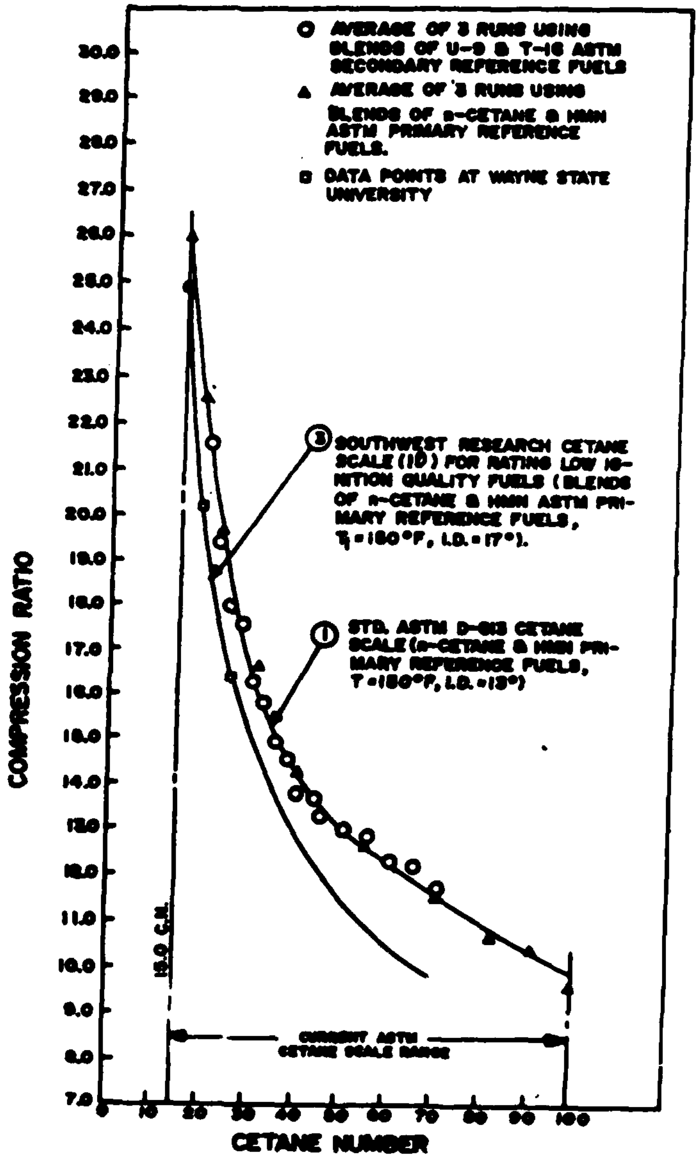

Fig. (2): Effect of increasing I.D. to 17°C.A. on the C.N.-C.R. relationship.

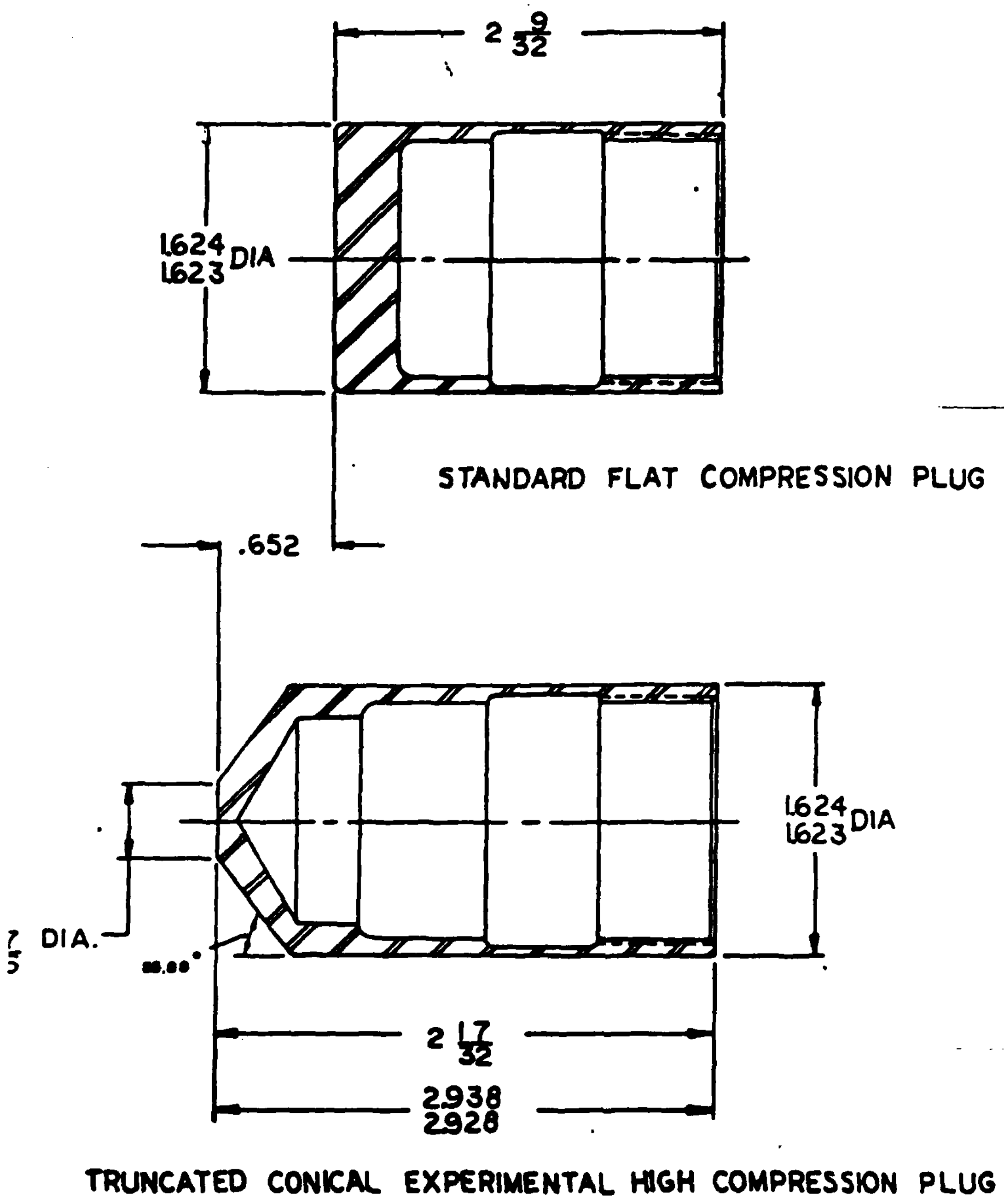
2 9/32
1.624
1.623 DIA
STANDARD FLAT COMPRESSION PLUG
.652
1.624
1.623 DIA
DIA.
2 17/32
2.938
2.928
TRUNCATED CONICAL EXPERIMENTAL HIGH COMPRESSION PLUG

Fig. (3): Truncated conical experimental high compression plug.

where E is the Global activation energy for the preignition reactions and depends mainly on the molecular structure of the fuel.

Both the air temperature and pressure increase with C.R. in the CFR engine. The relative effects of temperature and pressure on the ignition delay are discussed in details in a previous publication [14]. The effect of the increase in temperature with C.R. is much more than the effect of the increase in pressure on the I.D. This has been found to be particularly true for low C.N. fuels which have relatively higher activation energies. Based on this analysis, it becomes clear that raising the inlet air temperature above the 150°F, used in the D-613 method, would reduce the C.R. needed to produce an I.D. of 2.41 m sec. for the low ignition quality fuels. This has been verified experimentally by Elias [15]. Figure 4 shows 2 cetane scales: the original cetane scale at determined by using ASTM D-613 method, with an air inlet temperature of 150°F, and the scale developed after increasing the inlet air temperature from 150°F to 350°F. With the new scale it is possible to rate low ignition quality fuels without reaching the very high C.R.s needed in the original scale. A zero C.N. fuel can be autoignited with an I.D. of 2.41 m sec., at 900 RPM at a C.R. = 19.4:1.

The solution to this problem is to raise the inlet temperature above the 150°F specified by the ASTM D-613 procedure. This requires the use of an electric air heater of a higher capacity than the heater currently used on the CFR engine.

Ratings with inlet air temperatures between 150°F and 350°F need to done to choose a temperature which can be reached by using an electric heater of a reasonable capacity.

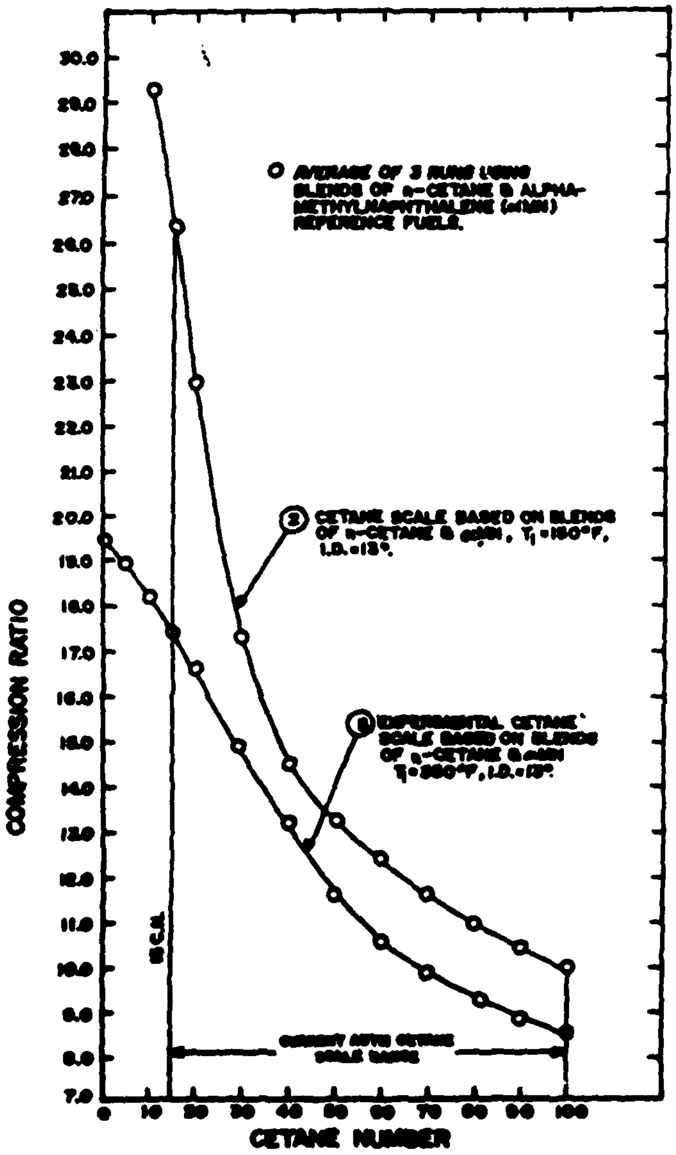

Fig. (4): Comparison between C.N.-C.R. relationship with 150°F and 350°F inlet air temperatures.

2.3.2 Problem 2: Instability of the Ignition Delay Meter in Rating Low Ignition Quality Fuels:

Many investigators observed that the ignition delay meter becomes unstable and performs erratically as the C.N. of the sample drops below twenty. Urban and Gray [10] proposed the use of an oscilloscope and associated pressure transducers instead of the standard ASTM ignition delay meter, to measure the I.D. of the low C.N. fuels. They reported that the accuracy of the rating depended on the operator's ability to average continuous cycles on the oscilloscope due to cycle-to-cycle variations in the pressure trace.

The reason for such instability has not been known till Sczomak [16] proved experimentally that it is caused by the cycle-to-cycle variation in the autoignition of low C.N. fuels. Figure 5 shows traces for the gas pressure in the prechamber, the rate of change of the gas pressure, the needle displacement, the needle velocity and the fuel injection pressure before the injector. Each of the figures (5a) to (5f) is for twenty superimposed consecutive cycles. It is noticed that the variations in the cylinder pressure are caused by variations in the I.D., and these variations increase as the C.N. decreases. It should be noted that the other traces for the needle displacement, needle velocity and fuel injection pressure showed no cycle-to-cycle variations for all the fuels.

Many attempts have been made to reduce the cycle-to-cycle variations in I.D., which result in the instability of the I.D. meter. Figure 6 from reference [16] shows the effect of increasing the inlet air temperature from 150°F to 350°F on the coefficient of variation in the I.D. It is clear that the cycle-to-cycle variations are reduced for

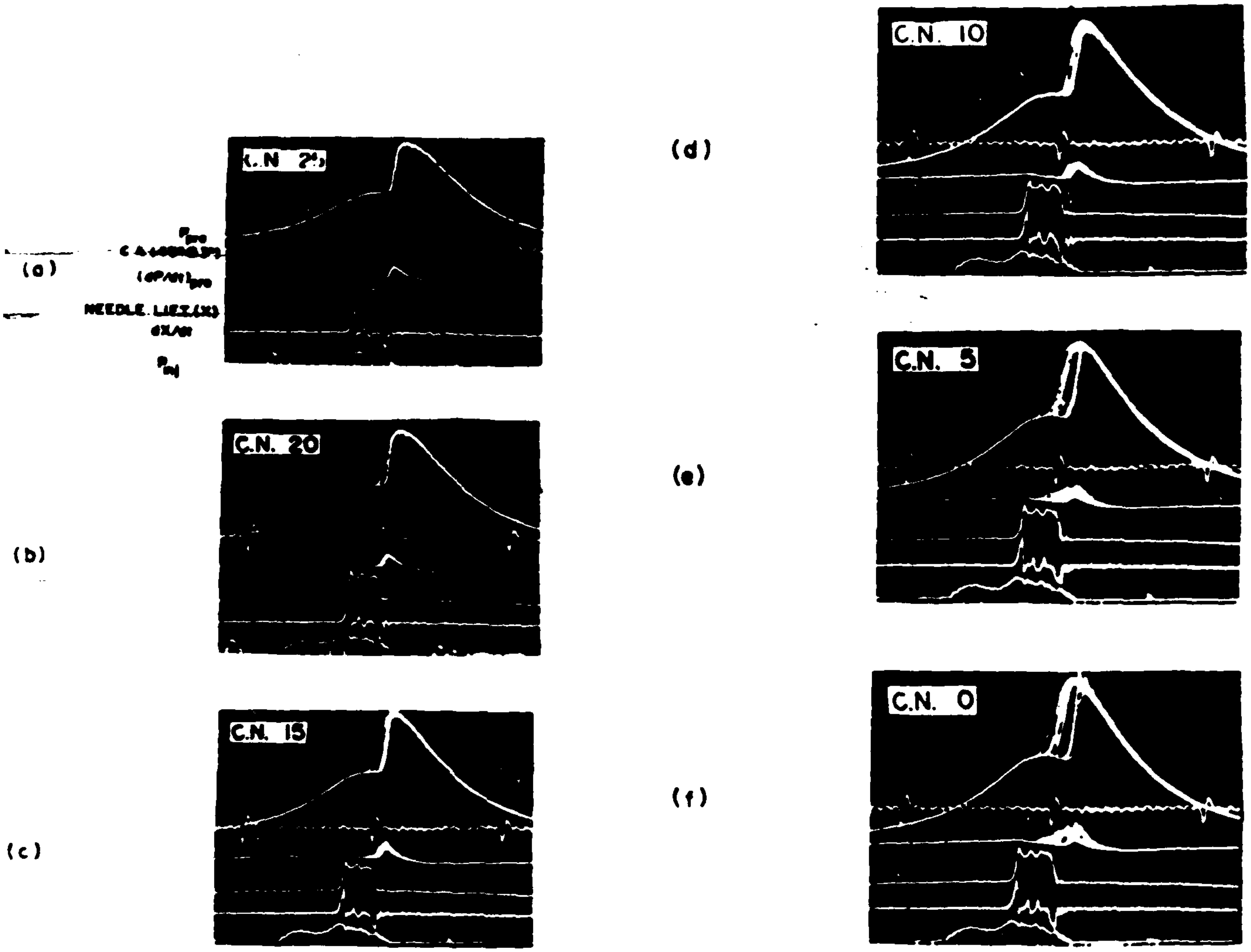

Fig. (5): Cycle-to-cycle variation for low ignition quality blends of different cetane numbers.

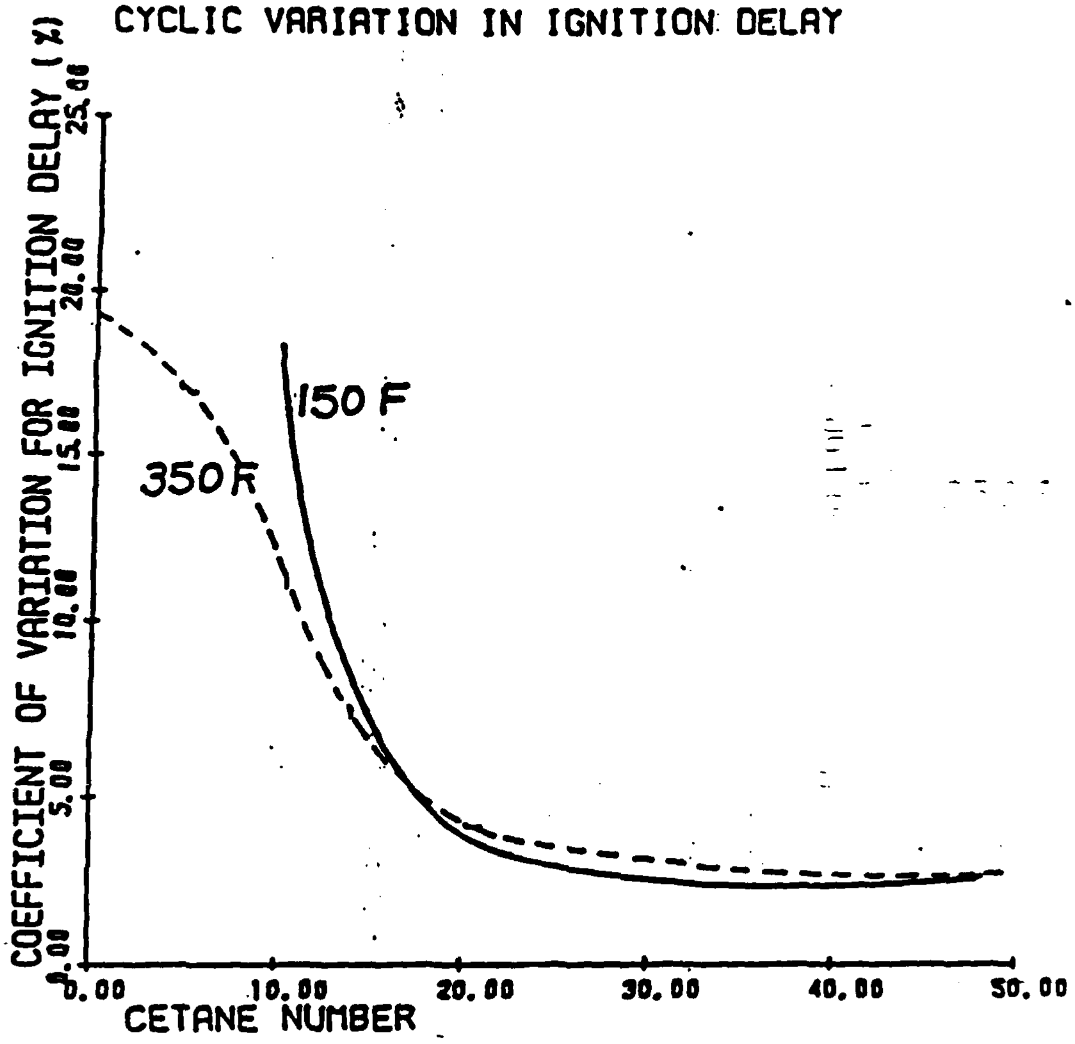

Fig (6): Effect of fuel cetane number on cycle-to-cycle variation in ignition delay at 350°F & 150°F air temperature.

C.N.s less than 18. However, these variations still exist even at this very high inlet air temperature.

At the present time the processes which result in the cycle-to-cycle variations in the autoignition process are not known. Further investigations in this area are needed.

2.3.3 Problem 3: Inconformity of the CFR Combustion System with Actual Diesel Combustion Systems:

The autoignition of fuel sprays injected in an engine is the result of two main sets of processes: physical and chemical. The physical processes lead to the formation of a combustible mixture, with an equivalence ratio close to the stoichiometric ratio. The chemical processes are mainly decomposition processes leading to the formation of the combustion redicals and the oxidation processes which release the energy of the combustion reactions: In actual diesel engines the combustion systems are designed to allow the above processes to take place and keep the ignition delay within certain limits such that the majority of the combustion energy is released close to TDC of the engine. This requires the optimization of the combustion system, which consists of the injection system and combustion chambers, to suit the properties of the fuel. The injection parameters include the nozzle type and size, injection pressure, and injection timing.

In the CFR-Cetane engine the shape of the combustion chamber varies according to the C.R. which in turn varies according to the ignition quality of the fuel being rated. Figures 7,8, and 9 give different views of the CFR prechamber, main chamber and injector. The C.R. of the engine is controlled by varying the volume of the prechamber by moving

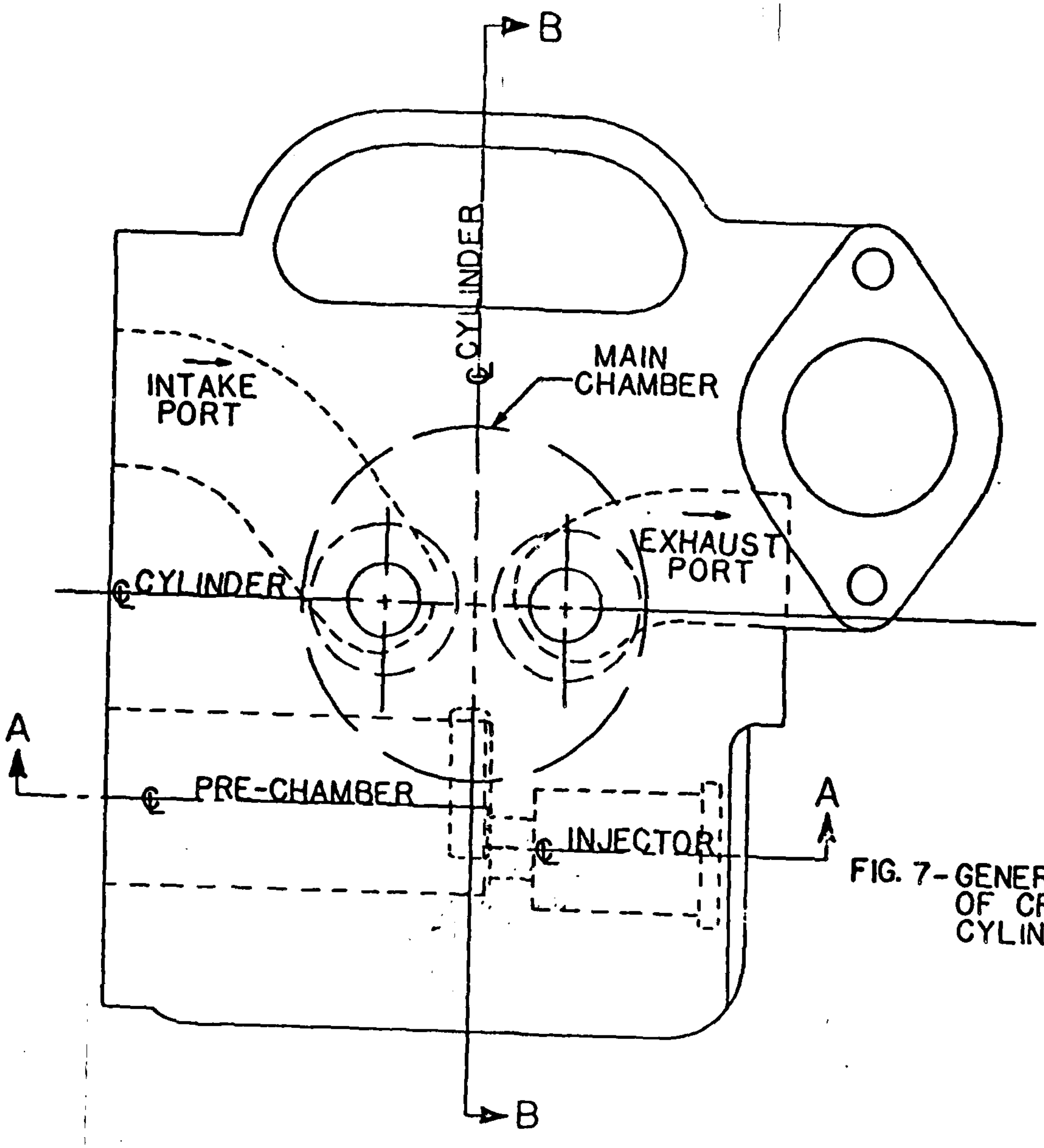

FIG. 7-GENERAL PLAN VIEW OF CFR CETANE CYLINDER HEAD.(25)

FIG. 8
CROSS-SECTION B-B OF FIGURE (6), SHOWING INSTALLATION OF AVL 12QP 300CVK WATER COOLED PRESSURE TRANSDUCERS IN BOTH PRE AND MAIN CHAMBERS. (25)

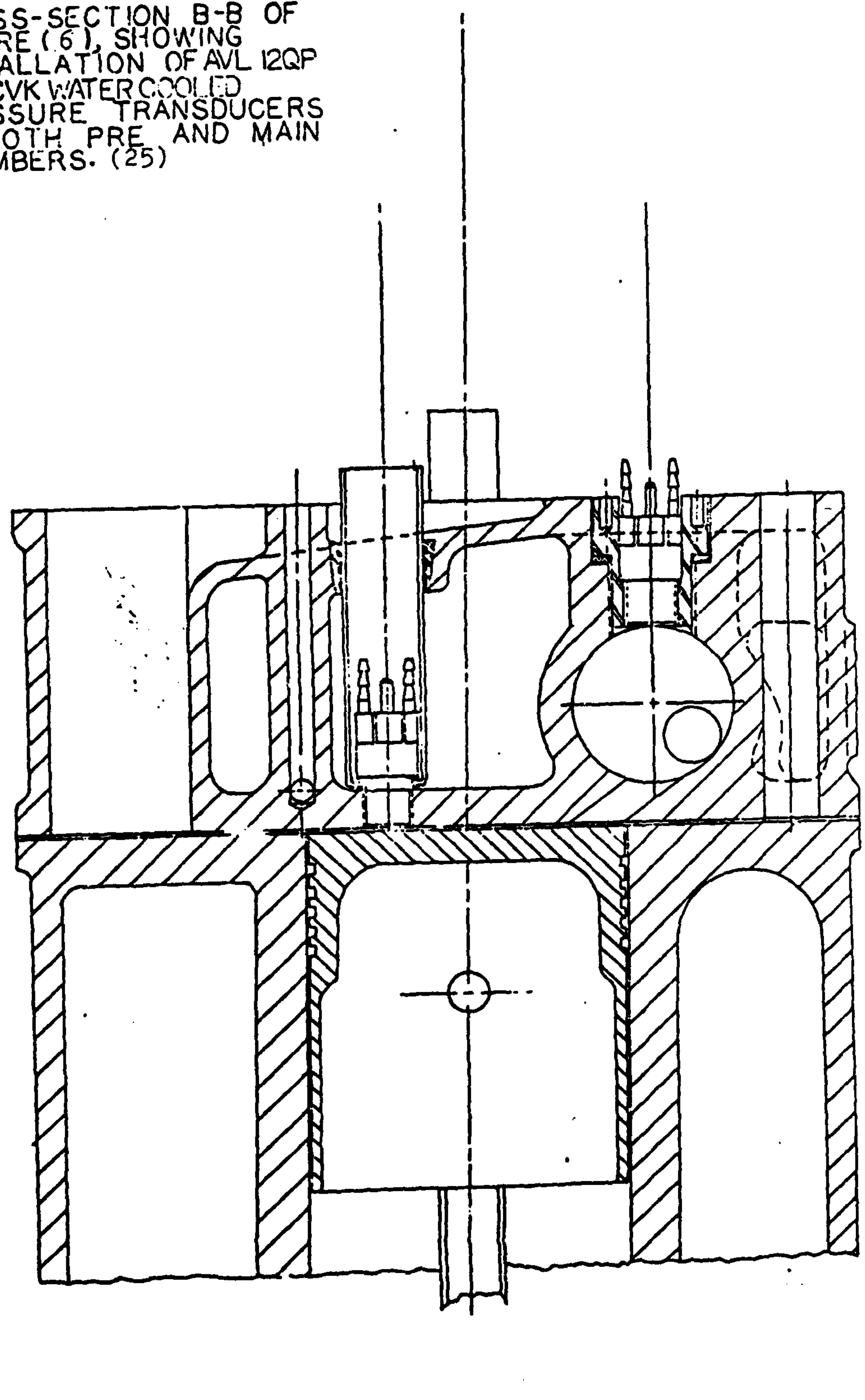

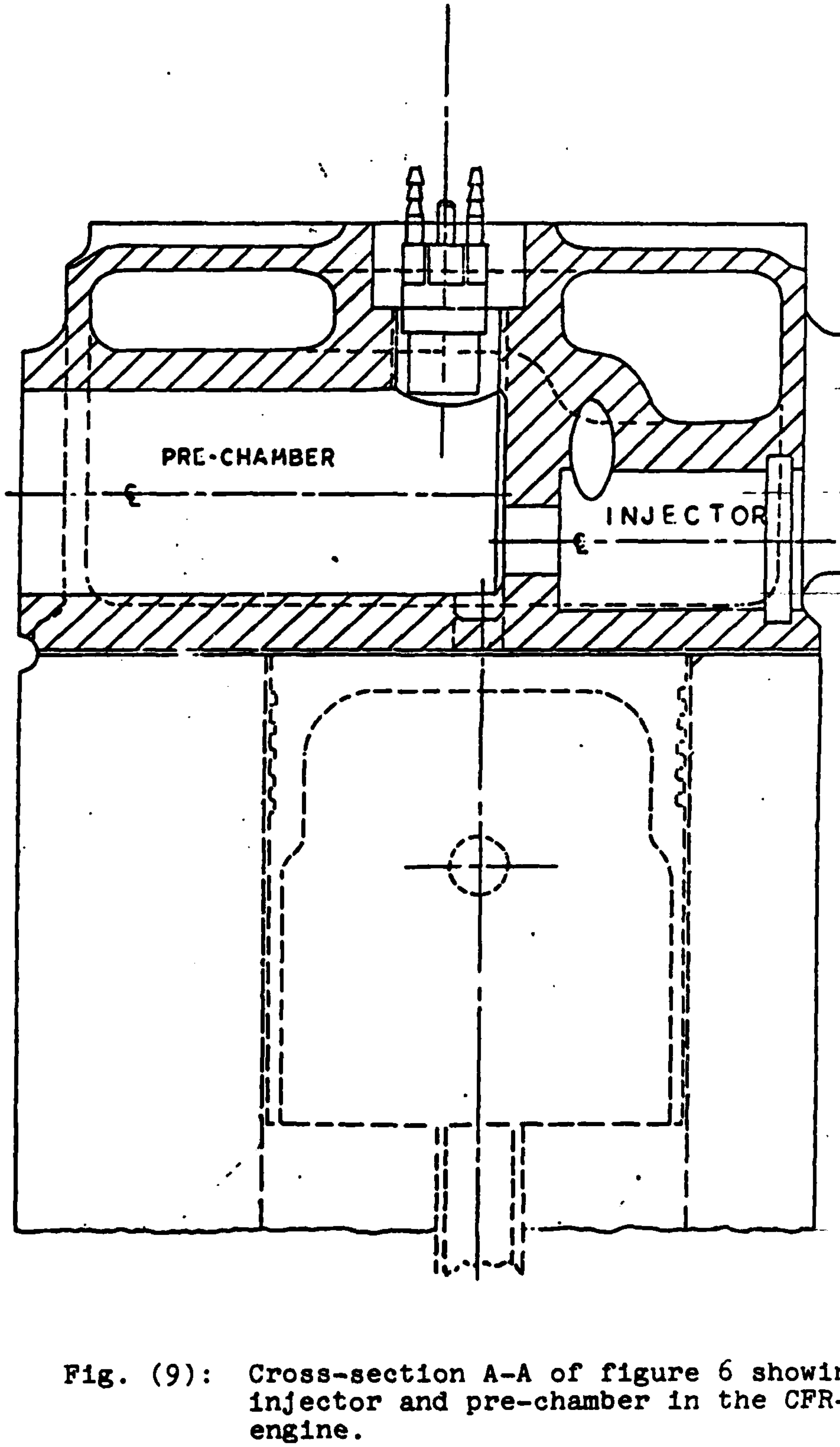

Fig. (9): Cross-section A-A of figure 6 showing the injector and pre-chamber in the CFR-Cetane engine.

the compression plug in the prechamber. The distance between the flat surface of the compression plug and injector nozzle tip decreases from 2.435" at C.R. = 7.92 to 0.435" at C.R. = 31. Figure 10 from reference [15] shows the shape of the prechamber at different C.R.s. An estimation of the spray penetration indicated that the sprays impinges on the surface of the compression plug, at all compression ratios during the ignition delay period of 2.41 m sec. [15]. It is not clear at this time whether ignition starts in the fuel spray before or after it impinges on the compression plug, particularly at the high compression ratios.

In actual diesel engines the ignition delay is mainly controlled by the chemical preignition processes rather by the physical processes even at the low ambient temperatures [17]. The physical processes are mainly dependent on the injection system and the extent of spray atomization. For a fixed nozzle configuration the atomization process depends to a large extent on the injection pressure, which is controlled by the needle opening pressure. If an increase in the injection pressure produces a decrease in I.D., this is an indication that the atomization process is not appropriate.

Figure 11 shows the effect of increasing the needle opening pressure on the I.D. of different fuels in the CFR engine at C.R. = 13.6 [20]. The fuels used range from light fuels n-C_7, typical Japanese fuel JPN with 50% boiling point of 263.5°C, heavy fuel 1 with 50% boiling point of 398°C and a heavier fuel 2 with 50% boiling point of 459°C. Figure 11 shows that the I.D. of the two light fuels decrease as the injector opening pressure increases from 1000 psi to 1500 psi, and remains constant at higher needle opening pressure. The I.D. for the two heavier fuels decreased continuously with the increase in injection

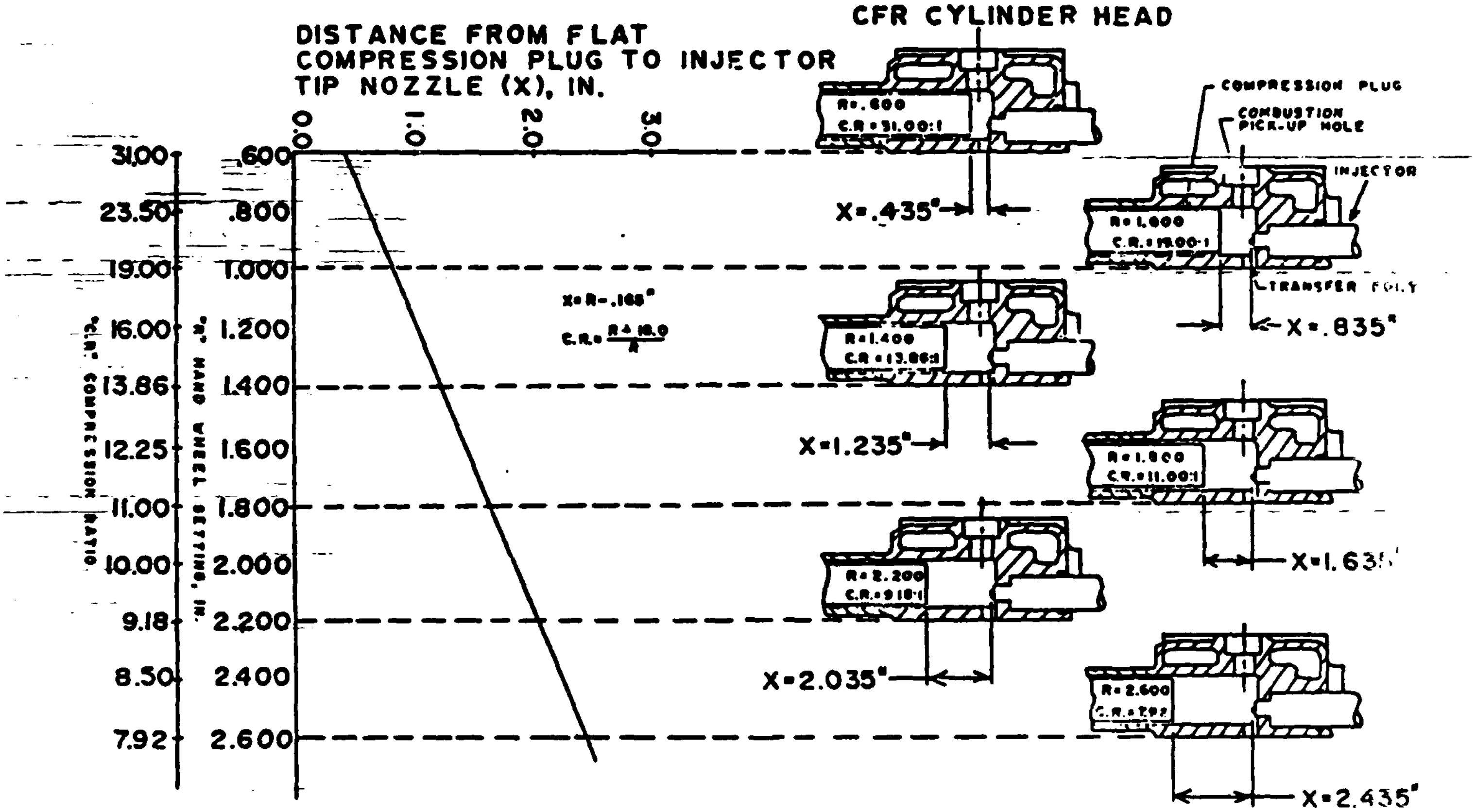

Fig. (10): Variation of Pre-chamber depth with C.R. in the CFR-Cetane Engine.

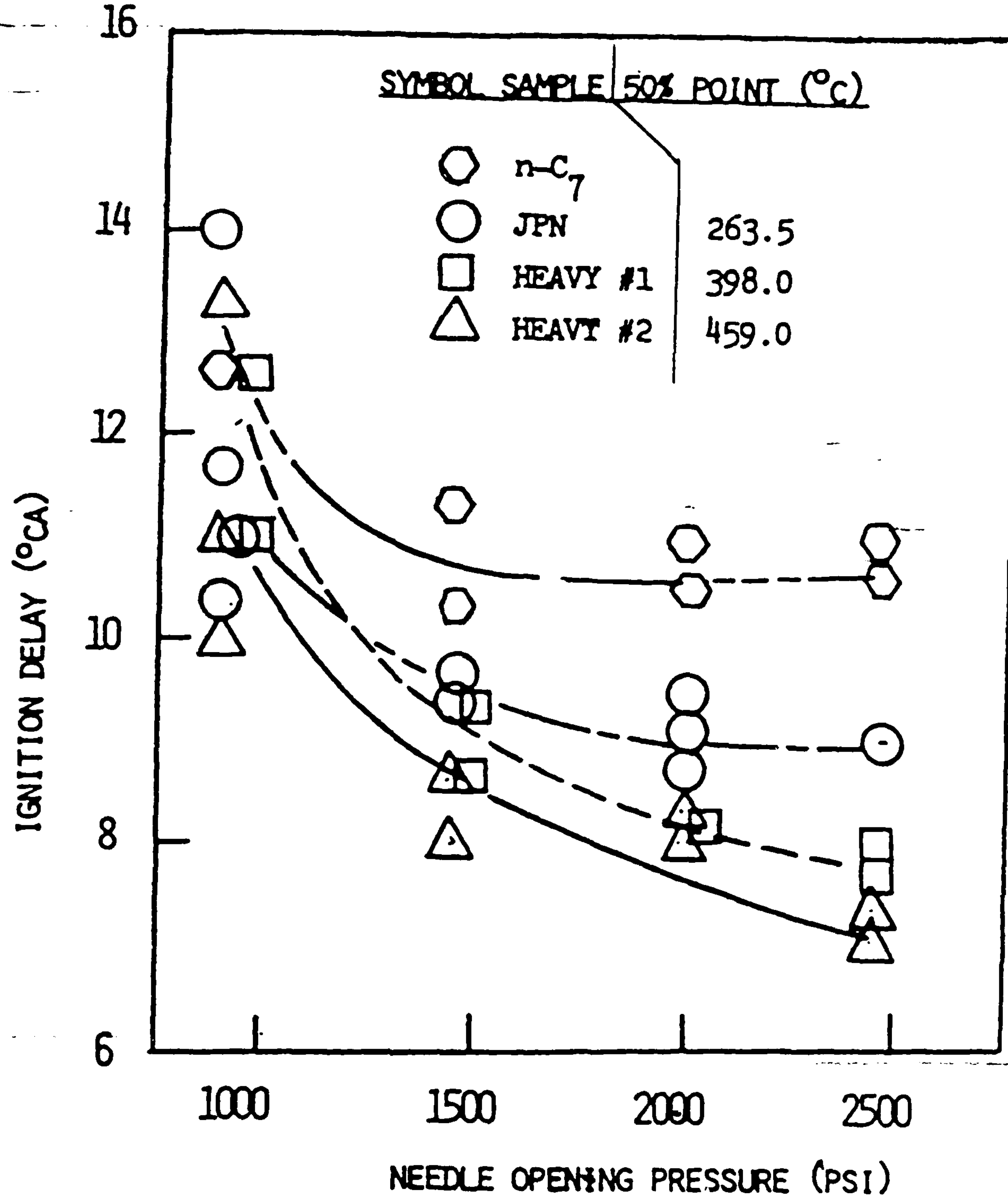

Fig. (11): Effect of needle opening pressure on I.D. in the CFR-Cetane engine.

pressure. This indicates that part of the increase in I.D. is due to the improper atomization process. The same effect has been reported by Lyn et al., [18] and Pederson et al., [19].

A possible solution of this problem is to increase the needle opening pressure for the heavier fuels. This would require rating the fuels in the CFR engine at different needle opening pressures. The rating would be done with a needle opening pressure beyond which the rating is independent of the fuel pressure.

2.3.4 Problem 4: Invalidity of C.N. in Correlating the I.D. for Different Fuels, Engines and Operating Conditions

There has been concern over the validity of the C.N. in rating the ignition delay of fuels in actual diesel engines. Many experiments have been conducted recently in engines [21,22,23] and constant volume bombs [24,25] to determine the I.D. of a wide range of fuels and correlate I.D. with the C.N as determined by the D-613 procedure.

Doyle and Needham [21,22] reported the results of extensive tests on a single cylinder engine using ten fuels in both IDI and DI combustion systems. The main fuel properties are listed in Appendix C. The fuels included DF-2, 2 middle distillates of different viscosities and aromatic contents, a high volatility broad cut fuel composed of 66% Naphtha and 34% DF-2, degummed sunflower oil, a more volatile less viscous sunflower monoester, shale derived fuel, a blend of 58% DF-2 and 42% coal derived SRC II, a blend of 78% DF-2 and 10% Methanol and 12% Hexan-1-01, and 1990 Canadian Diesel Fuel from tar sands. The fuels covered the following ranges: C.N.: 29 to 50.6, molecular weight: 172 to 635, Aromatic contents of hydrocarbon fuels: 19% to 57% and kinematic viscosity at 40°C: 0.91 to 33.93. The tests covered a wide range of engine operation conditions: low speed, peak torque and rated speeds, full load, light load and idle. Doyle and Needham reported that there is overall reasonable agreement between I.D. and C.N. in both D.I. and I.D.I. engines for petrolium and synthetic derived mid-distillates and the sunflower ester. However, I.D. of sunflower oil and volatile blends of Naphtha and Methanol with DF-2 showed varying delay response to load and speed.

The sunflower oil produced shorter I.D. than the other fuels having the same C.N. at high speeds and loads. Two factors might have contributed to this descrepency. The first in the Cetane rating of 29 for the sunflower oil is done in the CFR at the standard D-613 procedure. As indicated earlier this procedure calls for a constant injector opening pressure of 1500 psi which is enough to produce a proper spray for light or medium petroleum derived fuels. The author feels that the cetane rating of the Sunflower oil does not represent its autoignition quality, because of the CFR injection system being unsuitable for sunflower oil. The sunflower oil has a molecular weight of 635 as compared to 187 for DF-2. The molecular weight for the petroleum, shale or coal derived fuel tested ranges between 172 to 208. The viscosity of the sunflower oil is 33.93 CST, at 40°C, while the viscosity of all other fuels ranges between 0.91 and 4.37. It is clear that both the molecular weight and viscosity of sunflower oil are quite different from the rest of the fuels. Accordingly it appears that the C.N. rating of sunflower oil should take this into consideration and adjust the injection parameters in such a way as to develop a proper fuel spray in the CFR engine. The second factor is related to the optimization of the injection systems on the engines for the use of sunflower oil.

Siebers [24] used a constant volume bomb to measure the I.D. of several fuels, some of which were tested by Needham and Doyle [22], as explained earlier. Other fuels were blends of n-Cetane and HMN with C.N. ranging from 15 to 100. A premixed charge of $C_2H_4/H_2/O_2/N_2$ mixture was ignited and burned to form the high pressure, high-temperature environment and simulate the diesel thermodynamic conditions. The pressure ranged from 10 atm. to 50 atm., and the temperature ranged from 600°K to 1400°K. Siebers [24] concluded that the C.N. cannot provide a consistent and accurate measure of I.D. of fuels whose I.D. dependence on temperature and type of ignition process (single-stage or two-stage) different from those of the reference fuel blends of n-cetane and HMN. Sieber observed a pronounced two stage ignition for HMN at temperatures less than 900°K at a pressure of 30 atm.

The two-stage ignition has been reported in a recent study [20] to take place for fuels having C.N. between 19.4 and 73. The low C.N. fuels produced the two stage ignition at higher compression ratios than the high C.N. fuels.

In the author's opinion, C.N. cannot correlate the I.D. in all types of engines, for all fuels derived from different sources, under all engine operating speed and load conditions. This may be due to the fact that the Cetane rating is conducted only under a set of specified conditions in which the I.D. is kept constant and the air pressure and temperature are varied simultaneously by adjusting the C.R. at a constant speed and constant inlet air and coolant temperatures. In actual diesel engines the C.R. is kept constant while the ambient temperature varies for cold start to hot start conditions, the intake air pressure and temperature vary according to whether the engine in naturally aspirated or turbocharged, the engine speed varies form idling to rated speed and the load or F/A ratio vary from no load to full load. The autoignition process as reported by Siebers [24], even for the same fuel, may vary from a single stage under some of the above conditions to a double stage under other conditions. Accordingly it seems that using a C.N. value to rate the I.D. under all the above operating conditions is very optimistic.

The author feels than the I.D. can be correlated according to equation (3), in terms of three basic parameters:

i. Air temperature.
ii. Air pressure.
iii. A global activation energy for the preignition reactions.

The temperatures and pressures in equation (3) should represent the effective values for the preignition chemical reactions which control the preignition processes. The temperature at the start of fuel injection is often used for such correlations, while it does not represent the temperature which affect the rate of the chemical reactions. Figure 12 is an illustration on the variation in the temperature during the I.D. of three fuels.

$$C.N._{(A)} > C.N._{(B)} > C.N._{(C)}$$

The injection timing is the assumed the same for the three fuels for simplicity. It is clear that

$$Tm_{(C)} < Tm_{(A)} < Tm_{(B)}$$

and

$$Pm_{(C)} < Pm_{(A)} < Pm_{(B)}$$

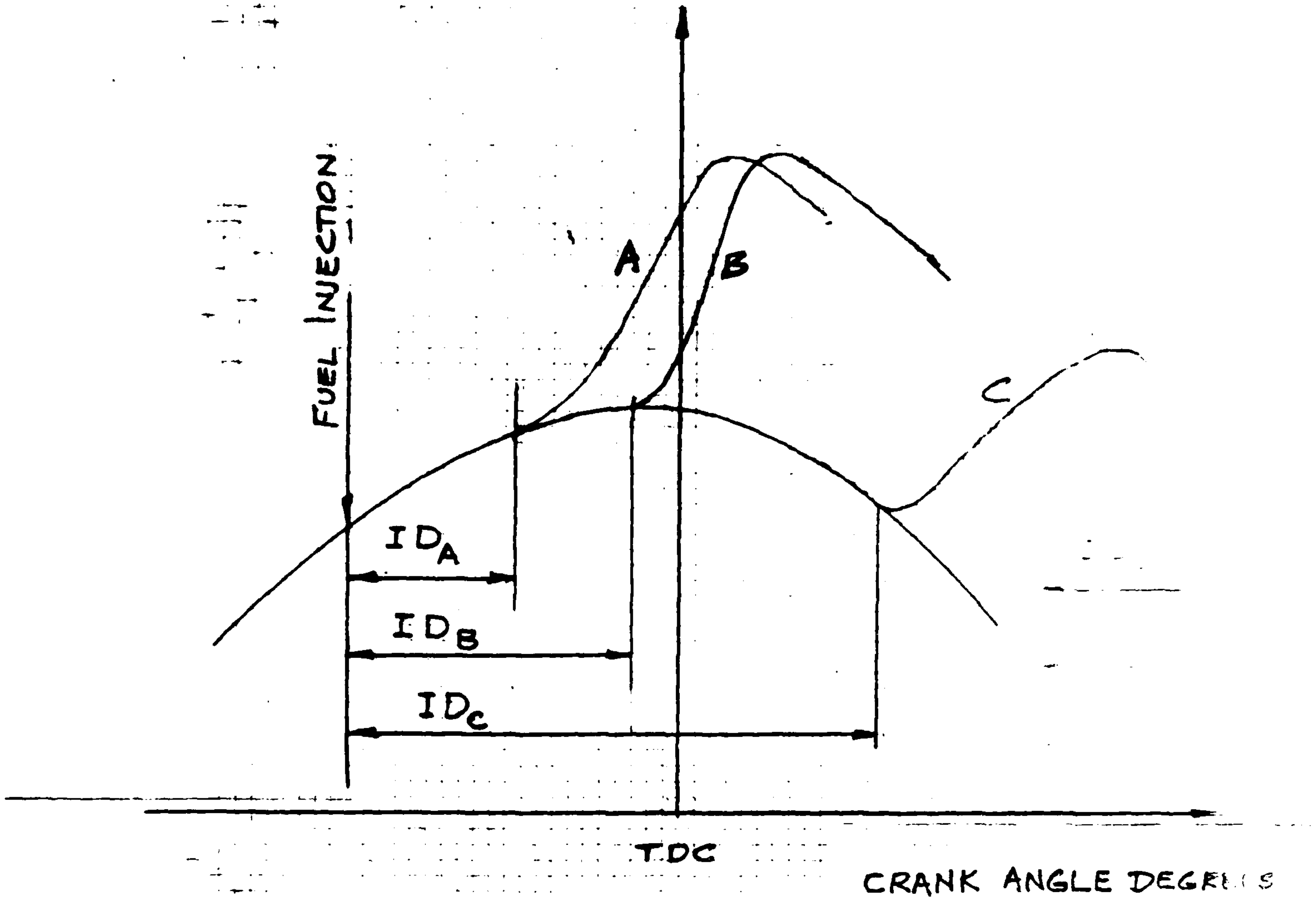

Fig. (12): Effect of I.D. on Mean Temperature and Pressure during I.D.

and Tm and Pm depend on both the injection timing and the length of I.D. period in crank angle degrees.

The results of tests conducted on a single cylinder research diesel engine under controlled temperatures and pressures during the I.D. are shown in figure 13. This figure shows the effect of C.N. on the I.D. of several distillates and blends of primary reference fuels in a D.I. single cylinder diesel engine. The data show the results obtained at inlet air temperatures varying from -4°F (-20°C) to 350°F (176.7°C). The inlet air pressure was adjusted to keep the mean pressure during the ignition delay at a constant value of 400 psia (KPa). For this, the inlet pressure had to be increased above atmospheric for temperatures above the normal room temperature and had to be decreased below atmospheric for tests at low ambient temperatures. The fuels used consisted of blends of primary reference fuels n-cetane (C.N. = 100) and αMN (C.N. = 0) and four distillates: DF-2, J.P4, Ref. 1 and Ref. 2 fuels. The properties of these fuels are given in Appendix D. Figure/4 shows the effect of changing the mean temperature during the I.D. for fuels having different C.N.s.

In addition to air temperature, the air pressure has an effect on I.D.. Figure 15 for DF-2 shows that increasing the mean pressure (during I.D.) reduces the I.D. of the fuel at different air temperatures. This is believed to be mainly due to the effect of air pressure on the preignition chemical reaction rates. This effect has been reported recently by Cowell and Lefebure [26] for homogeneous hydrocarbon-air mixtures in a continuous flow apparatus. The gaseous fuels used are propane, ethylene, methane and acetylene. The temperatures ranged between 670°K to 1020°K, the pressures ranged between 1 to 10 atmos-

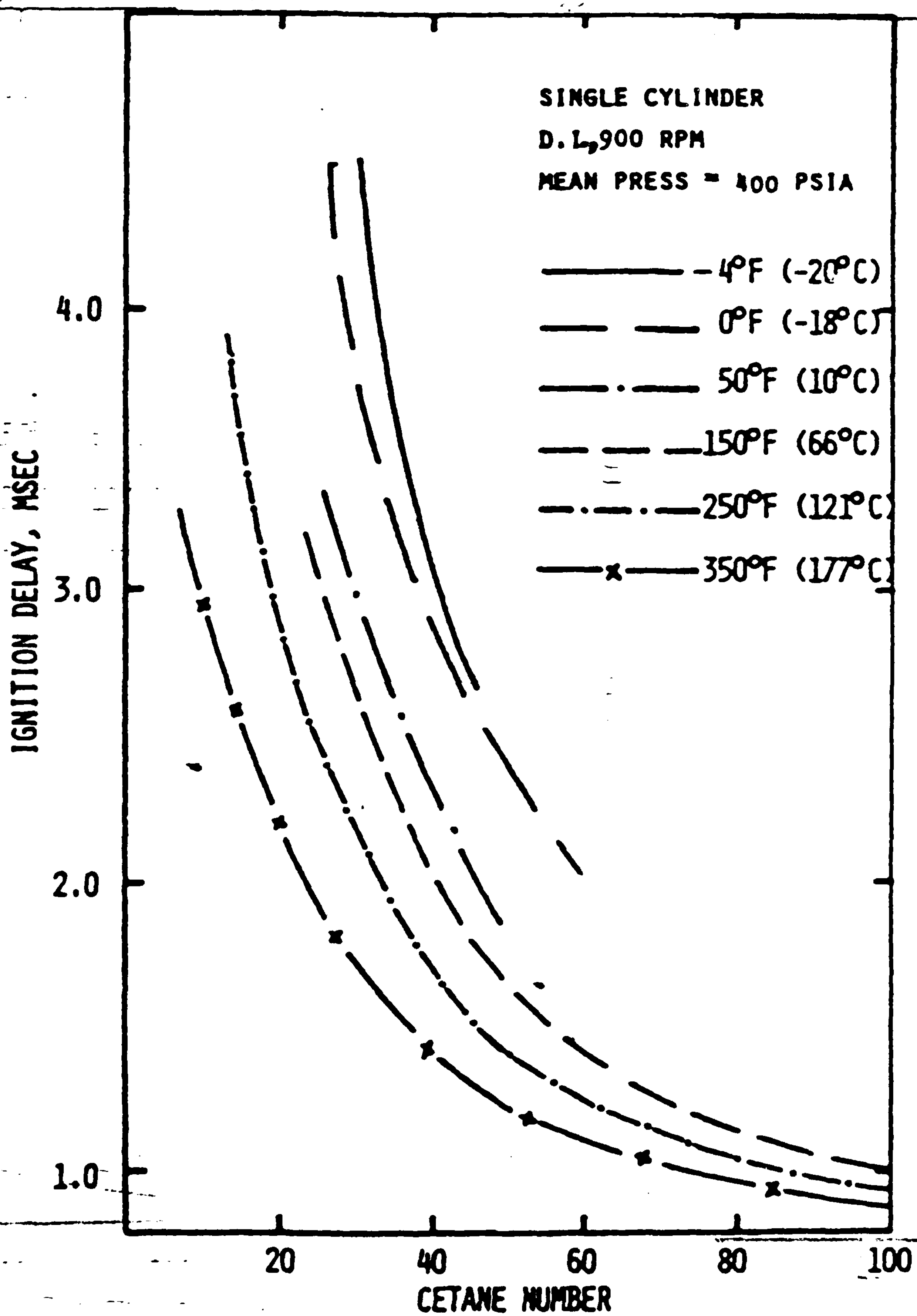

Fig. (13): Effect on C.N. on I.D. at different inlet air temperatures.

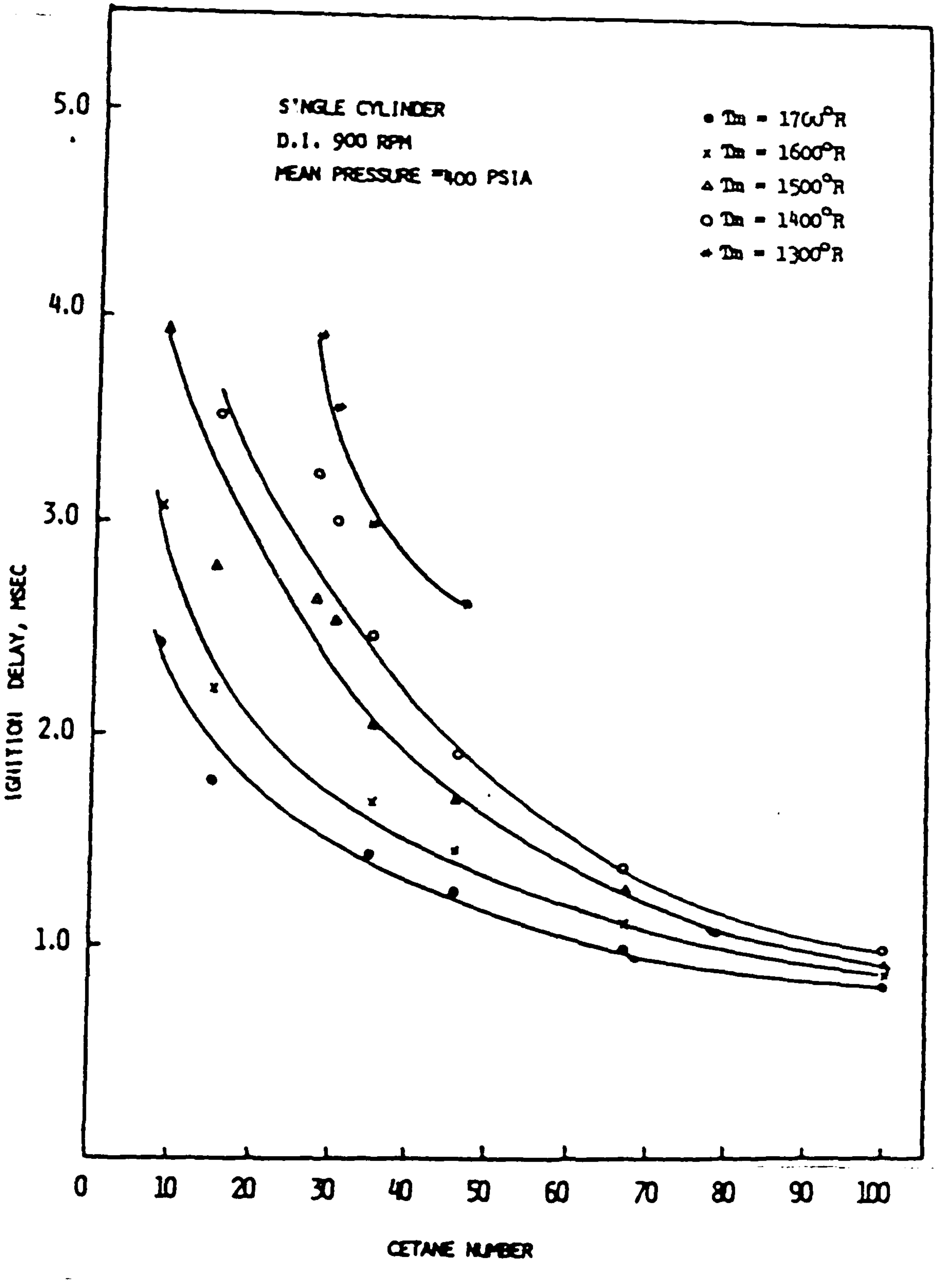

Fig. (14): Effect of C.N. on I.D. at different mean temperature during I.D.

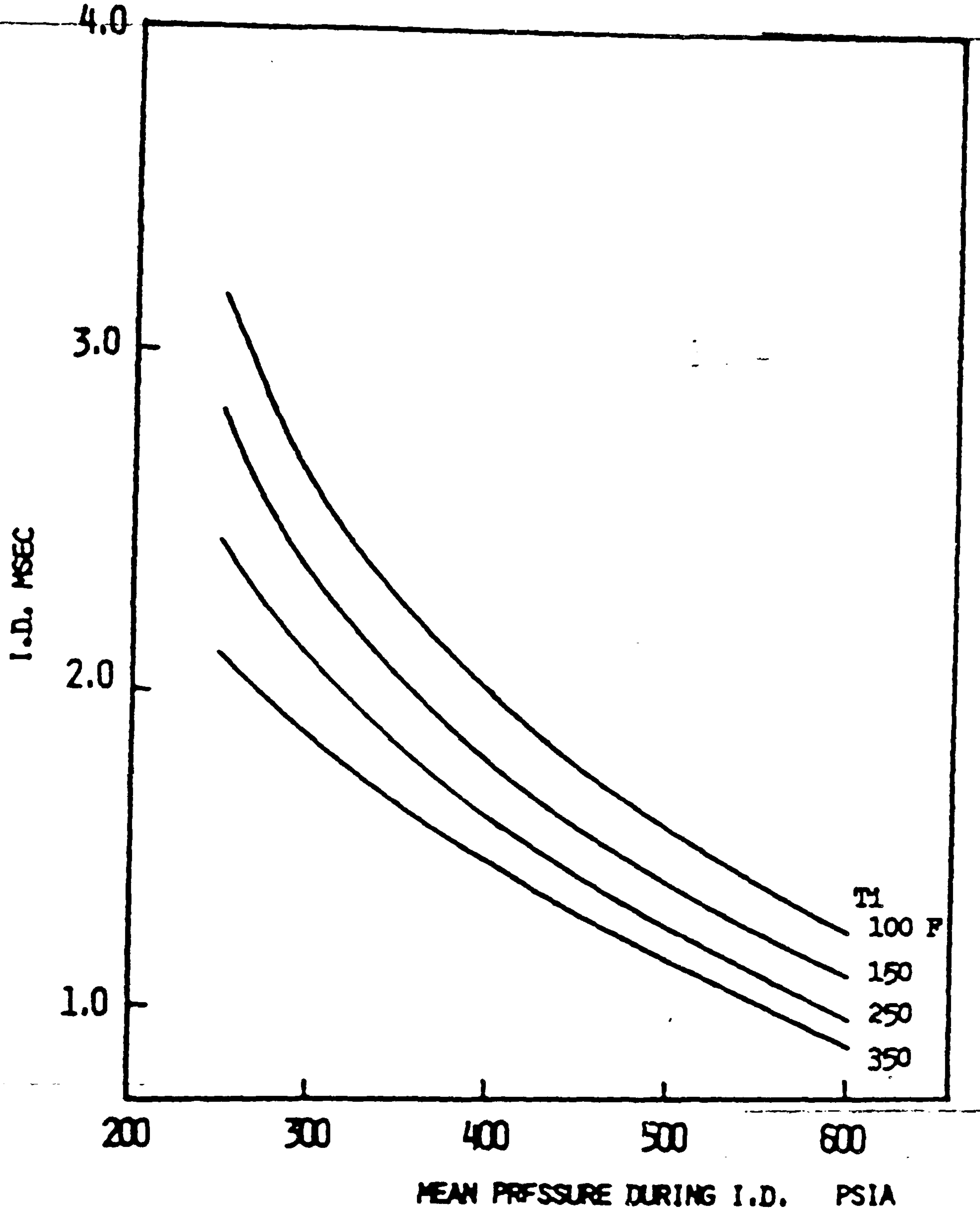

Fig. (15): Effect of mean pressure on I.D.

pheres, the equivalence ratios ranged between 0.2 to 0.7 and velocities ranged between 55 and 30 m/sec. The dependence of I.D. on pressure has the following form

$$I.D. \propto P^{-n}$$

where n varies from 1 for methane to 0.66 for acetylene. For liquid fuel sprays injected in diesel engines the results of figure 15 show that n is 1.2 for DF-2 (27).

The value of E in equation (3) can be obtained by plotting log I.D. vs $\frac{1}{Tm}$ at constant Pm, as shown in figure 16 for the data of figure 15. The slope of the straight line in figure 16 indicate that the activation energy E for DF-2, at Pm = 400 psi is 4965 BTU/16 mole. Birdi [27] found that E is a function of the mean pressure during I.D. in addition to the C.N. of the fuel. Figure 17 shows the variation in E with the C.N. at Pm = 400 psi, for all the reference and distillate fuels and their blends, tested in this program, at ambient air temperatures ranging between -4°F (-20°C) and 350°F (176.7°C).

It is recommended that such relationships between E and C.N. be obtained at different Pm. Then equation (3) would be able to correlate I.D. with C.N. of any fuel.

2.3.5 Inaccuracy or C.N. in Ranking the Overall Performance and Emission Bahaviour of Fuels in Diesel Engines

Many recent attempts have been made to characterize the overall performance and emission behaviour of fuels in diesel engines based on C.N. [21,22,28,29,30]. The following nine performance and emissions

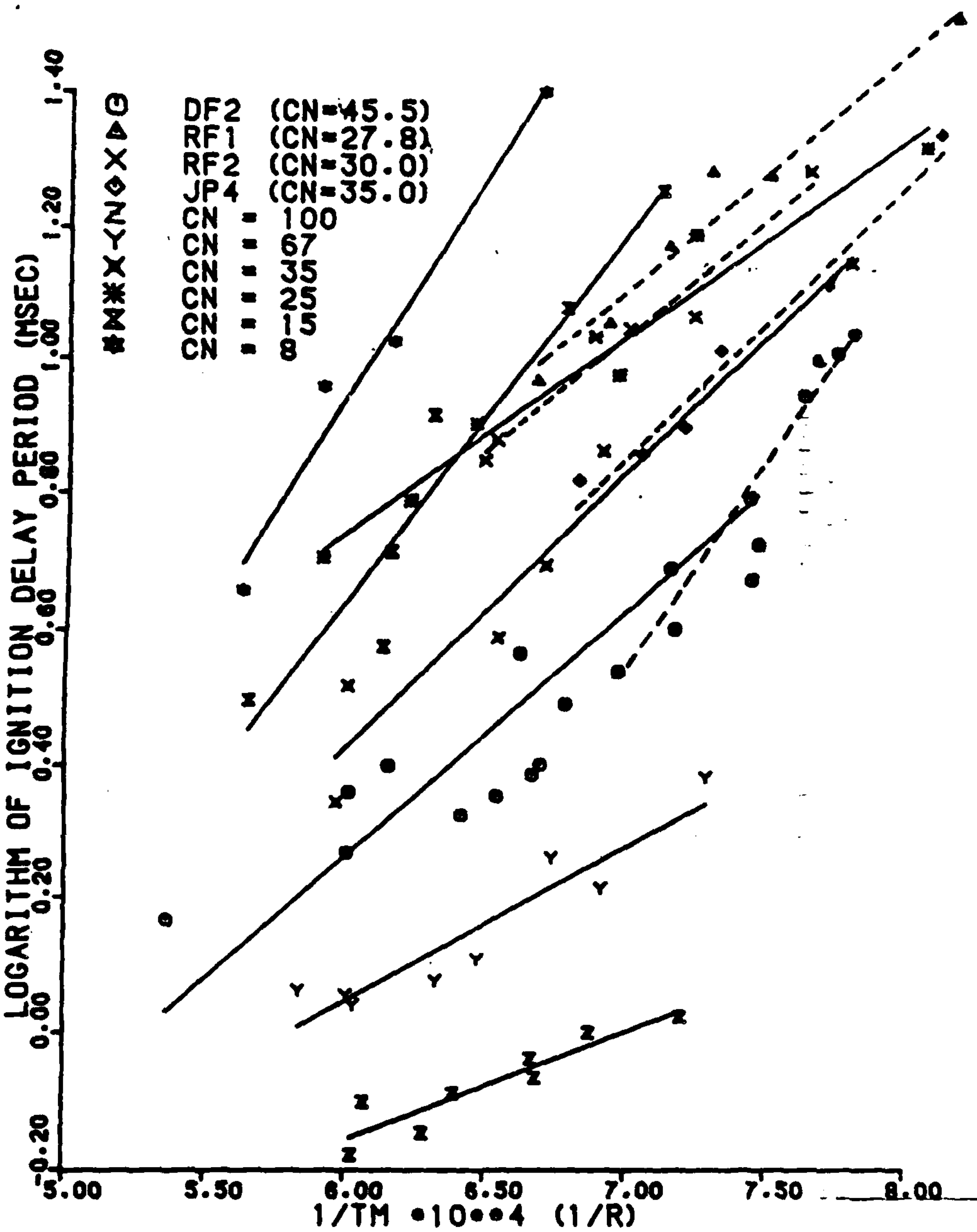

Fig. (16): Log I.D. plotted vs $\frac{1}{Tm}$ for fuels and blends of different C.N.S.

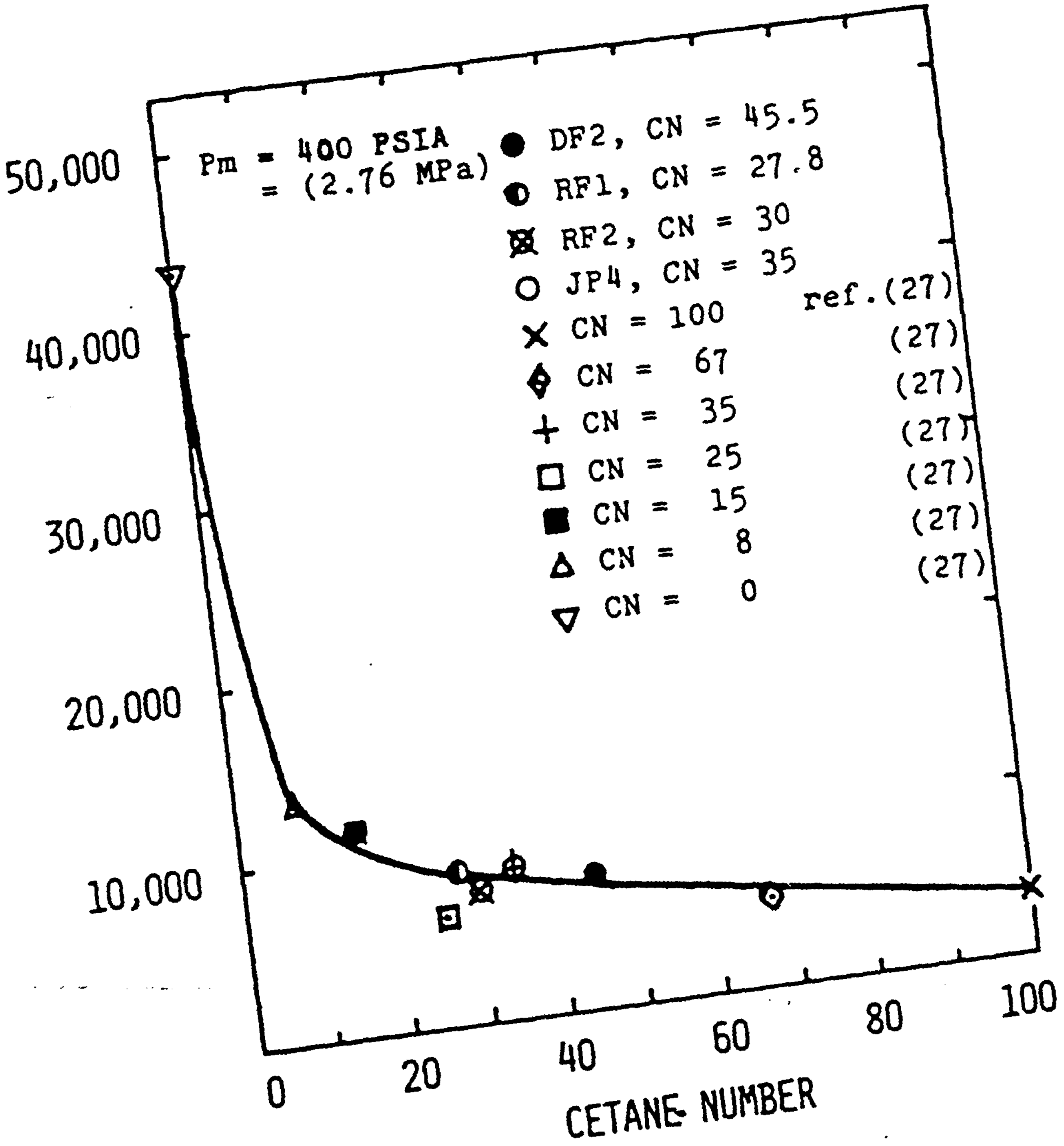

Fig. (17): Relationship between E and C.N. at Pm = 400 PSIA.

parameter have been considered: 1) Brake thermal efficiency, 2) Noise, 3) Unburned hydrocarbon emissions, 4) Nitrogen oxide emissions, 5) Carbon monoxide emission, 6) Black smoke intensity, 7) Particulate emissions, 8) Startability, and 9) White smoke.

In the author's opinion it is impossible to develop a single combustion parameter which would be able to rate the performance and emissions behaviour of fuels in diesel engines of different designs. The reasons behind this opinion are:

1. Any rating requires a scale with arbitrary reference states representing the lowest and the highest ratings on the scale. In order to develop a scale which would be able to rate the nine performance and emission parameters two fuels are needed: (i) a fuel which will produce the highest brake thermal efficiency, lowest noise, lowest HC, CO, NO_X, smoke, particulates, and white smoke. This in addition to be the easiest to start the engine on; (ii) similarly another fuel would be needed which would produce the worst performance. It is clear that it is impossible to find these two reference fuels which has the extremes in all the nine categories. Probably n-cetane does not represent the best fuel in fuel/engine performance parameters nor HMN represents the worst fuel.
2. Even if the above two references fuels are identified it is almost impossible that different fractions in their blends would give corresponding rating on the scale for the nine parameters. Each of these parameters is dependent in a very complex manner on many independent fuel, air, and engine variables. Even most of the relationships between many per-

formance parameters and the independent variables are not known or well identified.

The C.N. is one of the parameter which affect the I.D. of fuels as explained earlier. Any performance parameter which is a strong function of I.D. might be roughly rated by the C.N. Doyle and Needhan [20,21] reported that I.D. defines cold start, noise, light load hydrocarbons, and light load CO. In this respect C.N. might be a rough indicator of the behaviour of fuels in engines. Doyle and Needham [20,21] found that the peak rate of heat release (PRHR) correlated well with NO_X emissions. PRHR is not only a function of I.D., but also of the rate of mixing during the ignition delay and the premixed combustion periods, and the rate of the oxidation reactions during the premixed combustion period. Accordingly C.N. should not be able to rate NO_X at all operating conditions which affect the premixed combustion rates.

In the authors opinion an approach based on the work of Wade and Hunter [30] may be useful in correlating the fuel/engine performance parameters and the C.N.. Wade and Hunter [30] introduced the following three combustion parameters, as illustrated in figure 18:

i. Premixed Combustion Fraction (PCF).
ii. Premixed Combustion Index (PCI).
iii. Diffusion Combustion Index (DCI).

The premixed combustion fraction P, is the fraction of the total heat released at the end of the premixed combustion mode. The premixed combustion index P/P_A is the fraction of the total energy available in the fuel present in the cylinder at the end of the premixed mode. The diffusion combustion index is the ratio of the minimum period of time for diffusion combustion θ_{D_M} to the actual period of time for the diffu-

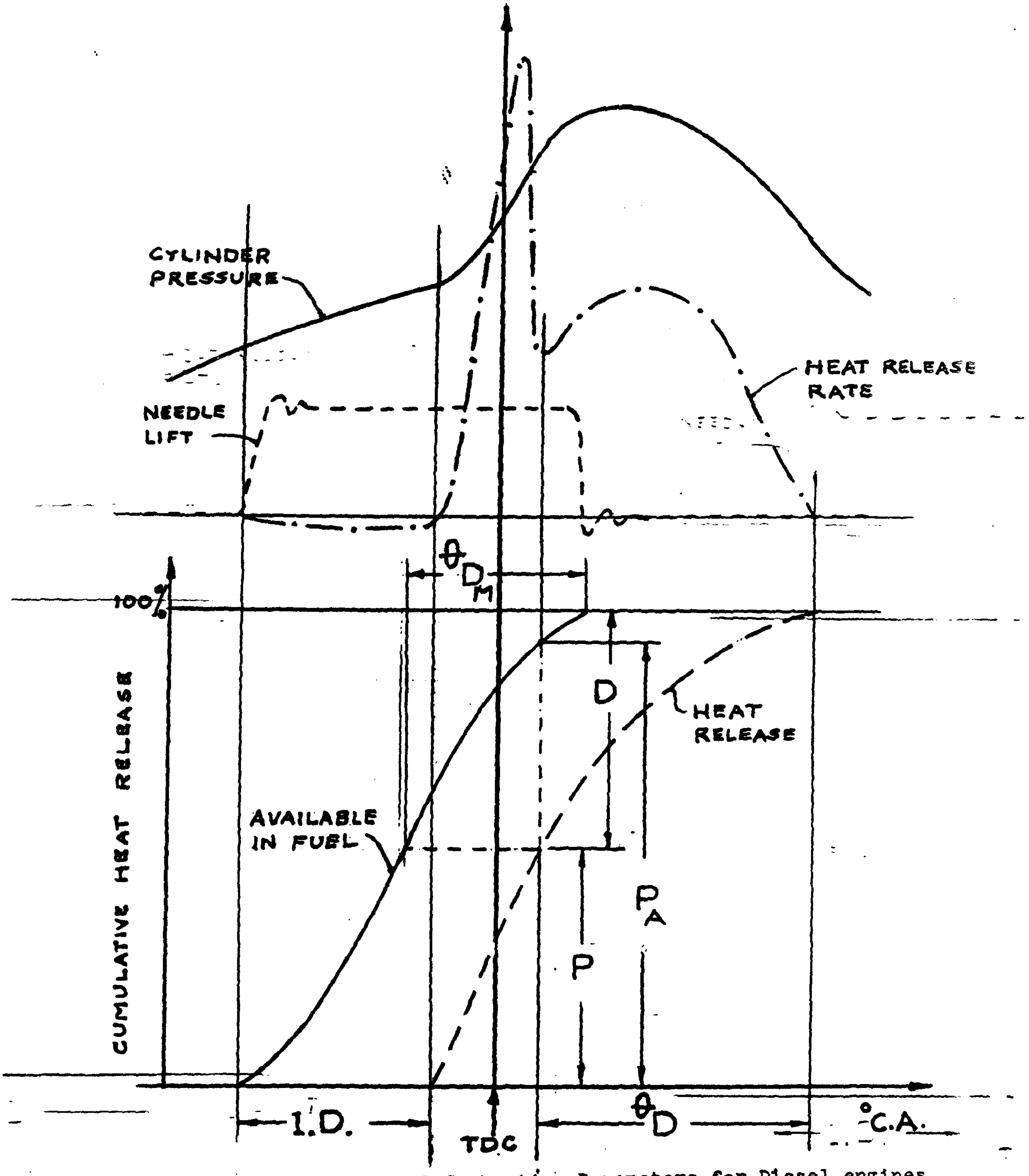

Fig (18): Global Combustion Parameters for Diesel engines.

sion combustion, θ_D. A diffusion combustion fraction D may be defined as the fraction of the total energy released in the diffusion combustion mode. Wade and Hunter applied their proposed technique to several types of diesel engines including D.I. and I.D.I. engines. Two fuels having C.N. = 47.5 and C.N. = 35 were used. The effect of reducing the C.N. on the proposed parameters were as follows:

i. I.D. increased.

ii. Both the premixed combustion fraction and the premixed combustion index increased by more than 100% due to the long I.D. of the low C.N. fuel.

iii. The diffusion combustion index decreased indicating that the burning rate of the low C.N. fuel had decreased.

The PCF affects HC, and NO_X and combustion noise, and the DCI affects BSFC and smoke.

2.3.6 Problem No. 6: Inability of C.N. in Rating the Cold Startability of Diesel Engines on Different Fuels:

The difficulty in starting diesel engines in low ambient temperatures represents one of the serious concerns of diesel engine designers, particularly when alternate fuels are used. The engine startability depends on a combination of factors among which the combustion failure is the most common. Combustion failure during starting may result from improper preignition or post ignition processes, assuming the the fuel flow is not interrupted at the low ambient temperatures. The preignition processes control the length of I.D. and the post ignition combustion processes control the rate and extent of the oxidation reactions. These processes are affected by the conditions during engine starting, which are characterized by:

i. Low ambient air temperatures which result in low temperatures near the end of the compression stroke.

ii. Low engine rotating speeds which result in

  (a) low compression pressures and temperatures,

  (b) poor injection process resulting in poor atomization,

  (c) low air turbulence resulting in low heat and mass transfer rates between the liquid and gaseous phases, and poor mixing.

The fuel properties play a big role in achieving successful ignition and subsequent combustion. The most important parameter to achieve successful ignition is the length of the ignition delay period. High C.N. fuels have short ignition delays and can produce successful ignition. Needham and Doyle [21,22] indicated that for the three middle distillate fuels tested [1,2, and 10] cold startability correlates well with the cetane rating.

Ignition may occur, however the engine may not start because of the low rate of post ignition oxidation processes. This may result from the lack of fuel evaporation or mixing the vapor with the air. It seems, then, that the fuel volatility should play a big role in the post ignition processes.

Combustion failure tests have been conducted on a single cylinder research diesel engines, in which the ambient temperature is lowered till combustion failed. The test are conducted on DF-2 (C.N. = 45), a light fuel (C.N. = 27.8), and a heavy fuel (C.N. = 30). The properties these fuels are given in Appendix D.

Figure 19,20 and 21 show the cylinder pressure, needle lift and crankangle degree marks for different ambient temperatues. The traces are for 0°C and lower ambient temperatures. The traces for higher ambient temperatures, in the range between 0°C and the normal room temperature, are not included in the figures because they have been found to be very close in shape to those at 0°C for the three fuels tested. Figure 19 is for DF-2, figure 20 is for Reference 2 (Heaviest) fuel, and figure 21 is for Reference 1 (most volatile) fuel. The fuel properties are given in Appendix D. Figure 19 shows that all the traces are reproducible. The I.D., rate of pressure rise and maximum pressure increase gradually with the drop in ambient temperature. This indicates an increase in the premixed combustion fraction.

Figure 20 is for Reference 2 fuel and shows the following:

i. I.D. increases with the drop in ambient temperature, indicating a decrease in the rates of the preignition processes. It is not clear at this time whether the physical or the chemical preignition processes has contributed to the increase in the I.D. because the fuel is very heavy.

ii. The injection process appeared not to suffer as the ambient temperature decreased. The fuel pressure and needle lift showed no cycle-to-cycle variations except at an ambient temperatue of -26°C, when misfiring took place.

iii. The slope of the pressure rise due to premixed combustion decreased gradually with the drop in ambient temperature, inspite of the increase in I.D. This indicates a reduction in premixed combustion index.

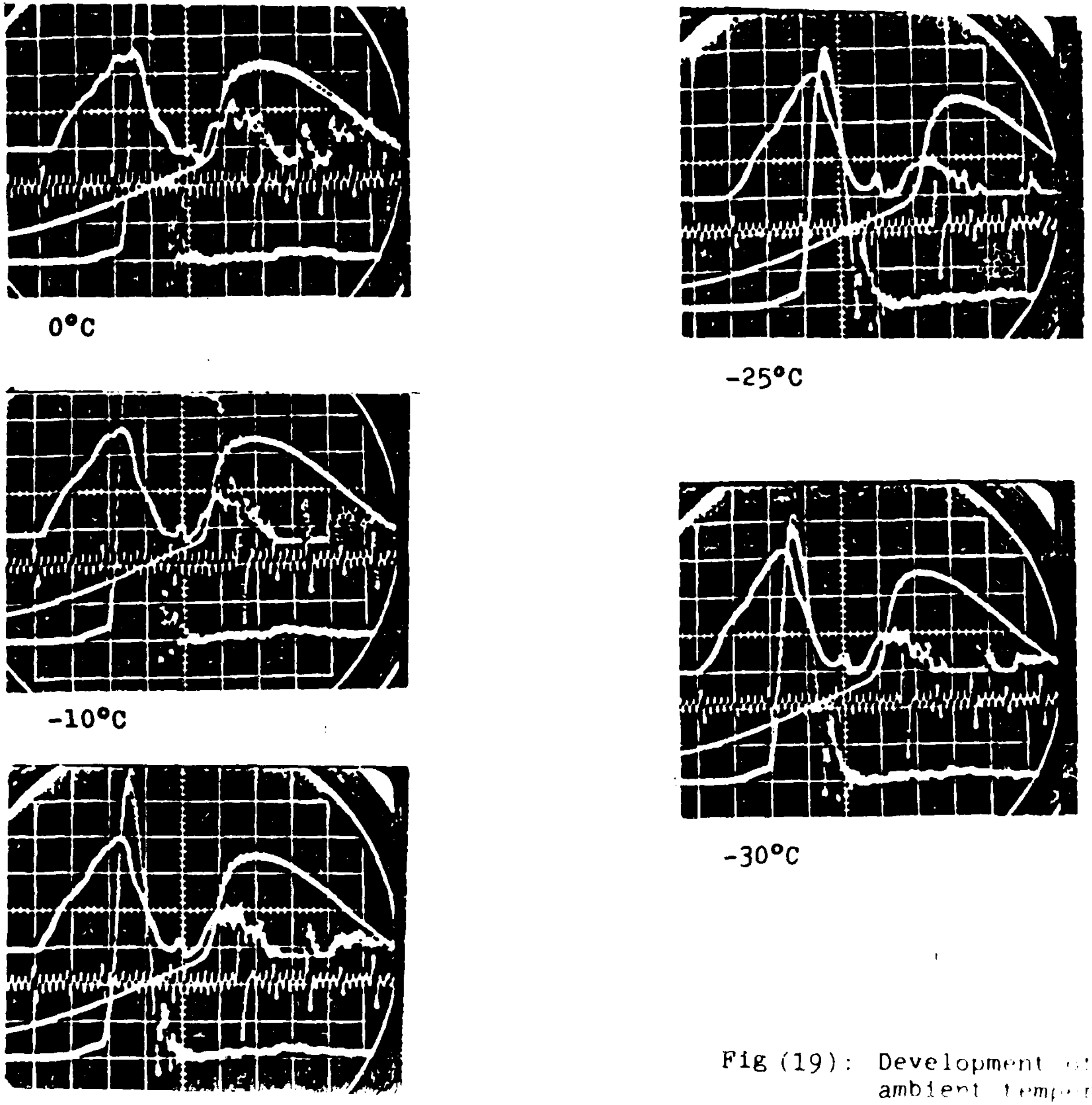

0°C

-10°C

-20°C

-25°C

-30°C

TACOM ENGINE
RPM = 900
DF-2 FUEL

Fig (19): Development of combustion at low ambient temperatures with Df-2

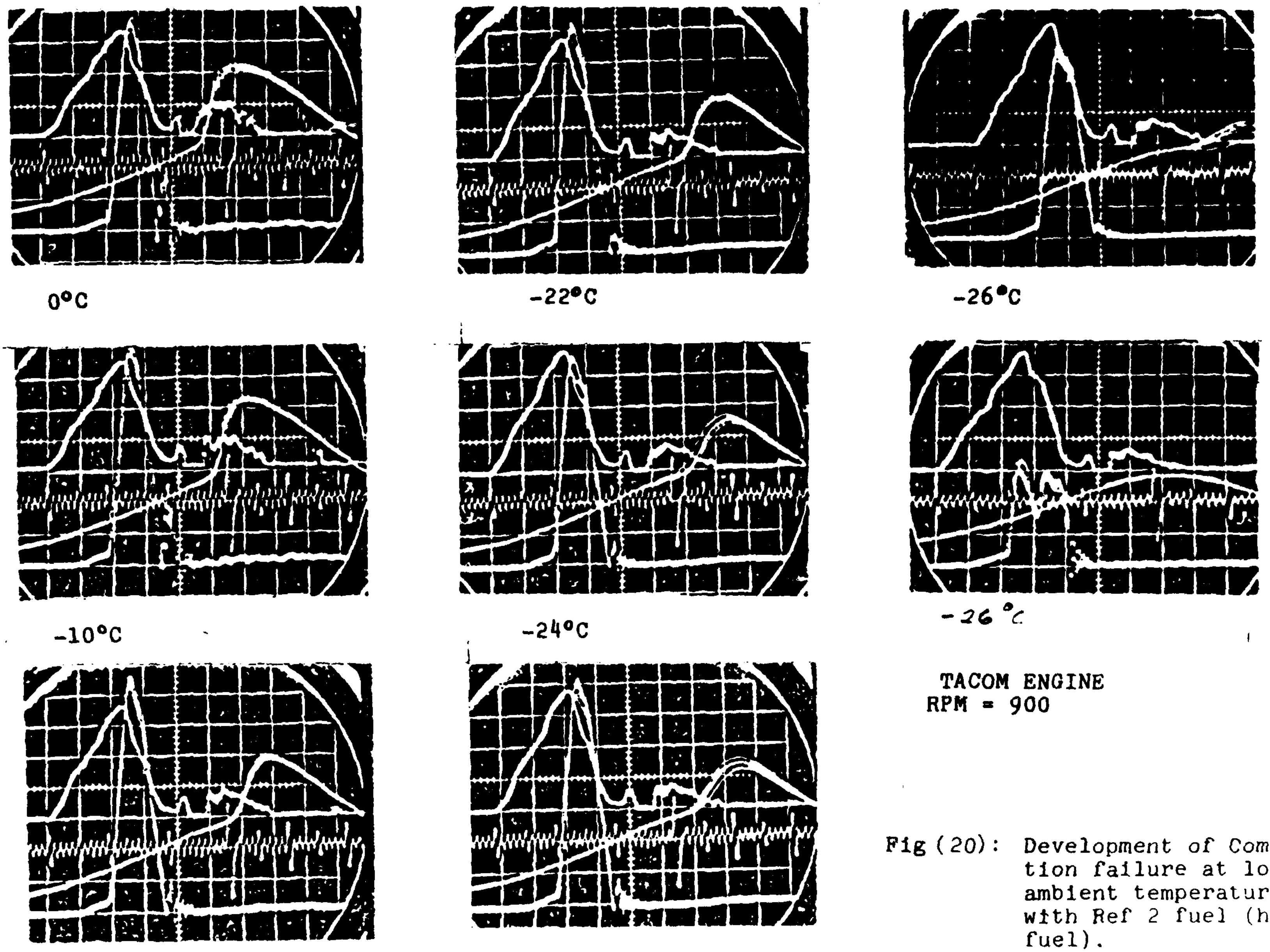

0°C

-22°C

-26°C

-10°C

-24°C

-26 °C

-20°C

-25°C

TACOM ENGINE
RPM = 900

Fig (20): Development of Combustion failure at low ambient temperatures with Ref 2 fuel (heavy fuel).

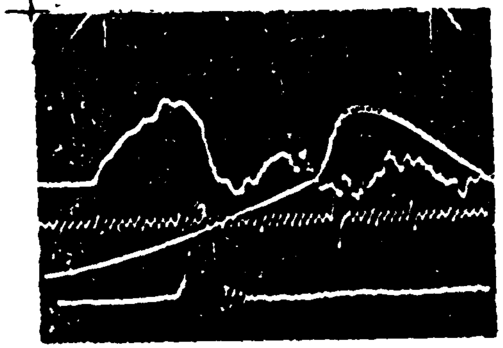

0°C

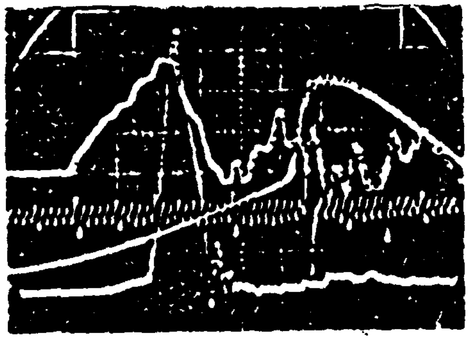

-10°C

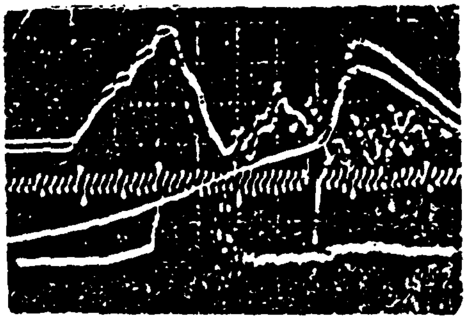

-20°C

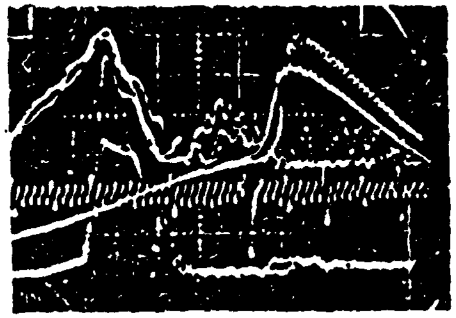

-25°C

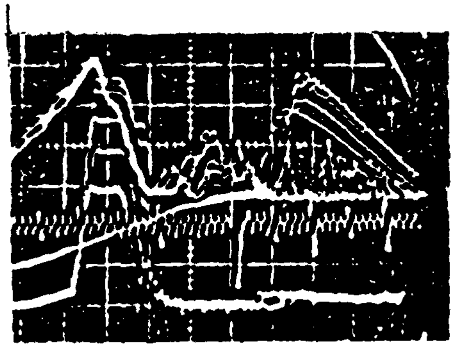

-26°C

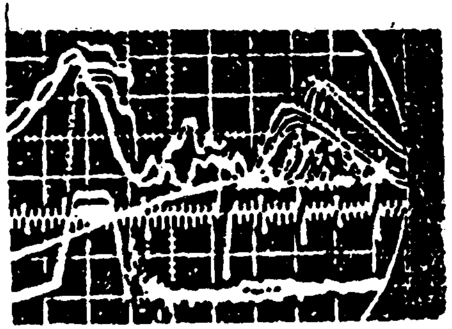

-27°C

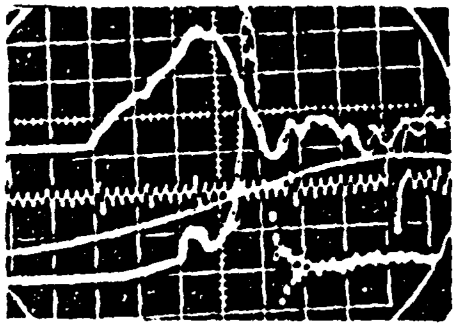

-28°C

TACOM ENGINE
RPM = 900
Ref 1 fuel

Fig (21): Development of Combustion failure at low ambient temperatures with Ref 1 fuel(volatile fuel).

iv. The total pressure rise due to combustion decreased with the drop in temperatue. This indicates a drop in the total heat release.

v. Misfiring is being caused by the failure of the premixed combustion regime which resulted in the failure of diffusion combustion.

Figure 21 is for Reference 1 (most volatile fuel) and shows the following:

i. The injection process, particularly the needle lift showed cycle-to-cycle variations at a temperature of -20°C, and increased with further drop in temperature.

ii. I.D. increased with the drop in ambient temperatures.

iii. Cycle-to-cycle variations occurred at a temperature of -20°C, and increased with further drop in temperature. The cause of this variation is not clear, whether it is from the injection or the preignition chemical processes. For this volatile fuel it is clear that the preignition physical processes do not suffer from the drop in temperature.

iv. The rate of pressure rise due to premixed combustion showed cycle-to-cycle variation, corresponding to that of the I.D.

v. The failure of combustion cannot, at this time, be attributed to the failure in the premixed combustion regime.

The above analysis of the experimental results on combustion failure at 900 RPM for the three fuels indicates the following:

i. The volatility has a great effect on the behaviour of fuels at low ambient temperatures.

ii. The failure of combustion at low ambient temperature is caused by the failure of the premixed combustion for the heavy fuel.

iii. The cause of the failure of combustion of the volatile fuel is not very clear, because of the deterioration of the injection process. However, it appears that the premixed combustion did not suffer as it did with the heavier fuel.

Needham and Doyle [21,22] reported similar results with some volatile fuels. They found that the broadcut fuel (no. 4), which has the highest volatility (distillation range 64°C to 312°C), lowest molecular weight and lowest viscosity of all the fuels, produced the worst performance in the D.I. engine by a large margin, in spite of a similar C.N. to that of tar sands fuel (no. 10).

It is clear that the cold startability, like the other fuel/engine parameters depends on other parameters, in addition to the C.N. of the fuel.

Montemayor and Owens (1985) determined the "Minimum Unaided Starting Temperature" for fuels of different physical properties and cetane numbers. They reported that the Minimum Unaided Starting Temperature for a 4 cylinder, 2-cycle D.I. diesel engine to be related to viscosity, 50% Boiling Point, and an autoignition temperatue, in addition to C.N.

The problems of cold startability and white smoke have not been well researched and deserve a careful investigation.

2.4 CONCLUSIONS

1. The basic function of the Cetane Scale is to rate the autoignition behaviour of a fuel by matching its ignition delay to that of a blend of two primary Reference fuels under specified conditions of inlet temperature, engine speed, coolant temperature, fuel-air ratio, injection timing and injector opening pressure. The only engine variable is the compression ratio. The Cetane Scale was not intended to rate any other combustion, performance or emissions parameter.

2. Three intrinsic problems exist in the cetane rating of fuels.

    2.1 Inability to rate low ignition quality fuels. The solution is to raise the inlet air temperature above the 150°F specified in the ASTM D-613 procedure.

    2.2 Instability of the ignition delay meter in rating low ignition quality fuels. This has been found to be due to the cycle-to-cycle variation in the I.D. of these fuels. No solution is known at this time.

    2.3 Inconformity of the CFR Combustion System with Actual Diesel Combustion Systems. A possible solution is to redesign the combustion system. Part of the problem may be solved for the existing system by optimizing the injection pressure such that the rating of the fuel is independent of the needle opening pressure.

3. Three fuel/engine preformance problems are examined:

    3.1 Invalidity of C.N. in correlating the I.D. for different fuels in different engines under all operating conditions. The I.D. should be correlated in terms of three basic parameters: mean temperature, mean pressure, and a global activation energy. The global activation energy can be correlated with the C.N.

3.2 Inaccuracy of C.N. in rating the overall performance and emissions behaviour of fuels in diesel engines. This correlation should be done in terms of I.D. and the combustion parameters which characterize the premixed and diffusion combustion regimes.

3.3 Inability of C.N. in rating the cold startability of diesel engines on different fuels. Startability depends on the success of both the autoignition and the subsequent combustion reactions. Many parameters other than C.N. need to be included.

2.5 RECOMMENDATIONS

1. Study the cetane rating at inlet air temperatures higher than the 150°F specified by the ASTM D-613 procedure. Determine the most suitable temperature which allows a suitable size of electric heater to be used.
2. Invistigate the phenomena of cycle-to-cycle variation in the autoignition process of fuels.
3. Investigate the effect of optimizing the needle opening pressure for each fuel on the cetane rating.
4. Develop correlations between the C.N. and the global activation energy for the preignition reactions for different fuels, to be used for correlating I.D. with C.N., temperatue and pressure.
5. Develop correlations between I.D. and the combustion parameters for the premixed and diffusion combustion and the fuel/engine perfor-

mance parameters. Relate these parameters to C.N. by using C.N.-I.D. correlations.

6. Make a combustion failure analysis during engine starting on different fuels and ambient temperatures. This will identify the engine and fuel parameters, other than C.N., which affect engine startability.

2.6 APPENDICES

2.6.1 APPENDIX A

CFR ENGINE SPECIFICATIONS

Bore	3.25 in.
Stroke	4.50 in.
Displacement	37.33 cu in.
Compression Ratio	7 to 28
Connecting-rod, center-to-center	10.00 in.
Number of piston rings	5
Crankcase	Highspeed CFR
Injection Pump	Bosch Type of variable injection timing
Injector	Bosch, ADN-30S-3/1
Injector Pintle valve lift	.004 to .006 in.
Valve timing	
Intake opens	10° ATDC
Intake closes	34° ABDC
Exhaust opens	40° BBDC
Exhaust closes	15° ATDC

2.6.2 APPENDIX B

SUMMARY OF OPERATING CONDITIONS SPECIFIED BY ASTM-D-613 CETANE METHOD

Engine speed, rpm	900 ± 9
Crankcase oil, SAE grade	30
Oil pressure at operating temperature	25 to 30 psi
Crankcase oil temperature	135 ± 15°F
Coolant Temperature:	
Range	212 ± 3°F
Constant within	± 1°F
Intake Air Temperature	150 ± 1°F
Valve clearances	.008 in., measured with the engine hot and running under standard operating conditions on a reference fuel of 50 C.N.
Fuel Injection Pump, Bosch:	
Advance, deg btdc	13.0
Opening pressure, psi	1500 ± 50
Injector:	
Water jacket temperature	100 ± 5°F
Fuel injection rate	13.0 ± .2 ml/min.

2.6.3 APPENDIX C

Properties of DOE Fuels Tested by Reference [21,22]

	FUEL DESCRIPTION - NUMBER				
PROPERTY FUEL NUMBER	PHILLIPS D2 NO. 1	MID-DISTILLATE NO. 2	MID DISTILLATE NO. 3	NAPHTHA/ D2 NO. 4	SUNFLOWER OIL NO. 5
SPECIFIC GRAVITY (15°C)	0.846	0.867	0.881	0.788	0.922
DISTILLATION (°C)					
IBP	189	183	219	64	477
10%	215	208	252	93	548
50%	261	267	288	138	588
90%	300	351	345	279	-
FBP	324	384	406	312	-
CETANE NUMBER	50.1	40.7	41.6	36.2	35.8
CETANE INDEX	47.1	42	42.2	14.8	-
VISCOSITY (cSt 40°C)	2.40	2.76	4.37	0.91	33.93
POUR POINT (°C)	-18	-15	-10	-39	-11

Properties of DOE Fuels Tested by Reference [21,22]
(continued)
(NOS. 6 through 10)

	FUEL DESCRIPTION - NUMBER				
PROPERTY FUEL NUMBER	SUNFLOWER OIL NO. 6	SHALE D2 NO. 7	SRC11/D2 BLEND NO. 8	METHANOL/ D2 BLEND NO. 9	TAR SANDS NO. 10
SPECIFIC GRAVITY (15°C)	0.887	0.828	0.890	0.836	0.881
DISTILLATION (°C)					
IBP	339	180	189	64	170
10%	359	207	224	74	197
50%	368	251	259	245	267
90%	372	304	303	296	352
FBP	411	341	331	321	383
CETANE NUMBER	59.9	51.1	35.6	38.9	35.2
CETANE INDEX	-	51.2	34.1	46.4	38.2
VISCOSITY (cSt 40°C)	4.96	2.44	2.47	1.98	2.82
POUR POINT (°C)	-5	-18	-21	-21	-45

Properties of DOE Fuels Tested by Reference [21,22]
(continued)

PROPERTY FUEL NUMBER	PHILLIPS D2 NOS. 1	MID-DISTILLATE NO. 2	MID DISTILLATE NO. 3	NAPHTHA/ D2 NO. 4	SUNFLOWER OIL NO. 5
	FUEL DESCRIPTION - NUMBER				
HC TYPE (% VOL)					
SATURATES	70.8	52.2	62.5	80.8	-
OLEFINS	1.2	0.5	1.0	0	-
AROMATICS	28.0	47.3	36.5	19.2	-
ELEMENTAL ANALYSIS					
C (%M)	86.69	87.27	86.82	86.04	77.09
H (%M)	12.96	12.19	12.62	13.63	11.59
S (%M)	0.2	0.38	0.22	0.07	0.01
O (%M)	0.045	0.058	0.33	0.020	11.13
N (%M)	0.004	0.015	0.017	0.001	5 ppm
HEAT OF COMBUSTION (NET MJ/kg)	42.61	42.21	42.25	43.36	37.03

Properties of DOE Fuels Tested by Reference [21,22]
(continued)
(NOS. 6 through 10)

	FUEL DESCRIPTION - NUMBER				
PROPERTY FUEL NUMBER	SUNFLOWER OIL NO. 6	SHALE D2 NO. 7	SRC11/D2 BLEND NO. 8	METHANOL/ D2 BLEND NO. 9	TAR SANDS NO. 10
HC TYPE (% VOL)					
SATURATES	-	81.0	47.5	70.0	51.2
OLEFINS	-	1.2	1.2	2.0	0.7
AROMATICS	-	17.8	51.3	28.0	48.1
ELEMENTAL ANALYSIS					
C (%M)	76.78	86.03	87.08	79.77	87.15
H (%M)	11.95	13.80	11.28	13.08	11.98
S (%M)	0.01	0.04	0.34	0.14	0.59
O (%M)	13.73	0.060	0.209	4.72	0.056
N (%M)	8 ppm	0.094	0.306	0.005	0.026
HEAT OF COMBUSTION (NET MJ/kg)	37.23	43.07	41.21	39.72	41.98

2.6.4 APPENDIX D

Properties of Fuels Tested at WSU

Fuel Properties

Property Fuel	Specific Gravity (15°C) [D1298]	Kinematic Viscosity (40°C) cts [D445]	Distillation (°C) [D82] 10% Recover	50% Recover	90% Recover	Aniline Point (°C) [D611-77]	Cetane Number [D-613]
DF-2	0.8547	2.705	209.25	256.5	319	55.2	45.5
Reference #1	0.7883	0.779	108.5	167.5	235.5	38.8	27.8
Reference #2	0.9296	3.791	212.5	255.5	319.5	35.0	30.0
JP-4	0.7640	0.779	94	149.5	225	55.2	35.0

2.7 List Of References:

1. L.J. Lemesurier and R. Stansfield, J. Inst. Petroleum Tech., 17,387,1931.
2. G.D. Boerlage and J.J. Broeze, Engineering 132, 603-6, 687-9, 755-6, 1931.
3. A.W. Pope, Jr. and J.A. Murdock, S.A.E. Journal 30, 136, 1932.
4. P.H. Schweitzer, H.A. Dickinson and M.J. Reed, "Status of Diesel Fuel Oil Standardization in the United States". Paper 78, World Petroleum Congress, London, 1933.
5. T.B. Hetzel and P.H. Schweitzer, Automotive Ind. 73, 202, 1935.
6. P.H. Schweitzer, "Methods of Rating Diesel Fuels." School of Engineering, The Pennsylvania State College, 1937.
7. ASTM Manual for Rating Diesel Fuels by the Cetane Method, 1963.
8. J.A. Russell, B.K. Bailey, W.W. Wimer, "Emergency Fuels Utilization Guidebook", Southwest Research Institute Report DOE/cs/54269-01, Contract No. AC01-78CS54269, August 1980.
9. "Low Cetane Number Determinations." U.S. Army Fuels and Lubricants Research Laboratory, San Antonio, Texas, June 1965.
10. C.M. Urban and J.T. Gray of Southwest Research Institute, "An Investigation of Methods for Determining Cetane Numbers of Low Ignition Quality Fuels." Paper presented at S.A.E. mid-year meeting, Detroit, MI., May 20-24, 1968.
11. H.O. Hardenberg and E.R. Ehnert, "Ignition Quality Determination Problems with Alternate Fuels for Compression Ignition Engines." SAE paper no. 811212, 1981.
12. J.N. Bowden, A.A. Johnston and J.A. Russell, "Octane-Cetane Relationship." Final report AFLRL No. 33, U.S. Army Fuels and Lubricants Research Laboratory-Southwest Research Institute, San Antonio, Texas, March 1974.
13. Communication between J.G. Stewig of Waukesha Motor Company and Klaus Hebmuller of Ern Mototenteile K.G., Dusseldorf, West Germany, 1969. This information was obtained from Mr. Ivan Baxter of Waukesha Motor Company.
14. Naeim A. Henein, Nabil Y. Elias, "A Modified Cetane Scale for Low Ignition Quality Fuels." SAE paper no. 780640, June, 1978.

15. ASTM Manual for Rating Diesel Fuels by the Cetane Method, 1963.

16. D.P. Sczomak and N.A. Henein, "Cycle-to-Cycle Variation with Low Ignition Quality Fuels in a CFR Diesel Engine," SAE Fuels and Lubricants Meeting, Houston, Oct. 1979, paper no. 790924, 1979.

17. N.A. Henein and C.S. Lee, "Autoignition and Combustion of Fuels in Diesel Engines Under Low Ambient Temperatures" SAE International Off-Highway and Powerplant Congress and Exposition, Milwaukee, WI, paper no. 861230, 1986.

18. W.T. Lyn and E. Valdmanis, "The Effects of Physical Factors on Ignition Delay," Proc. Inst. Mechanical Engineers, Vol. 181, No. 1, PA2A, 1966-67.

19. P.S. Pederson and B. Quale, "A Model for Physical Part of the Ignition Delay in a Diesel Engine," SAE paper no. 740716.

20. Y. Takasi, "Effect of Fuel Properties on Autoignition in Diesel Engines," Internal Report, Wayne State Univ., 1986.

21. D.M. Doyle and J.R. Needham, "Investigation Into Alternative Fuel Rating Techniques," Final Report, DOE/CE/50010-1, November 1985. Symposium on the Chemistry of Cetane Number Improvement, The Division of Petroleum Chemistry, Inc., American Chemical Society, Miame Beach Meeting, April 28-May 3, 1985 Preprints Vol. 30, No. 2 March 1985.

22. J.R. Needham and D.M. Doyle, "The Combustion and Ignition Quality of Alternative Fuels in Light Duty Diesels" SAE International Fuels and Lubricants Meeting and Exposition, Tulsa, Oklahoma, Oct. 21-24, 1985, Paper no. 852101.

23. D.M. Yost, T.W. Ryan III, and E.C. Owens, "Fuel Effects on Combustion in a Two-Stroke Diesel Engine." SAE paper no. 8502104.

24. D.L. Siebers, "Ignition Delay Characteristics of Alternative Diesel Fuels:Implications on Cetane Number," SAE International Fuels and Lubricants Meeting and Exposition, Tulsa, Oklahoma, Oct. 21-24, 1985, SAE paper no. 852102.

25. T.W. Ryan III, "Correlation of Physical and Chemical Ignition Delay to Cetane Number" SAE International Fuels and Lubricants Meeting and Exposition, Tulsa, Oklahoma, Oct. 21-24, 1985, paper no. 852103.

26. L.H. Cowell and A.H. Lefebure, "Influence of Pressure on Autoignition Characteristics of Gaseous Hydrocarbon-Air Mixtures" SAE International Congress and Exposition, Detroit, MI, Feb., 1986, paper no. 860068.

27. P. Birdi, "General Correlation for Ignition Delay Period in Diesel Engines" Ph.D. Dissertation, Wayne State Univ., 1979.

28. H. Ng, G. Borman, "An Investigation of Effects of Alternate Fuel Properties on Combustion and Emission Mechanisms in Direct Injection Engines," DOE/CS/5006-1 Report, April, 1985.

29. D.L. Sutton, "Investigation Into Diesel Operation With Changing Fuel Property," SAE International Congress and Exposition, Detroit, MI, paper no. 860222, 1986.

30. W.R. Wade, C.E. Hunter, "Analysis of Combustion Performance of Diesel Fuels," CRC Workshop on Diesel Fuel Combustion Performance, Atlanta, Georgia, Sept. 14, 1983.

SECTION 3

C.N. RATING OF COLD STARTABILITY OF DIESEL ENGINES ON DIFFERENT FUELS

The inability of C.N. scale in rating the cold startability of diesel engines on different fuels is of great concern to the military and industry. This seciton of the report deals with the research conducted to find out why the C.N. fails to predict the cold startability of diesel engines.

This section describes the experimental work conducted on a single cylinder engine to determine the effect of the Cetane number and other fuel properties on cold startability.

3.1 ENGINE AND INSTRUMENTION:

The engine is a single cylinder, Deutz, 4-stroke-cycle, direct injection air cooled diesel engine $d = 0.095$ m, and C.R. = 17:1.

The cylinder gas pressure is measured by using a quartz crystal pressure transducer, and a charge amplifier. Before each run the engine was soaked at the controlled ambient temperature for at least 5 hours.

The instantaneous angular velocity is determined from the time taken by the crankshaft to rotate through a fixed angle. An electromagnetic pick up installed in the flywheel housing, produces a pulse signal to indicate the present of a tooth on the flywheel ring gear.

The data acquisition system consists of a 24 bit high speed counter, four 10 bit analog to digital converters and a TDC identification circuit.

3.2 FUELS:

The following two fuels are used: DF-2 (Diesel fuel number 2) and JP-4 fuel. The fuel main specifications are given in item 2.6.4. JP-4 is a lighter fuel than DF-2, and has a lower C.N., but a higher volatility than DF-2.

3.3 EXPERIMENTAL RESULTS

A. DF-2 FUEL

Fig. 22 is a plot of the instantaneous angular velocity of the engine versus the engine revolutions, at an ambient temperature of 20°C, after a cold soak period of five hours. The engine started successfully and reached the idling speed of 130 radians per second after about 30 revolutions. Fig 23 is for starting the engine at an ambient remperature of 15°C, after a cold soak period of fire hours. The data for 20°C is plotted on Fig 22 at the same scale for comparison. The engine started successfully and reached the idling speed after 35 revolutions. The oscillations in the engine speed after the engine starts are under investigation at the present time. Fig 24 is at an ambient temperature of 10°C after a cold soak time 12 hours. The engine started and reach the idling speed after 45 revolutions. The oscillations in speed are more frequent and their amplitude is higher than at the higher ambient temperatures. Fig 25 is for an ambient temperature of 5°C and cold soak of 5.5 hours. The uniform cranking speed is 60 radians per second, for about 45 revolutions. Following this the engine began to accelerated at a very slow rate, which increased in time. A maximum speed of 138 radians per second is reached after 90 revolutions from the start of cranking, or after 45 revolutions from uniform cranking. Fig 25 shows that the oscillations increased in number and amplitude as the temperature decreased from 10°C to 5°C. Fig 26 is for an ambient temperature of 2°C. The engine is cranked at a uniform speed of 57 radians per second, for about 60 revolutions after which the speed increased very gradually, at a slow rate at fiist. The rate of increase in speed increased till it reached a maximum of 143 radians per second. The number of revolutions taken for the engine to accelerate from the uniform cranking speed to the maximum speed is 50. The oscillations in speed increased in number, and amplitude.

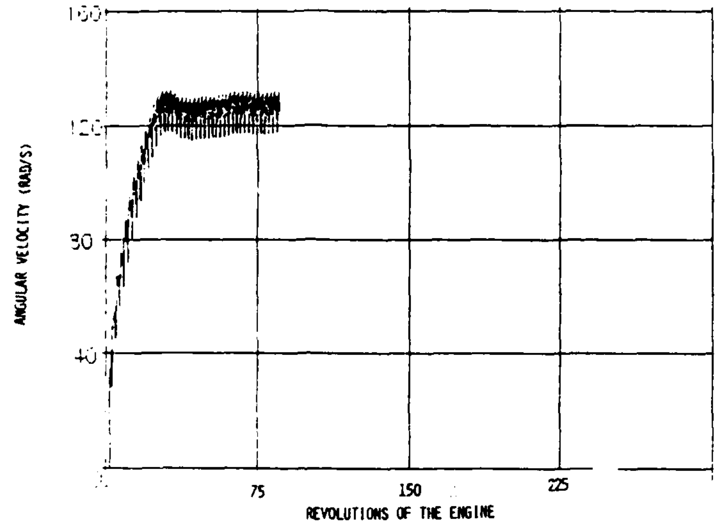

Fig. 22 Plot of angular velocity vs. engine revolutions, Fuel: DF 2, Oil: arctic oil, ambient temperature:20 C, cold soak time: 5 hrs., startability conditions Started easily.

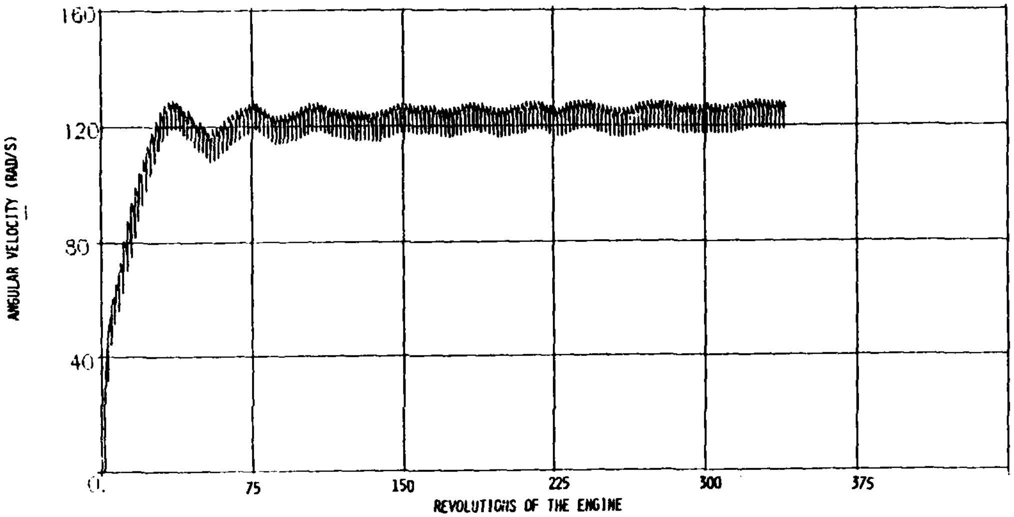

Fig. 23 Plot of angular velocity vs. engine revolutions, fuel: DF 2, oil: arctic oil, ambient temperature:15 C, Cold soak time: 5 hrs., startability condition: started easily.

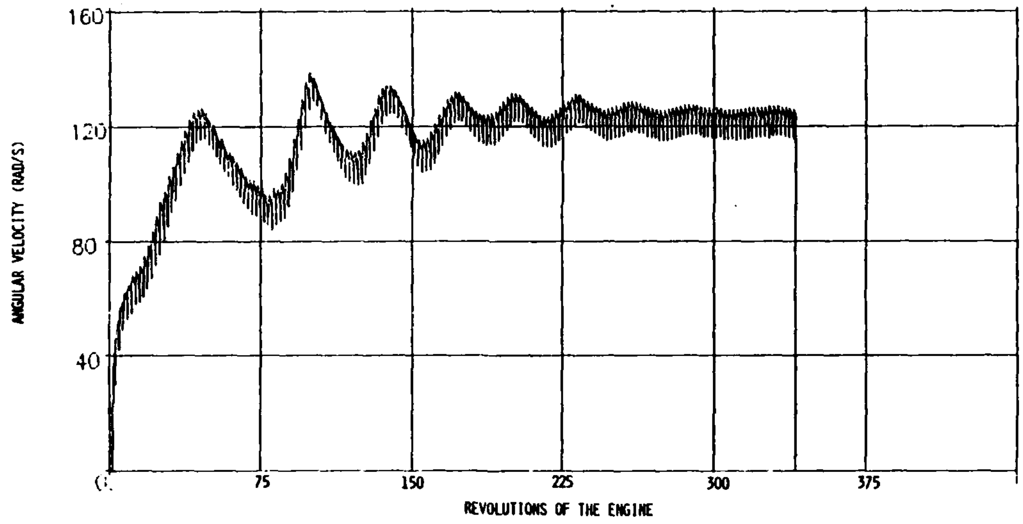

Fig. 24 Plot of angular velocity vs. engine revolutions, fuels DF 2, oil: arctic oil, ambient temperature: 10 C, cold soak time: 12 hrs., startability conditions started easily.

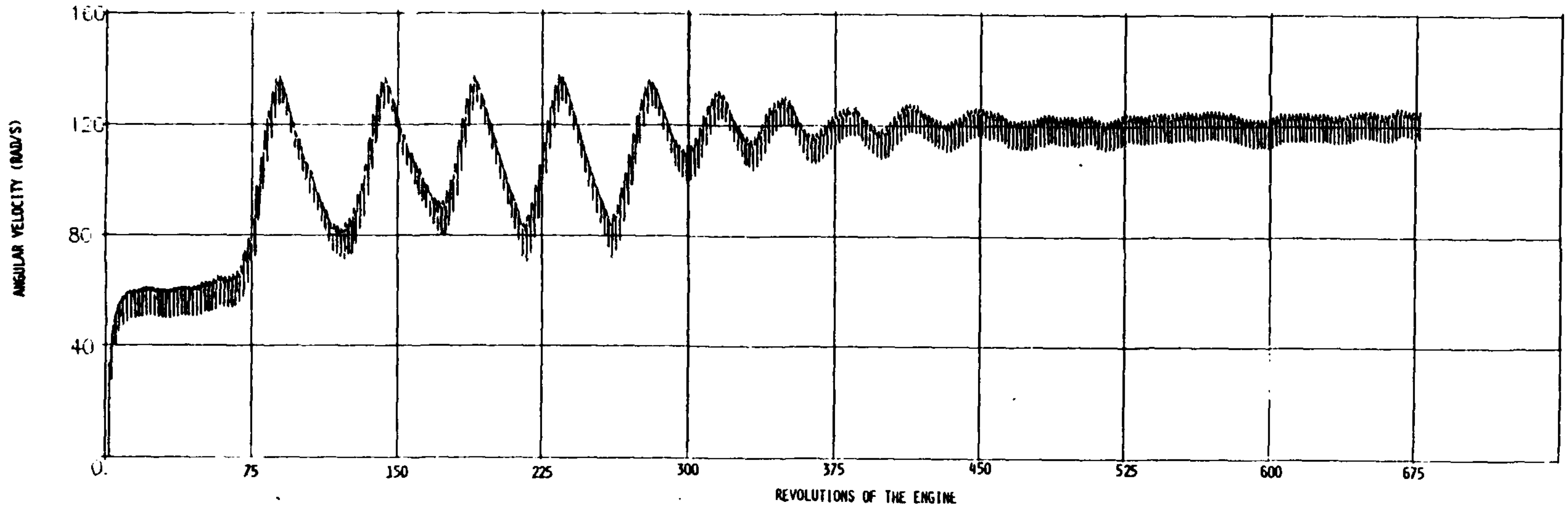

Fig. 25 Plot of angular velocity vs. engine revolutions, fuel: DF 2, oil:arctic oil, ambient temperature: 5 C, cold soak time: 5½ hrs., startability condition: started easily.

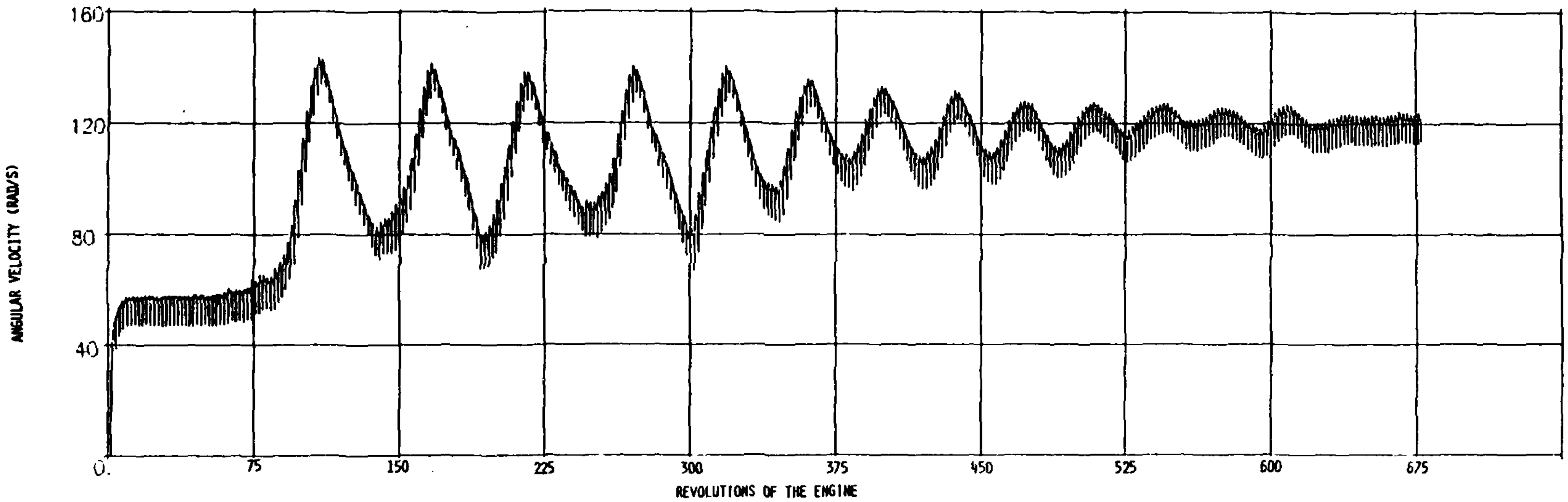

Fig. 26 Plot of angular velocity vs. engine revolutions, fuel: DF 2, oil: arctic oil, ambient temperature: 2 C, cold soak time: 5½ hrs., startability condition: started easily.

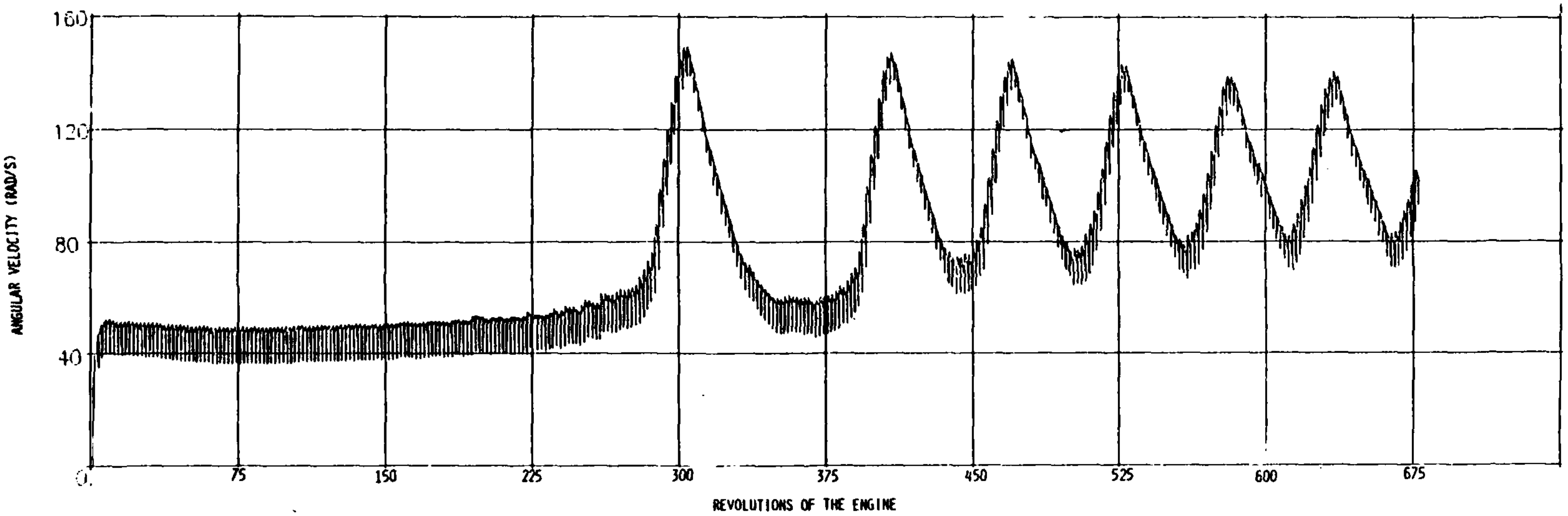

Fig. 27 Plot of angular velocity vs. engine revolutions, Fuel: DF 2, oil:arctic oil, ambient temperature:-5 C, cold soak time: 13 hrs., startability condition: started easily.

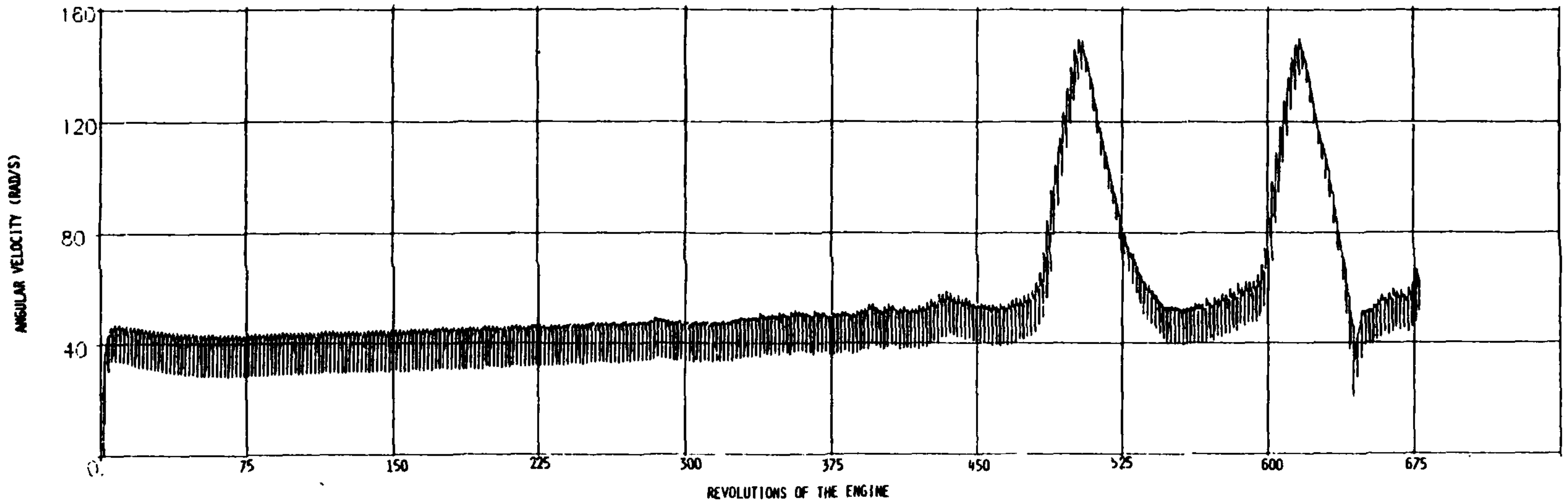

Fig. 28 Plot of angular velocity vs. engine revolutions, Fuel: DF 2, oil:arctic oil, ambient temperature: -8 C, cold soak time: 12 hrs., startability condition: with difficulty.

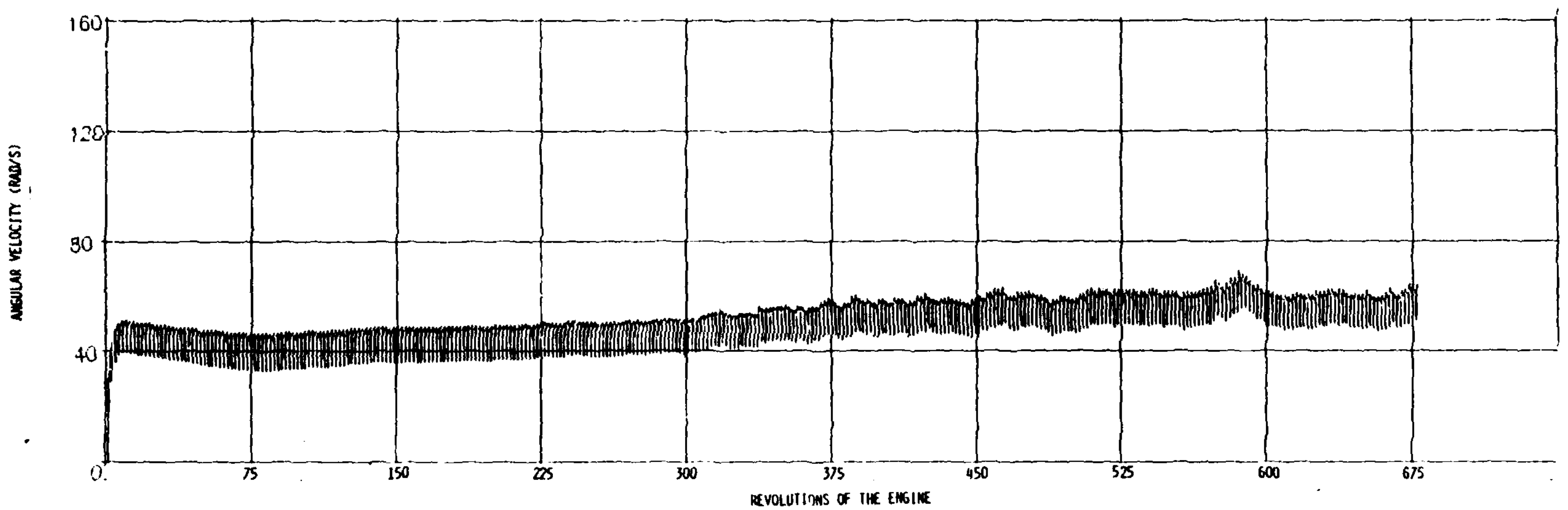

Fig..29 Plot of angular velocity vs. engine revolutions, fuel: DF 2, oil:arctic oil, ambient temperature:-10 C, cold soak time:5 hrs., startability condition: did not start.

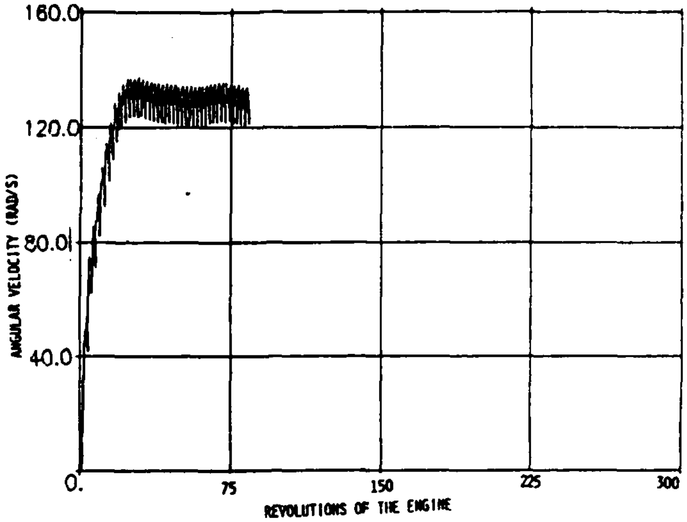

Fig. 30 Plot of angular velocity vs. crank angle , fuel: JP 4 oil:arctic oil, cold soak time: 12 hrs, ambient temperature: 25 C, startability condition: started easily.

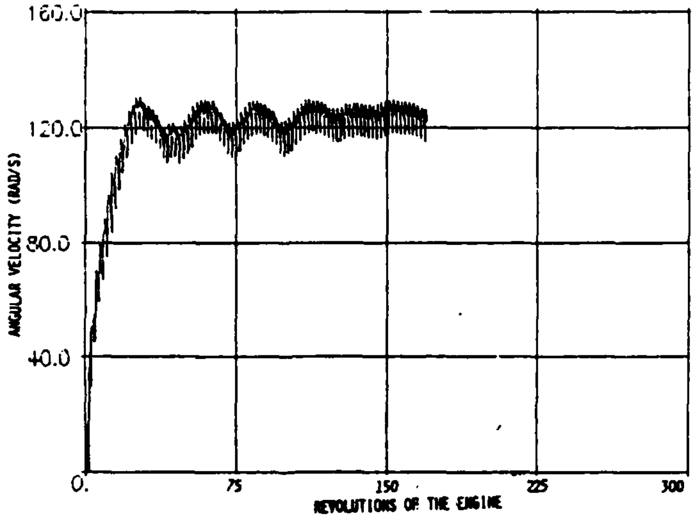

Fig. 31 Plot of angular velocity vs. crank angle, fuel: JP4, oil: arctic oil, cold soak time: 6 hrs., ambient temperature:10 C, startability condition: started easily.

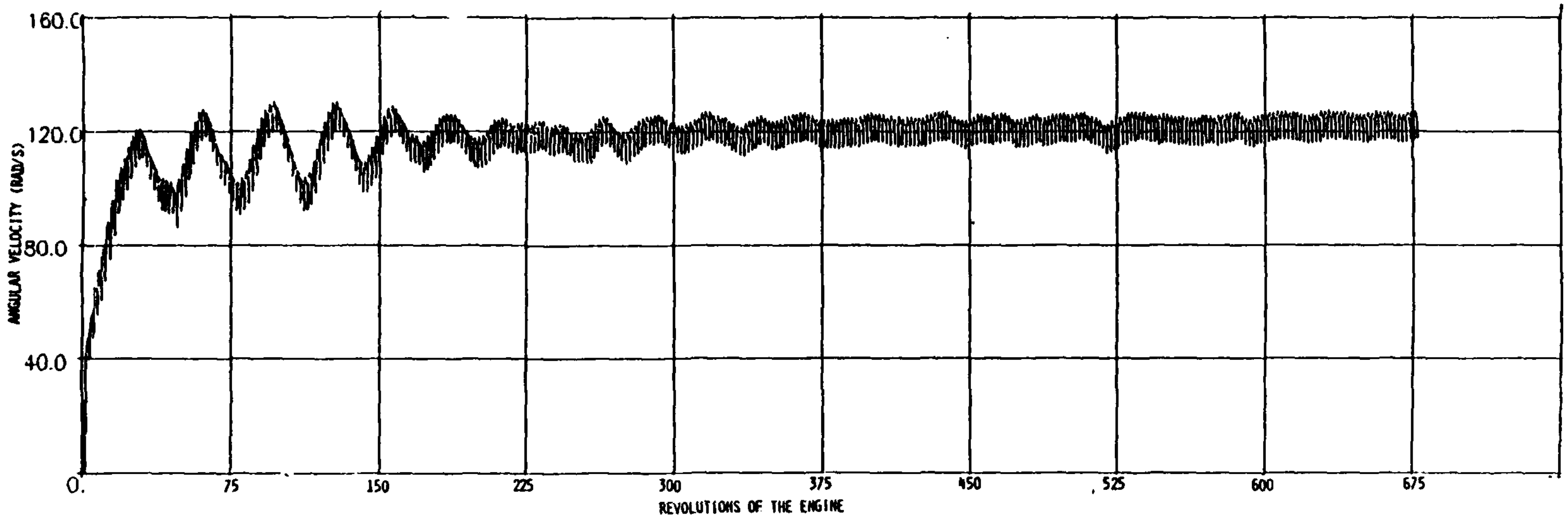

Fig. 32 Plot of angular velocity vs. crank angle, fuel: JP4 oil: arctic oil, cold soak time:5hrs., ambient temperature: 5 C, startability condition: started easily.

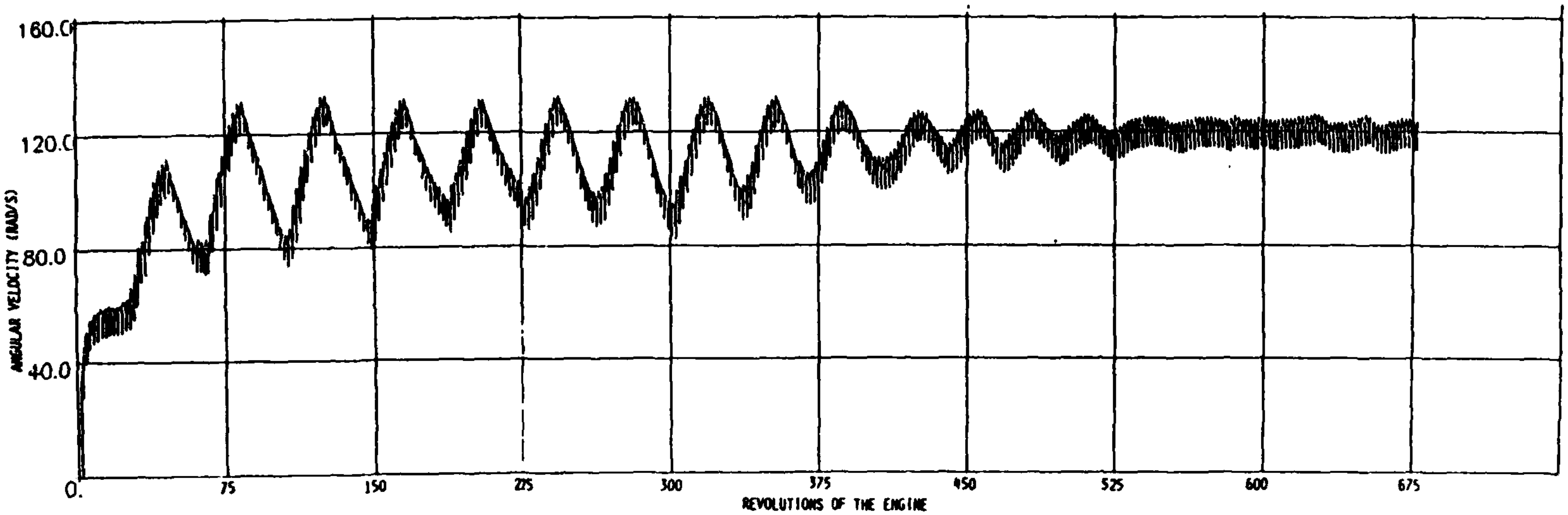

Fig. 33 Plot of angular velocity vs. crank angle fuel, JP4 oil:arctic oil: cold soak time: 12 hrs., ambient temperature: 0 C, startability condition: started easily.

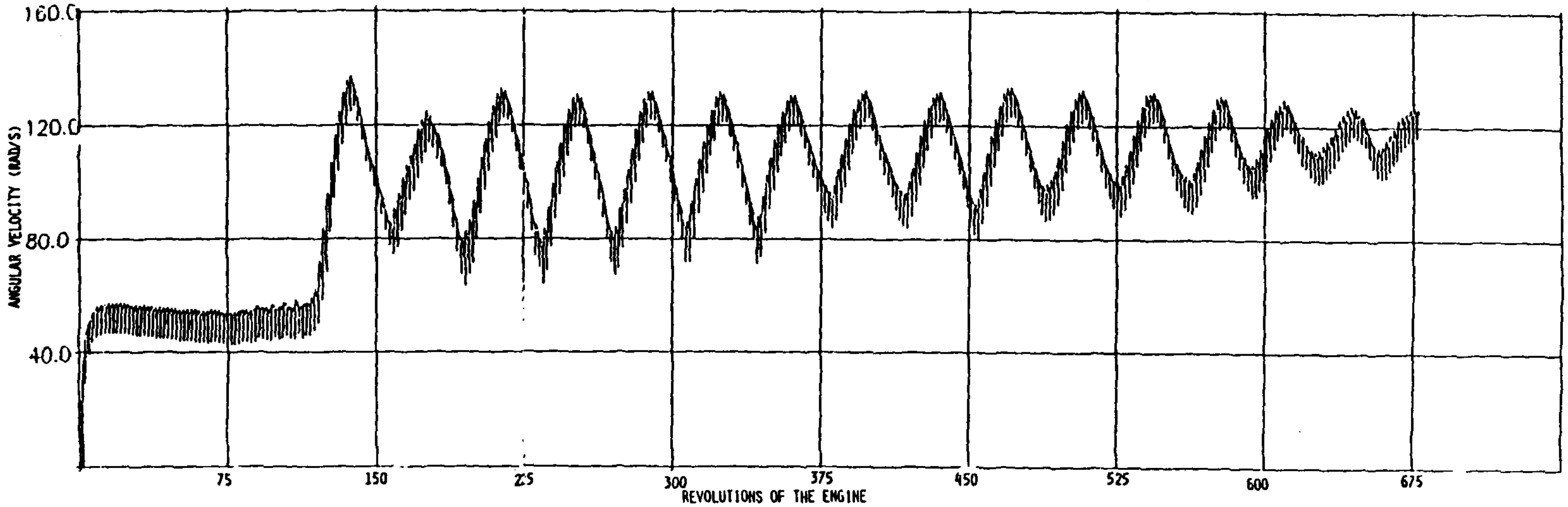

Fig. 34 Plot of angular velocity vs. crank angle, fuel: JP4, oil:arctic oil, cold soak time: 5½ hrs., ambient temperature:-5 C, startability condition: started easily.

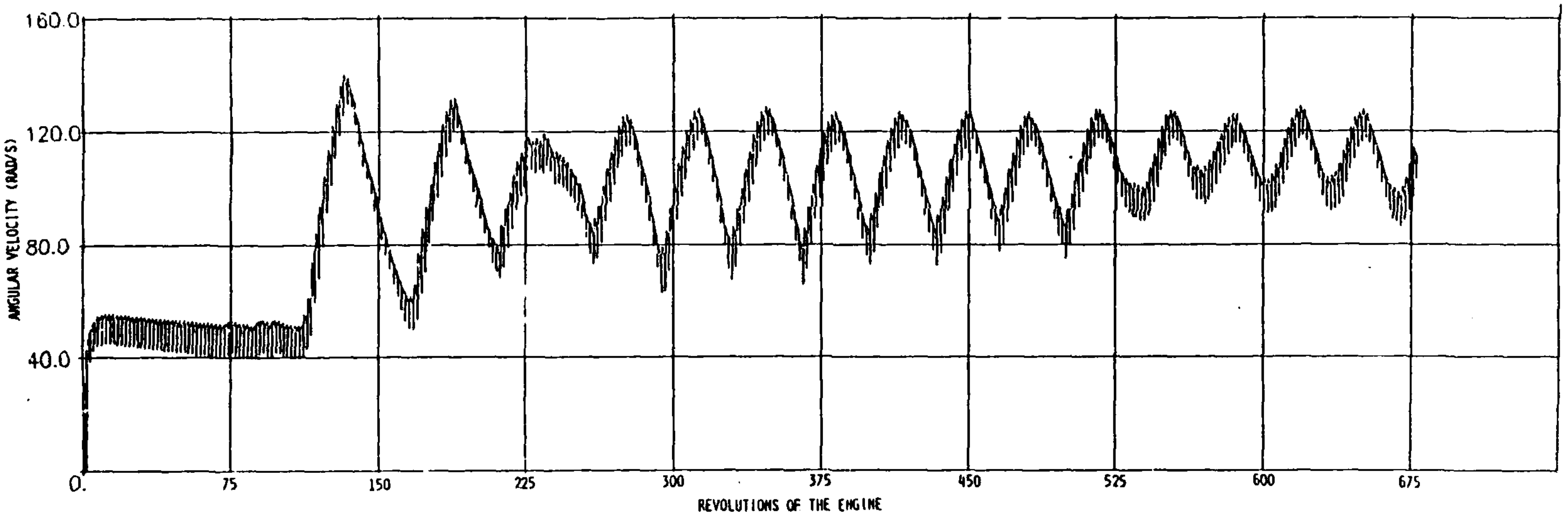

Fig. 35 Plot of angular velocity vs. Crank angle, fuel: JP4, oil: arctic oil, cold soak time:6 hrs., ambient temperature:-6 C, startability condition: started easily.

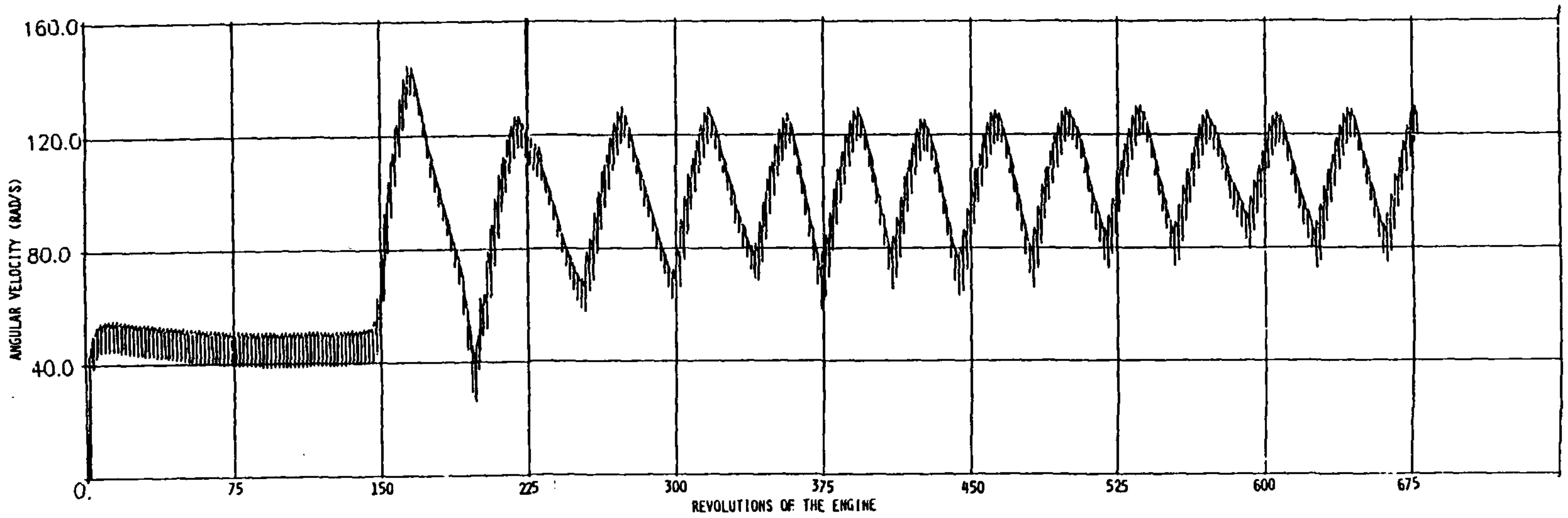

Fig. 36 Plot of angular velocity vs. crank angle, fuel: JP4, oil:arctic oil, cold soak time: 6 hrs., ambient temperature:-8 C, startability condition: started easily.

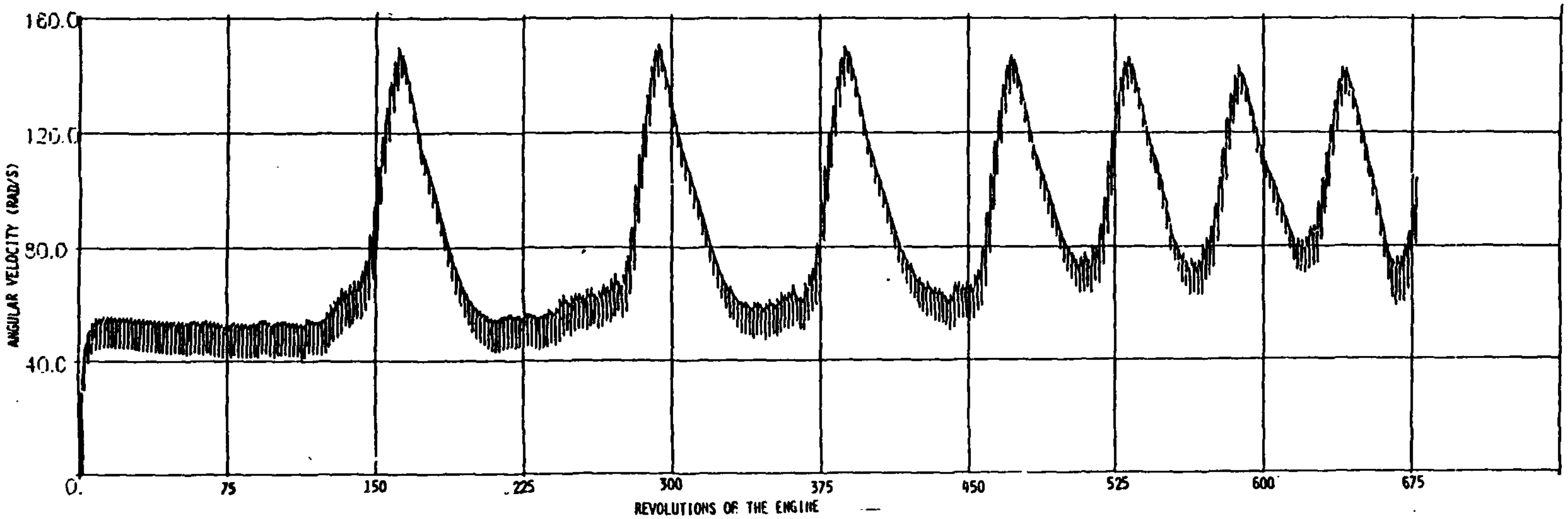

Fig. 37 Plot of angular velocity vs. crank angle, fuel: JP4 oil:arctic oil, cold soak time:5½hrs., ambient temperature:-9 C, startability condition: started easily.

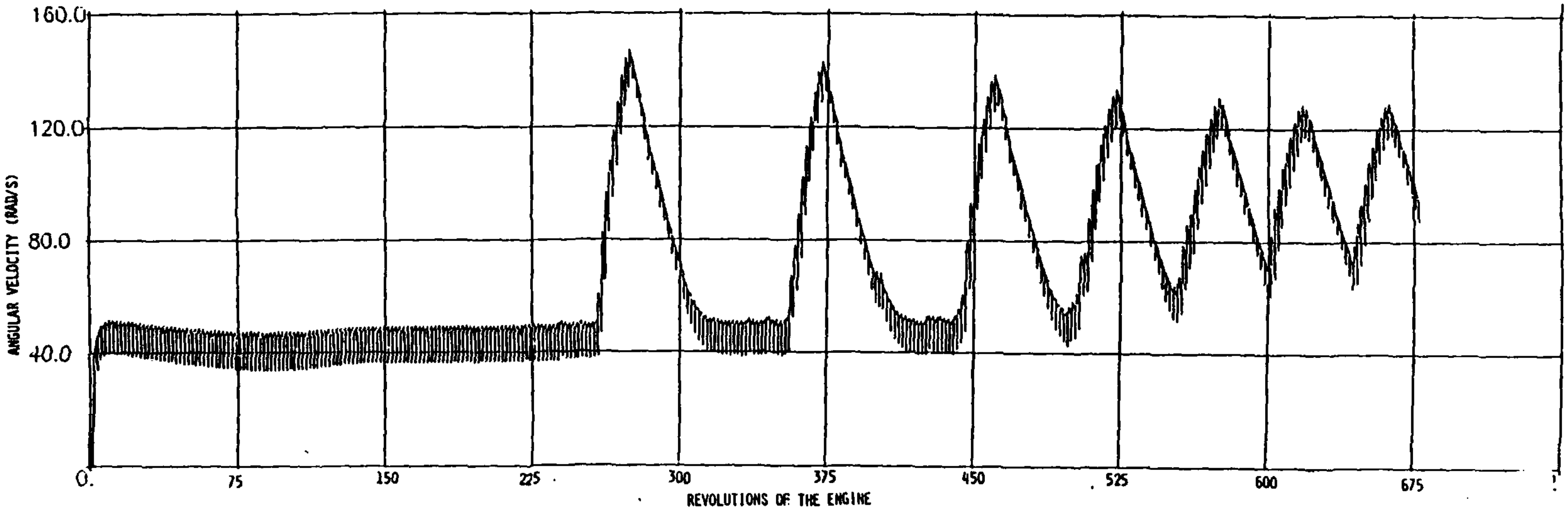

Fig. 38 Plot of angular velocity vs. crank angle, fuel: JP4, oil: arctic oil, cold soak time: 7½hrs., ambient temperature:-10 C, startability conditions: started with difficulty.

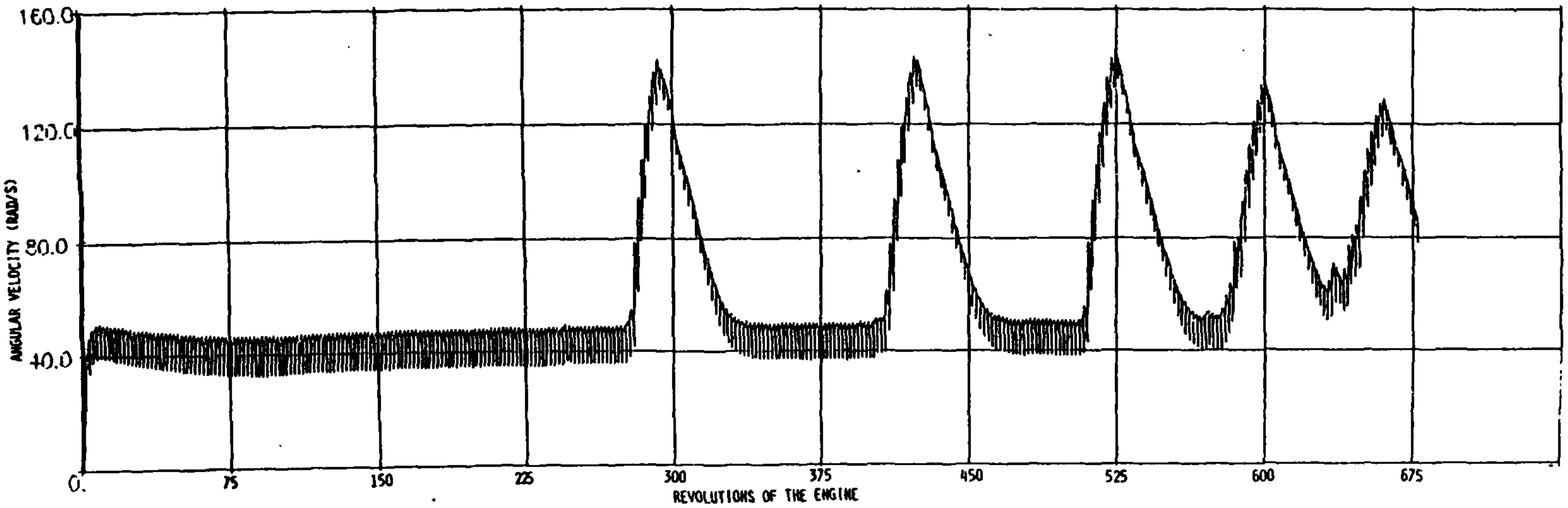

Fig. 39 Plot of angular velocity vs. crank angle, Fuel: JP4, oil: arctic oil, cold soak time: 6 hrs., ambient temperature: -11 C, startability condition: started with difficulty.

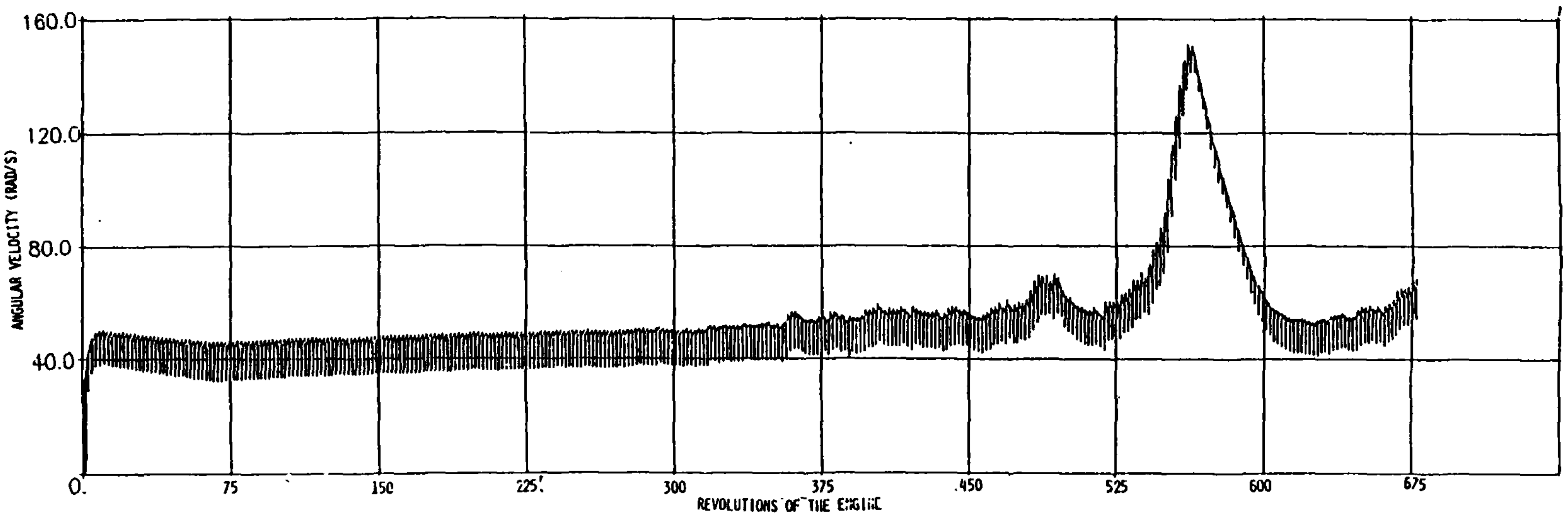

Fig. 40 Plot of angular velocity vs. crank angle, Fuel: JP4, oil: arctic oil, cold soak time:8hrs., ambient temperature: -13 C, startability condition: failure to start.

Fig 27 is for an ambient temperature of -5°C and Fig 28 is for an ambient temperaute of -8°C. By comparing the two figure it is clear that the drop in ambient temperature resulted in a decrease in the cranking speed, an increase in the cranking period, and an increase in the amplitude of the oscillations. Fig 29 is for an ambient temperature of -10°C. The engine failed to start even after cranking for 675 revolutions. Fig 30 is for engine startability with JP-4 at an ambient of 25°C and cold soak time of 12 hours. The engine started quickly and accelerated to 137 radians per second in 20 revolutions. Fig 31 is for JP-4 and an ambient temperature of 10°C. Fig 32 is for an ambient temperature of 5°C. Fig 33 is for an ambient temperature of 0°C. Fig 34 is for an ambient temperature of -5°C. Fig 35 is for an ambient temperature of -6°C. Fig 36 is for an ambient temperature of -8°C. Fig 37 is for an ambient temperature of -9°C. Fig 38 is for an ambient temperature of -10°C. Fig 39 is for an ambient temperature of -11°C. Fig 40 is for an ambient temperature of -13°C

COMPARISON BETWEEN STARTABILITY ON DP-2 AND JPA:

Fig 41 is a plot of the engine revolutions from the beginning of cranking to the time the engine reached its maximum starting speed, at different ambient temperatures. The difference between DF-2 and JP-4 is negligible at normal ambient temperatures. As the ambient temperature drops the difference between the two fuels increases. The engine failed to start on DF-2 after cranking the engine for 675 revolutions, at an ambient temperature of -10°C. At the same ambient temperature the engine successfully started on JP-4 after cranking for 270 revolutions. The engine did not fail to start on JP-4 at ambient temperatures down to -13°C.

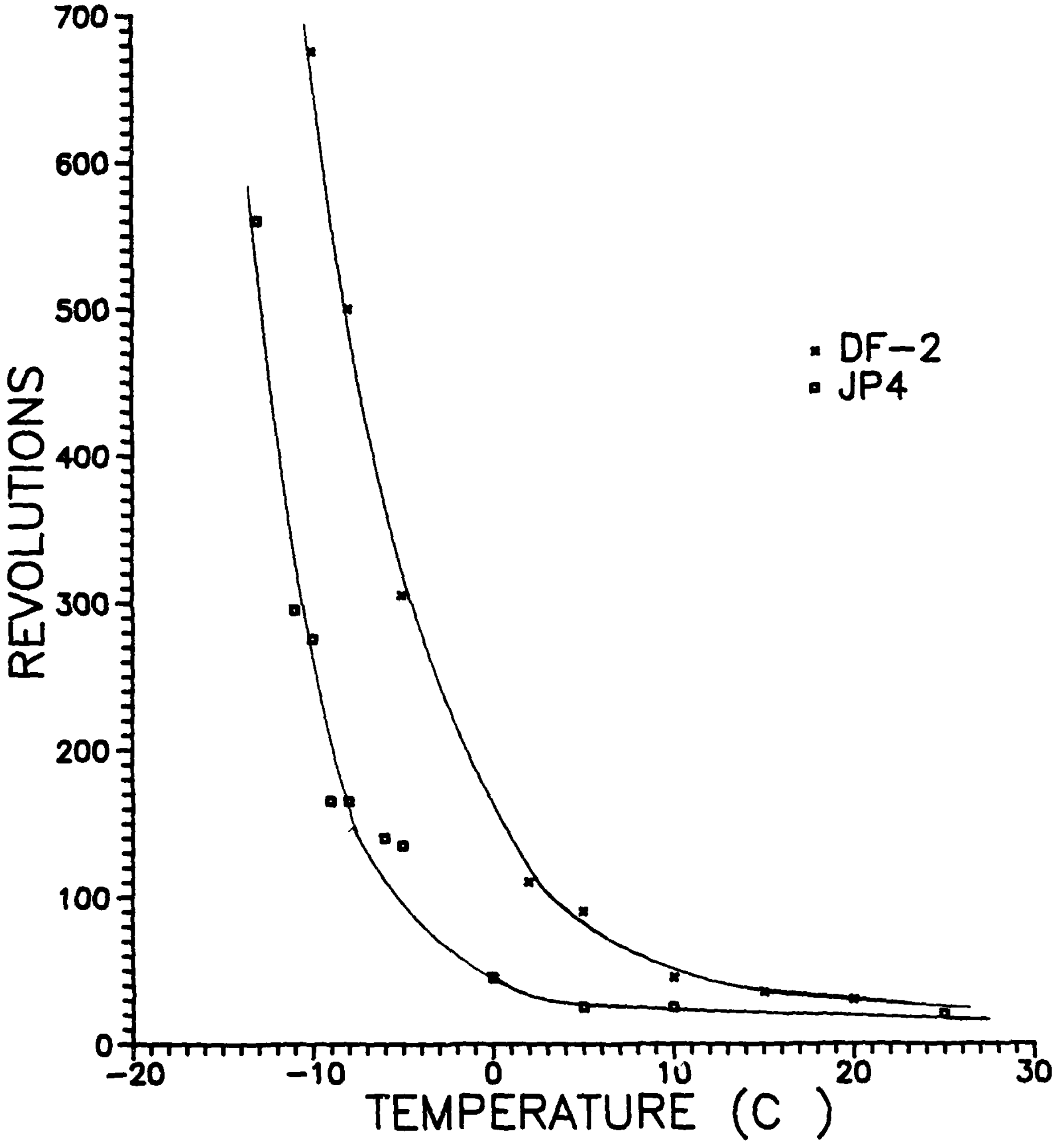

Fig. 41 Comparison between the engine revolution to maximum starting speed on DF 2 and JP4 fuels.

It is clear that JP-4 is more volatile than DF-2. However the Cetane number of JP-4 is less than DF-2.

The experimental results indicate very clearly that the fuel volatility plays a major role in the formation of the combustible mixture which is ready for autoignition at the low ambient temperatures. Since the Cetane number is determined, according to ASTM D-613 method, at hot air and engine temperatures it does not reflect the effect of fuel volatility.

It can be concluded that the C.N. alone cannot rate the autoignition characteristics of the fuel at air and engine temperatures lower than those used in the ASTM D-613 method. These temperatures are 150°F for inlet air temperature and 220°F for the engine coolant temperature. These temperatures do not represent at all the conditions during cold starting.

SECTION 4

EFFECT OF FUEL VOLATILITY ON AUTOIGNITION AND COMBUSTION AT LOW AMBIENT TEMPERATURES

The effect of fuel volatility on the ignition delay was investigated in a single cylinder research diesel engine, under steady state running conditions. The tests were conducted at low room temperatures. The ignition delay was measured. The ambient temperature was lowered till the engine misfired. A comparison was made between the misfiring temperatures and ignition delays of fuels having equal cetane numbers but of different volatilities. The low volatility fuels were composed by blending primary reference fuels so that they have cetane numbers equal to those of distillate fuels. The primary reference fuels are cetane ($C_{16}H_{34}$) and heptamethylnonane ($C_{16}H_{34}$). Cetane has a C.N. of 100 and heptamethylnonane has a C.N. of 15.

4.1 ENGINE

The engine is the ATAC.IH.LABECO single cylinder, direct injection diesel engine, 4.5x4.5 in, C.R.=16:1. The engine is coupled to a General Electric D.C. Motor/Generator Cradle type dynamometer. The dynamometer is provided with a speed and load control and a tachogenerator for measuring the speed. The intake and exhuast sides were connected to two steel surge tanks of 3 cubic feet capacity each in order to reduce pulsations on the measuring system.

4.2 INSTRUMENTATION

Figure 42 shows the layout of the equipments and general instrumentations. Intake air is taken from the cold room, which has vents to allow for the make-up air to flow into the room and be cooled before it reaches the intake air filter. A butterfly valve, remotely controlled, is used to control the air pressure in the intake system. The air pressure is adjusted so that the mean pressure during the ignition delay period is kept constant for all the runs. The flow rate was measured by a Meriam Laminar Flowmeter (50MW20-2), which is installed before the intake surge tank. The pressure differential across the flowmeter is measured by an inclined manometer with a scale division of 0.01 inch. The flowmeter was calibrated by the manufacturer. A Kistler (601B-SN 2922) quartz pressure transducer is installed in the cylinder head of the engine to measure the cylinder pressure. The signal from the transducer is amplified by a Kistler 504E charge amplifier. This signal is then fed to the voltage channel of the Textronix 565 oscilloscope, and

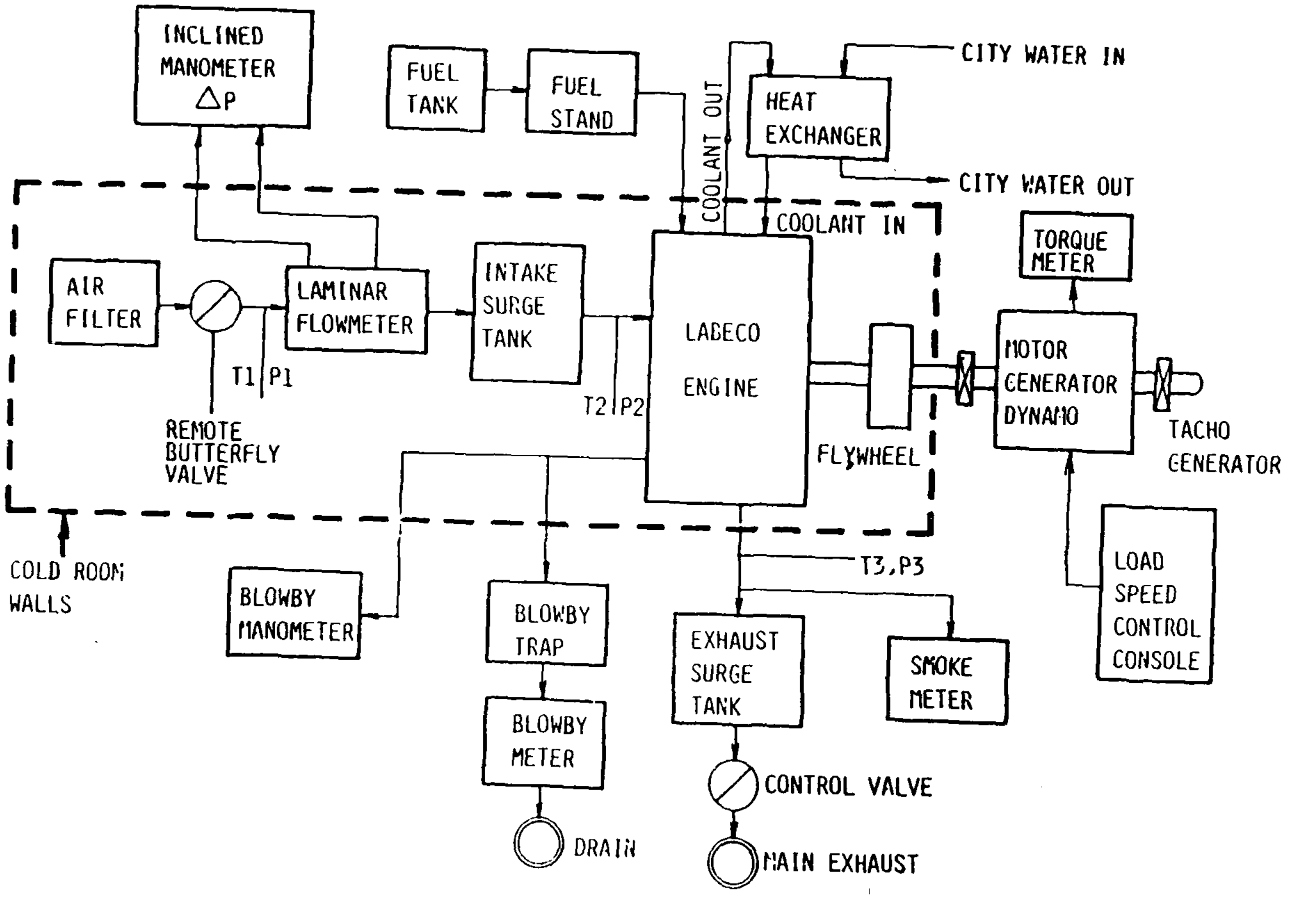

Figure 42 Layout of Experimental Setup

fed to a peak meter, in order to measure the peak cylinder pressure. The pressure transducer was statically calibrated using a dead weight tester machine, over a range 0-1500 psi.

Fig 43 shows the schematic of the electronic instrumentation used, to measure the needle lift of the injector, the triggering circuit, the injection pressure transducers and the pickup used to indicate the crank angle degrees.

4.3.1 MISFIRING TEMPERATURE

The misfiring temperatures for distillates and blend of primary reference fuels are:

DF2 (CN=45.5, distillate) : no misfiring was found at -32°c

Ref. 1 (CN=27.8, distillate) : -28°c

Ref. 2 (CN=30.0, distillate) : -26°c

JP4 (CN=35.0, distillate) : -27°c

CN=45.5 (blend) : -9°c

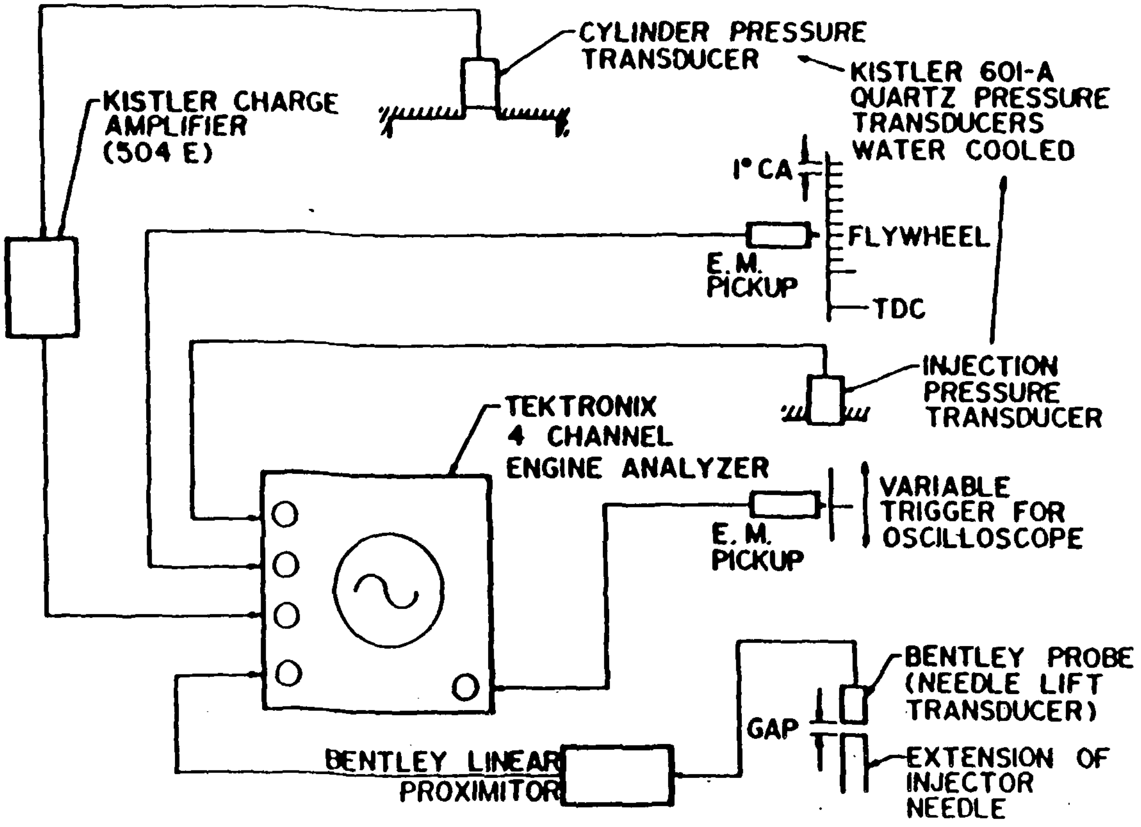
CYLINDER PRESSURE TRANSDUCER
KISTLER 601-A QUARTZ PRESSURE TRANSDUCERS WATER COOLED
KISTLER CHARGE AMPLIFIER (504 E)
1° CA
FLYWHEEL
E.M. PICKUP
TDC
INJECTION PRESSURE TRANSDUCER
TEKTRONIX 4 CHANNEL ENGINE ANALYZER
VARIABLE TRIGGER FOR OSCILLOSCOPE
E. M. PICKUP
BENTLEY PROBE (NEEDLE LIFT TRANSDUCER)
GAP
EXTENSION OF INJECTOR NEEDLE
BENTLEY LINEAR PROXIMITOR

Figure 43 Schematic of Electronic Instrumentation (Reference 12)

AD-A189 730 CETANE SCALE EVALUATION AND POSSIBLE MODIFICATION(U) 2/2
WAYNE STATE UNIV DETROIT MI CENTER FOR AUTOMOTIVE
RESEARCH N A HENEIN 23 DEC 87 ARO-21397.2-EG
UNCLASSIFIED DAAG29-84-K-0164 F/G 21/4 NL

END
DATE
FILMED
4 88

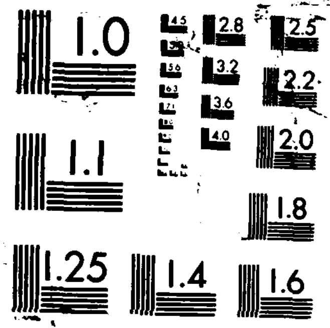
1.0
4.5
5.6
6.3
2.8
2.5
3.2
2.2
3.6
4.0
2.0
1.1
1.8
1.25
1.4
1.6

CN=27.8 (blend) : -10°c

CN=30.0 (blend) : -10°c

CN=35.0 (blend) : -14°c

Figure 44 shows the above results and indicates that the misfiring temperature of distillates is lower than that of the fuel blends. Because all the fuel blends in this research work were formed from N-Cetane (CN=100) and Heptamethylnonane (HMN, CN=15), they are less volatile than the distillates. This difference in volatility causes the large difference in their misfiring temperatures.

4.3.2 IGNITION DELAY

The effect of inlet air temperature on the ignition delay period of distillates and blends of primary reference fuels was studied. Figure 45 shows that the ignition delay periods of blended fuels are higher than those of distillated fuels, while they have the same cetane number.

Figure 46 shows variation of ignition delay with cetane number at different ambient air temperatures.

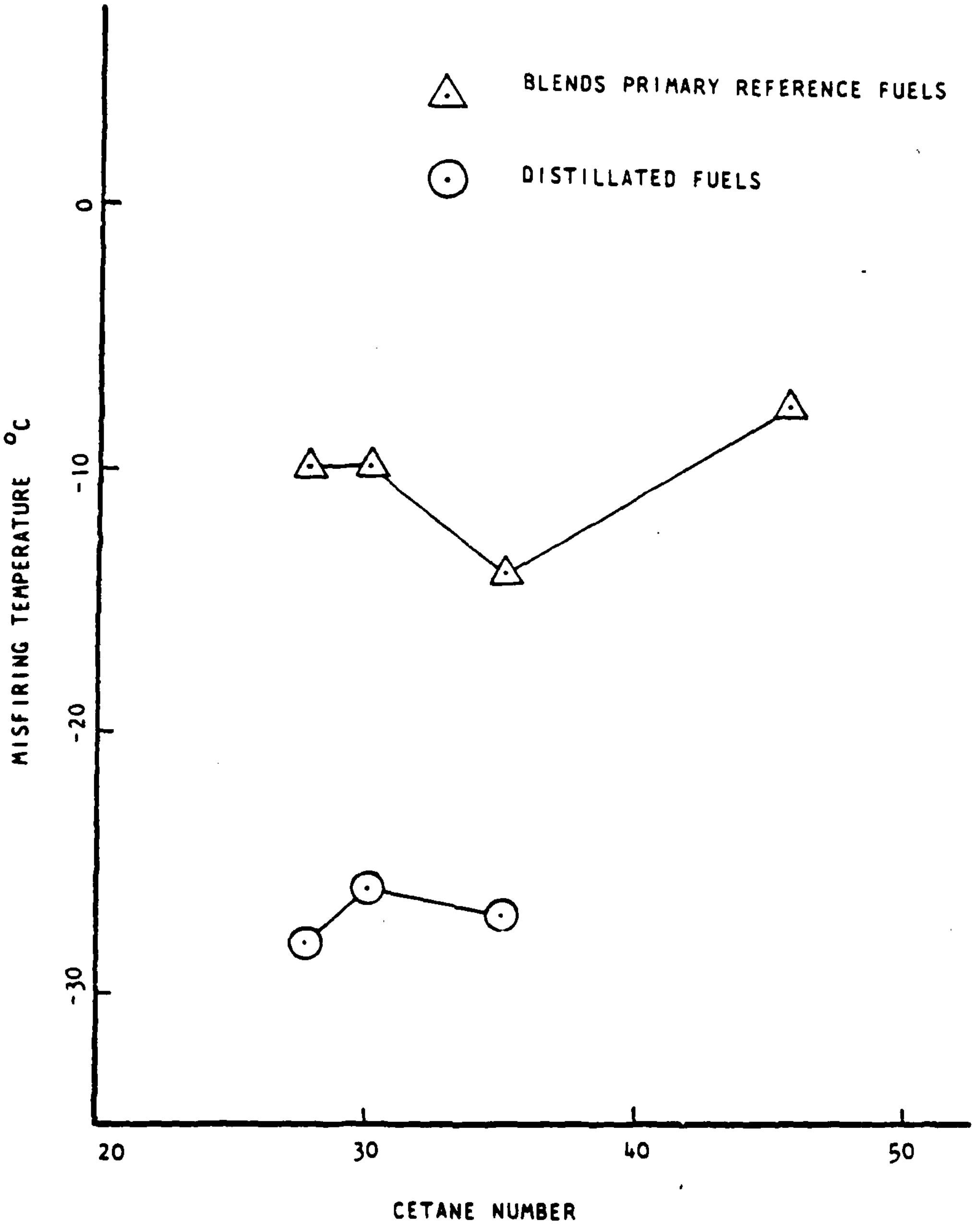

Figure 44 Variation of Misfiring Temperature with Cetane Number for Distillated and Blend Fuels

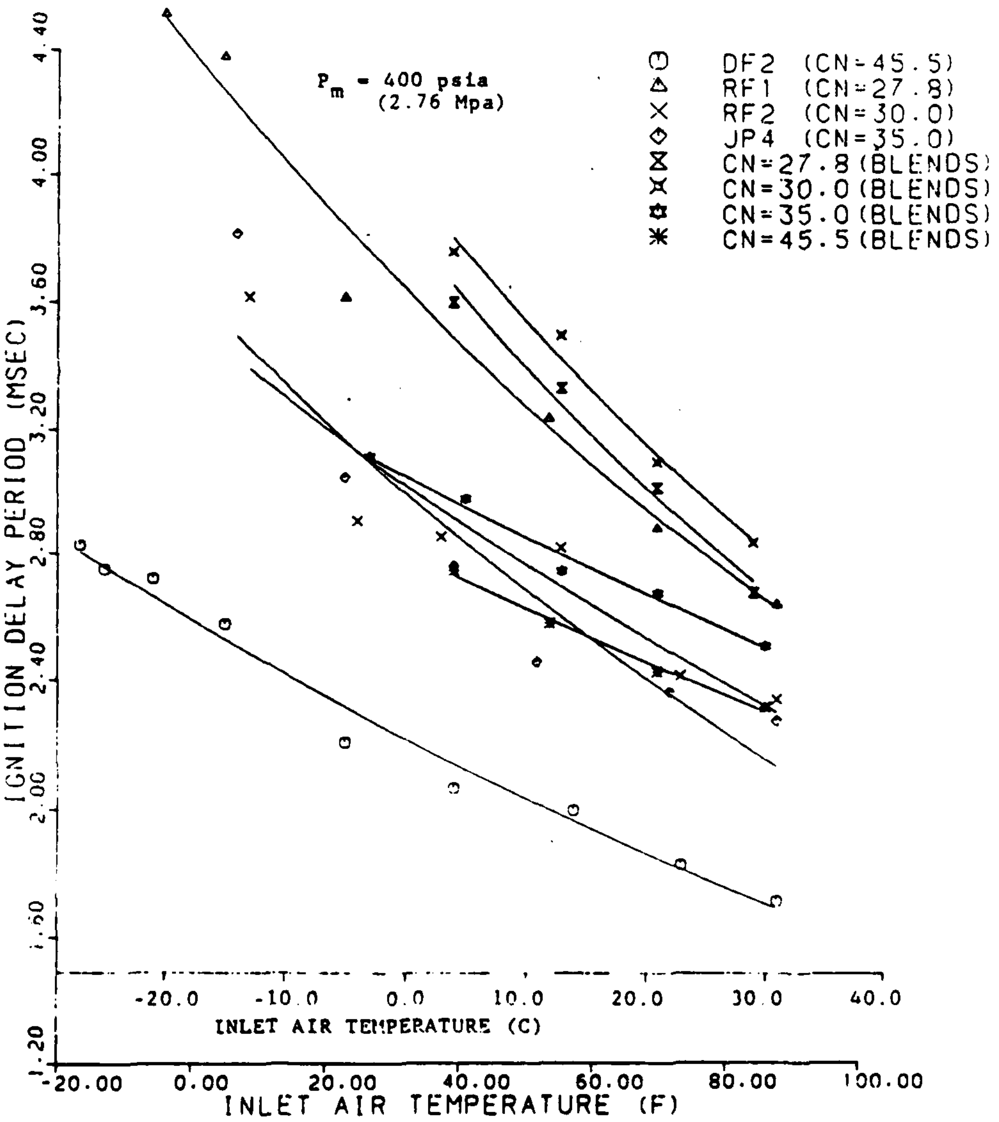

Figure 45 Variation of Ignition Delay Period with Inlet Air Temperature at Pm=400 psia (2.76 MPa), for Distillated and Blend Fuels

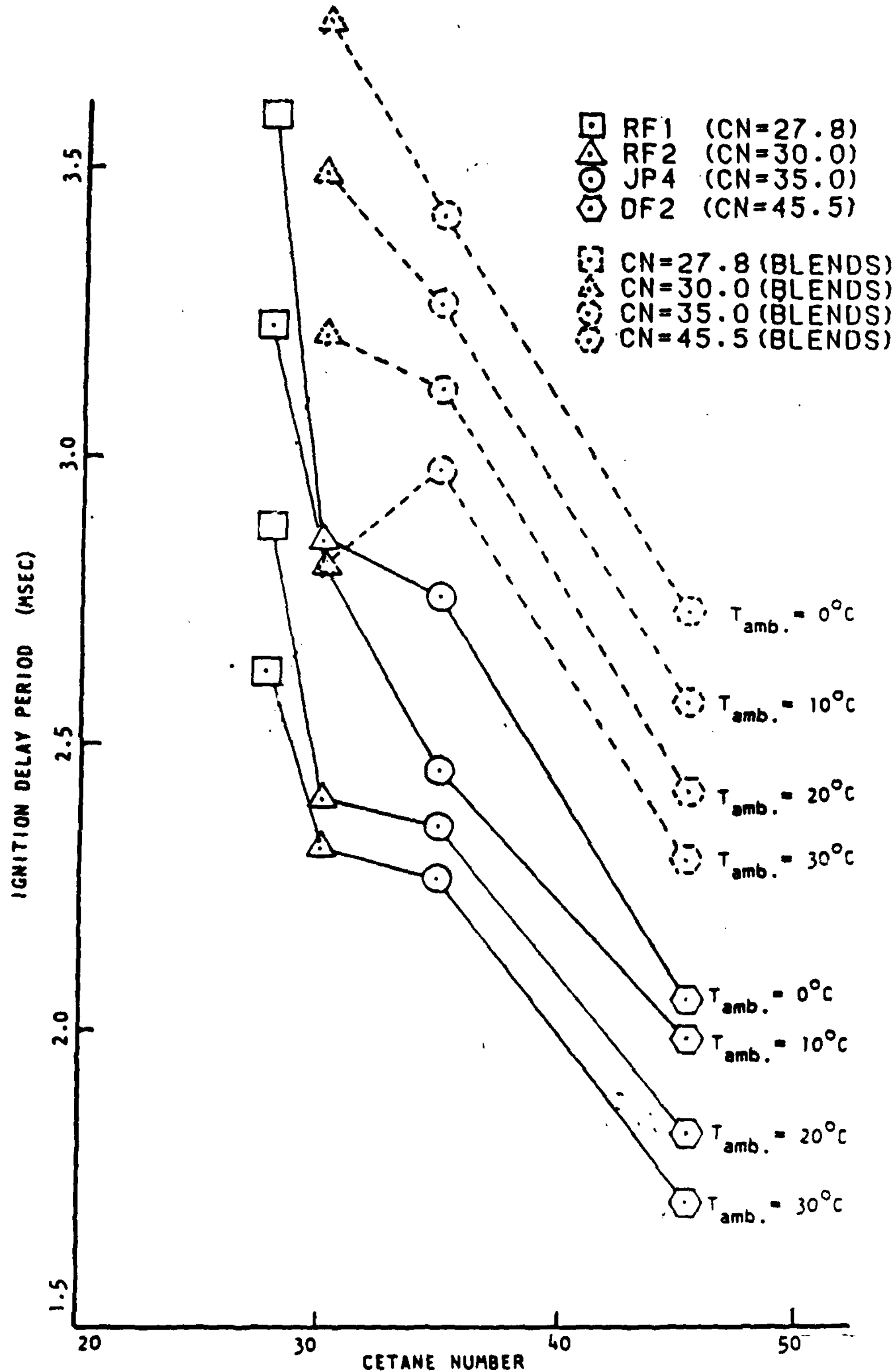

Figure 46 Variation of Ignition Delay Period with Cetane Number at Different Ambient Temperature (distillated and blend fuels)

The ignition delay period for distillates are lower than the ignition delay for the blends, both having the same cetane number.

4.4 CONCLUSIONS

This analysis clearly indicates that the cetane number of the fuel is not the only parameter which affect the autoignition process in diesel engines, particularly at low ambient temperatures. The shorter delay of the distillates and lower their misfiring temperature compared with the blends of primary reference fuels, both having the cetane number, support the above conclusion.

SECTION 5

MATHEMATICAL MODEL FOR ENGINE STARTABILITY

A mathematical model has been developed to predict the behavior of the engine during the cranking and starting process. The model will be presented in a paper in the SAE Annual Congress to be held in Detroit, Mi., February, 1978. The paper is duplicated in this section.

DIESEL STARTING: A MATHEMATICAL MODEL

Timothy P. Gardner
Ford Motor Company

Naeim A. Henein
Wayne State University

ABSTRACT

A mathematical model is developed to study the transient behavior of a four-stroke, single cylinder naturally-aspirated, DI diesel engine during cranking and starting. The model simulates the full thermodynamic cycle of the engine and includes detailed sub-models for the intake and exhaust gas flow processes, autoignition combustion, heat transfer, mechanical friction, blowby, and engine dynamics. The model considers the period of time from starter on until the engine reaches the idle speed.

Experimental data and results obtained from the engine are used to calibrate and validate the model. A comparison of results from the model and the experiments generally show good agreement for the starting conditions investigated.

MANY FACTORS CONTRIBUTE to the successful starting of diesel engines. In the absence of a positive ignition source in the diesel engine, the initiation of combustion is mainly temperature dependent. The air temperature near the end of compression, in turn, depends on the compression ratio and other engine operating conditions such as inlet air temperature and cranking speed. During cranking, the compressed air temperatures are lower than those during any other mode of engine operation. The low compression temperatures are caused partly by the low ambient temperature, and more importantly by the excessive heat losses between the cylinder gases and the walls and by the excessive blowby losses at the low cranking speeds. Consequently, the low compression temperatures result in poor ignitibility of the fuel, and hence, poor startability of the engine.

Most engine designers agree that starting requirements set the lower limit on the range of compression ratios used in diesel engines. Therefore, a model which could predict the minimum CR at the design stage, which would eventually lead to a successful start, would be of considerable interest to the designer.

This paper describes a general mathematical model of a naturally-aspirated, direct-injection (DI) diesel engine which can be used to investigate the effects of compression ratio, ambient temperature, fuelling rate, etc. on the starting process. The model simulates a full thermodynamic cycle in which cylinder pressure, temperature, equivalence ratio, etc. are calculated along with engine friction to determine the final compression temperatures in the cylinder as well as the engine cranking speed during starting. The model also calculates the instantaneous heat losses, blowby losses, and frictional losses during the starting process.

LITERATURE REVIEW

Many mathematical models have been developed to simulate the fluid mechanics and thermodynamic processes in internal combustion engines [1-11]. These models can be grouped into two broad categories; 1) steady-state models, and 2) unsteady-state or transient models.

In steady-state models, the engine speed, fuel rate, and load are usually held constant over the entire cycle. By definition, steady state operation requires that the conditions at the end of the cycle must equal those at the beginning. This criteria is used to obtain an energy balance.

In transient models, thermodynamic and gas flow processes are usually simulated by using one of two approaches. The first is a quasi-linear approach, in which empirical relationships are used for engine thermodynamics and gas flow. These are linked with dynamic models of the mechanical components [10]. The major disadvantage of quasi-linear models is their heavy reliance on experimental data which limits the usefulness of this approach. The second is a quasi-steady approach, in which engine thermo and fluid dynamics are treated on a quasi-steady basis employing the "filling and emptying" concept [4,7]. By using the quasi-steady approach, one can calculate the steady, or transient phenomena occuring in the engine regardless of its operating conditions. However, the formulation and solution procedure must be different than that used in steady models since the periodicity condition (constant speed) does not hold during transient operation.

Most filling and emptying models for diesel transient analysis reported in the literature have been used to calculate the performance characteristics of turbocharged diesel engines under changing speed or load, or to match the turbocharger to a new or uprated engine design. The authors know of no one who has applied the filling and emptying models to study the transient behavior of diesel engines during initial cranking and starting. Since the basic assumptions used in quasi-steady models are applicable to any operating condition in the engine, an attempt is made to use these models to develop a general model for engine startability and to investigate the effects of various design and operating parameters on the starting process of diesel engines.

The primary difference between the present filling and emptying model and some of the other models published in the literature is in the detailed treatment of the friction losses and blowby losses, which are particularly important during the cranking and starting process. Instantaneous values of friction and blowby losses, rather than cycle averaged values, are calculated along with instantaneous heat losses. The inclusion of these calculations in the filling and emptying model allows a more detailed investigation of the effects of various design and operating parameters on these losses, as well as provide additional insights into how these parameters affect engine startability.

CRITERIA FOR ENGINE STARTABILITY

The fact that ignition occurs in the combustion chamber does not necessarily mean that the engine will successfully start. Marginal conditions in the combustion chamber may result in partial ignition or even misfire, which may prevent the engine from starting. Therefore, a criteria must be established in the model for evaluating the startability of the engine.

A number of different methods have been used in experimental studies to evaluate engine startability. These methods are based on; 1) required cranking time, 2) time to start of combustion, 3) cranking torque & smoke measurements, 4) time-to-starter off, and 5) time-to-idle speed. The authors believe that the time-to-idle speed method is the most reliable, and the most repeatable of these methods, and hence, is adopted for the starting criteria in the present model.

MODEL FOR STARTING

The starting model used in this study is shown schematically in Figure 1. Initially, the engine is assumed to be at rest. Starting consists of cranking the engine while fuelling with the starter motor on until ignition occurs and the engine accelerates to an arbitrarily set cranking speed. The starter motor torque is then turned off, and the engine continues to accelerate with the aid of the gas pressure torque until it reaches its idling speed to complete the starting process. The starting attempt is considered to be successful if ignition occurs while cranking with fuelling, and the engine is able to accelerate, with no assistance from the starting motor, to its idle speed within a specified time. If ignition does not occur and/or the engine fails to reach its idle speed within a specified time (or number of cycles), the starting attempt is considered unsuccessful.

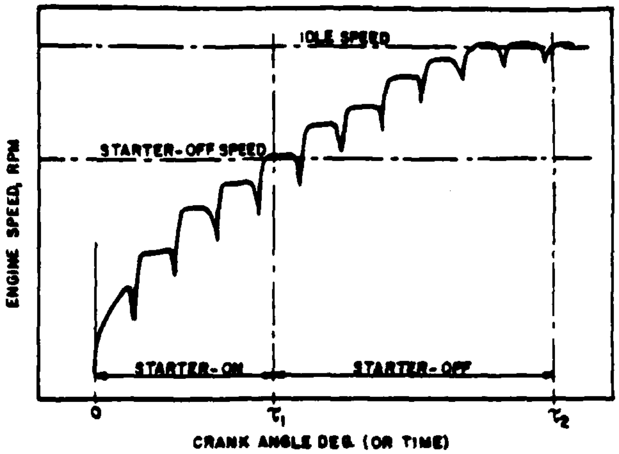

Figure 1 - Model for Starting Process

MATHEMATICAL FORMULATION

The mathematical formulation of the model is derived by applying the thermodynamic principles to the three control volumes shown in Figure 2; 1) the cylinder, 2) the intake manifold, and 3) the exhaust manifold. Heat, work and mass transfer across the control surfaces of these control volumes are calculated. The basic approach used to derive the governing equations for each control volume is to apply an energy balance, then combine the thermodynamic property relationships, and the mass continuity equation to obtain the final equations.

The rate of change of gas temperature with respect to time dT/dt, can be expressed in the form of an ordinary differential equation developed by Borman [3] as;

$$\frac{dT}{dt} = \frac{A - P\frac{\partial u}{\partial P}\left[\frac{1}{M}\frac{dM}{dt} - \frac{1}{V}\frac{dV}{dt} - \frac{1}{R}\frac{\partial R d\Phi}{\partial \Phi dt}\right] - \frac{\partial u d\Phi}{\partial \Phi dt}}{\frac{\partial u}{\partial T} + \frac{\partial u}{\partial P}\frac{P C}{T D}} \quad (1)$$

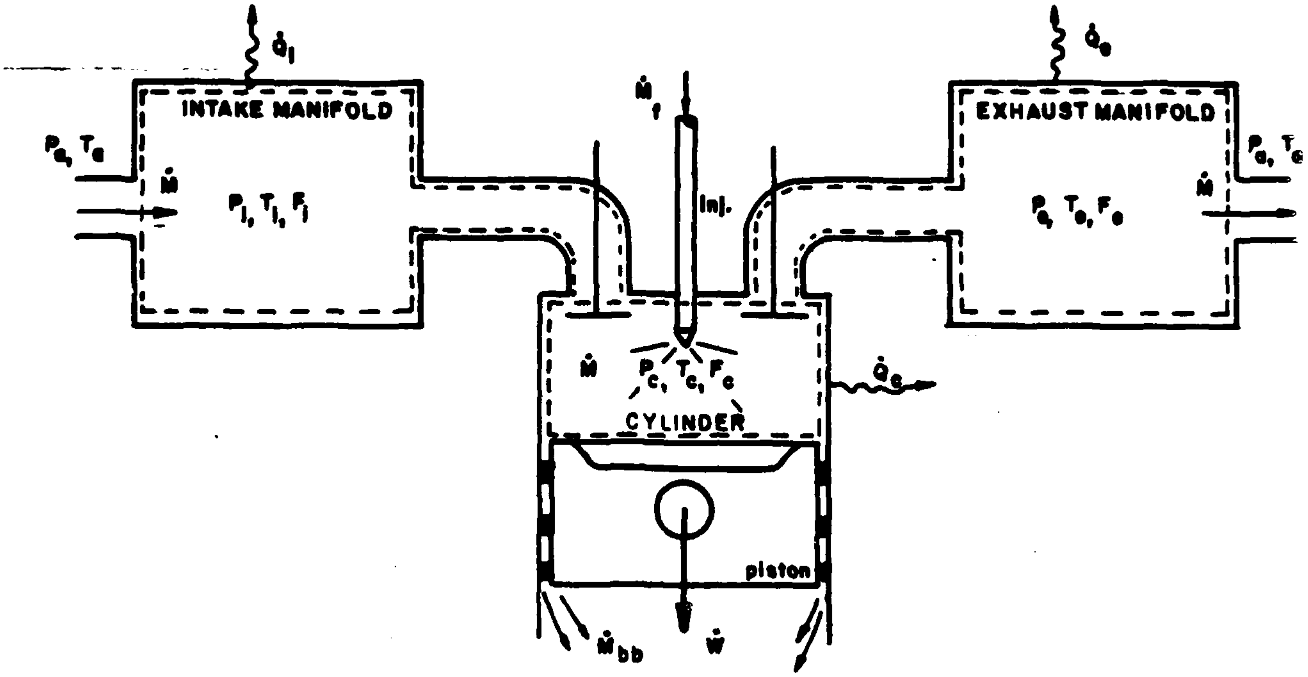

Figure 2 - Engine Thermodynamic System

where,

$$A = \frac{-RT}{V}\frac{dV}{dt} + \left[\Sigma\frac{dQ}{dt} + \Sigma\frac{h\,dM}{dt} - \frac{u\,dM}{dt}\right]\frac{1}{M}$$

$$C = 1 - \frac{T}{R}\frac{\partial R}{\partial T}$$

$$D = 1 - \frac{P}{R}\frac{\partial R}{\partial P}$$

Equation (1) is the basic form of the energy equation that is applied to each control volume at each instant, together with the continuity equation, and the perfect gas equation. All of the partial derivatives in Eq.(1) can evaluated from the gas property relationships which are of the form:

$u = u(P, T, \Phi)$
$R = R(P, T, \Phi)$

The rate-of-change of mass in the cylinder, dM/dt, obtained by considering the rates of flow through the intake and exhaust valve, fuel injection, and blowby past the piston rings:

$$\frac{dM}{dt} = \frac{dM_i}{dt} - \frac{dM_e}{dt} + \frac{dM_f}{dt} - \frac{dM_b}{dt} \qquad (2)$$

All values of enthalpy and internal energy used in the model are defined on the basis of one absolute reference state using the definition for absolute enthalpies given by Powell [34]. The absolute enthalpy of the pure fuel is calculated from the known enthalpy of combustion and the sensible enthalpy of the fuel according to:

$$h_f = h_f + Cp\,dt \qquad (3)$$

where,

h_f = the enthalpy of formation from the elements (at T=0 °K ,and P=1 atm)
Cp = the specific heat of the fuel.

The volume, V, and rate-of-change of volume, dV/dt, for the cylinder can be calculated from the engine geometry and speed according to [37] :

$$V = V_c + \pi D^2 S/4 \qquad (4)$$

$$S = r\,[1 - \cos\theta + L/r\,(1 - \sqrt{1 - r\sin^2\theta/L^2}\,]$$

$$\frac{dV}{dt} = \frac{\pi N D^2}{120}\frac{dS}{d\theta}$$

$$= \frac{N D^2}{120}\,r\sin\theta \quad 1 + \frac{\lambda\cos\theta}{(1 + \lambda^2\sin^2\theta)^{.5}} \qquad (5)$$

where,
V_c = the clearance volume at TDC
D = the cylinder bore

λ - the ration r/L
r - the crank throw radius
L - the connecting rod length
θ - the crank angle measured from TDC.

The rate of heat transfer, dQ/dt, at the gas-to-wall interface can be calculated by:

$$\frac{dQ}{dt} = h_c A_t (T_g - T_w) \qquad (6)$$

where,
h_c - the gas-to-wall heat transfer coefficient
A_t - the total wall area for heat transfer
T_g - the gas temperature
T_w - the cylinder wall temperature.

Calculation of the heat transfer coefficient (h_c) for the cylinder is discussed later.

The equivalence ratio Φ in the cylinder will change whenever mass enters or leaves the cylinder. The equation for Φ at any time t can be written in terms of the mass of air (M_a), mass of fuel (M_f), and the stociometric fuel/air ratio (f_s) as:

$$\Phi = \frac{Mf}{M_a f_s} \qquad (7)$$

where,

$$Ma = \frac{M}{1 + \Phi f_s} \qquad (8)$$

$$Mf = \frac{M \Phi f_s}{1 + \Phi f_s} \qquad (9)$$

Substitution of Eqs.(8) and (9) into Eq.(7), and differentiating the results gives:

$$\frac{d\Phi}{dt} = \frac{F1}{M} \left[\frac{F1}{f_s} \frac{dM_a}{dt} - \frac{\Phi \, dM}{dt} \right] \qquad (10)$$

where,

$$F_1 = 1 + \Phi f_s$$

By using Eqs.(1), (2), and (10) to evaluate dT/dt, dM/dt, and dΦ/dt, new values of T, M, and Φ can be calculated at the end of each crank angle step. The pressure, P, can then be calculated using the perfect gas equation.

THERMODYNAMIC GAS MIXUTRE PROPERTIES - The equilibrium thermodynamic properties for the products of combustion of air and C_nH_{2n} are assumed. Algebraic expressions derived by Krieger and Borman [13] are used for lean mixtures, and expressions by Marzouk [35] for rich mixtures.

GAS EXCHANGE PROCESSES - A one-dimensional quasi-steady compressible flow model is used to describe the gas exchange between the engine cylinder and the intake and exhaust manifolds. The manifolds are treated as infinite plenums with specified pressures, thus, neglecting any dynamic effects in the flow due to pressure waves. From a knowledge of the gas conditions in the cylinder and manifolds, plus a geometric valve area and discharge coefficient, the instantaneous mass flow through the valves (and ports) can be calculated by:

$$M = C_d A_e P_1 [Z g_c/R_1 T_1]^{0.5} \qquad (11)$$

where,

$$Z = \frac{2\gamma}{\gamma - 1} \left[\left(\frac{P_2}{P_1} \right)^{2/\gamma} - \left(\frac{P_2}{P_1} \right)^{(\gamma+1)/\gamma} \right]$$

C_d - the discharge coefficient
A_e - the effective flow area
P_1 - the upstream stagnation pressure
P_2 - the downstream stagnation pressure at the effective flow area
T_1 - the upstream gas temperature
γ - the ratio of specific heats.

Due to the large pressure difference between the cylinder and the exhaust manifold when the exhaust valve just begins to open, the flow through the exhaust valve can become choked. In that case, when sonic conditions prevail at the exhaust valve, the critical pressure ratio is evaluated from:

$$\left(\frac{P2}{P1} \right)_{crit} = \left(\frac{2}{\gamma + 1} \right)^{\gamma/(\gamma - 1)} \qquad (12)$$

COMBUSTION PROCESS - The combustion model used in the present simulation program is that developed by Watson, Piley, and Marzouk [12]. It is based on algebraic expressions describing the fuel burnig rate as a function of the dominant controlling parameters, such as ignition delay and equivalence ratio. Chemical reactions are considered to commence at the dynamic injection point and to take place in two distinct periods: an ignition delay followed by a period of heat release. The ignition delay is considered to be the time interval between the dynamic injection point (when injector needle starts to lift) and the ignition point (start of heat release due to combustion),. The total length of the ignition delay is related to the cylinder gas temperature and pressure, the engine speed, and the ignition quality of the fuel according to an empirical expression by Hardenberg and Hase [30]:

$$ID_a = (0.36+0.22Vp) \exp \left[EA \left(\frac{1}{R\,T_m} - \frac{1}{17190} \right) + \frac{21.2}{P_m - 12.4} \right]^{0.63} \qquad (13)$$

where,

ID_a = the ignition delay in crank angle degrees
V_p = the mean piston speed
EA = the apparent activation energy
= $618{,}840/(C_n + 25)$
C_n = fuel cetane number
P_m = the absolute cylinder pressure
T_m = the absolute cylinder temperature.

The ignition delay in seconds can be determined by simply dividing the result from Eq.(13) by the quantity 6N, where N is the engine speed in rev/min.

The combustion correlation consists of two algebraic expressions, one for pre-mixed fuel burning and the other for diffusion controlled fuel burning. The total instantaneous fuel burning rate is given by the sum to the two components;

$$M_t = M_p + M_d \qquad (14)$$

where the subscripts t, p, and d denote total, pre-mixed, and diffusion, respectively. In order to quantify the proportion of the fuel burnt by either mechanism, a 'mode of burning factor', B_m, is used to express the cumulative fuel burnt by pre-mixed burning as a fraction of the total fuel injected.

$$B_m = M_p / M_t \qquad (15)$$

The mode of burning factor is calculated from:

$$B_m = 1.0 - 0.746\, \Phi_{tr}^{0.35}\, ID_s^{-0.35} \qquad (16)$$

where, Φ_{tr} is the equivalence ratio of the trapped gas, and ID_s is the ignition delay in seconds. Substituting Eq.(15) into Eq.(16), the non-dimensional fuel burning rate can be expressed as:

$$M_t = B_m M_p(t) + (1-B_m) M_d(t) \qquad (17)$$

For the pre-mixed phase, the burning rate is given by:

$$M_p(t) = C_{p1} C_{p2}\, T^{C_{p1}-1} \left(1 - T^{C_{p1}}\right)^{C_{p2}-1} \qquad (18)$$

For the diffusion phase, the burning rate is given by:

$$M_d(t) = C_{d1} C_{d2}\, T^{C_{d2}-1} \exp(-C_{d1} T^{C_{d2}}) \qquad (19)$$

where,

$C_{p1} = 2.0 + 0.002703 \times ID_a^{2.0}$
$C_{p2} = 5000$
$C_{d1} = 10.0\, \Phi_{tr}^{-1.505}$
$C_{d2} = 0.48\, C_{d1}^{0.423}$

The variables C_{p1}, C_{p2}, C_{d1}, and C_{d2} are experimentally determined 'shape factors' which describe the fuel burning rate as a function of engine operating parameters [12].

GAS-TO-WALL HEAT TRANSFER IN THE CYLINDER- Numerous correlations for the gas-to-wall heat transfer coefficient have been proposed over the years [14]. In the present model, the correlation by Hohenberg [39] was used. Hohenberg presented a simplified correlation for heat transfer coefficient which made allowance for the rise in gas velocity with increasing engine speed as well as the variation in velocity with time (crank angle) expressed as;

$$h_c = C_1\, V_d^{-0.06}\, p^{0.8}\, T^{-0.4}\, (Vp + C2)^{0.8} \qquad (20)$$

where the constants C_1 and C_2 are empirical constants which can be adjusted for local variations due to intake swirl or combustion chamber geometry. Based on comprehensive measurements on various types of DI diesel engines, Hohenberg recommends values of 130 for C_1 and 1.4 for C_2. Although the Hohenberg correlation does not explicitly include a term for radiative heat losses in the cylinder, the empirical basis of the multiplying constant implicitly allows for radiation.

HEAT TRANSFER DURING INTAKE AND EXHAUST- The heat transfer in the intake and exhaust ports is modeled using a quasi-steady heat transfer correlation, in the form of a Nussult-Reynolds number relationship given by Malchow et al [15]:

$$Nu_D = K\, Re_D^{\,a} \qquad (21)$$

where Re_D denotes the Reynolds number, the subscript D denotes the diameter of the intake or exhaust pipe, and K and a denote empirical constants taken to be 0.0774 and 0.769, respectively.

CALCULATION OF METAL WALL TEMPERATURES - A simple one-dimensional heat conduction model is used to evaluate the mean inner metal surface temperature of the combustion chamber. Additional heating of the cylinder wall by friction, and cooling of the wall by the flow of oil over the surface, is neglected. It is known from experiments that the wall temperature changes in the actual engine are very small compared to the changes in gas temperature. The model, therefore, takes this fact into account by updating the wall temperature only at the end of the cycle rather than at each step during the cycle.

MECHANICAL FRICTION - A number of empirical correlations have been proposed to model total or cycle averaged mechanical friction in internal combustion engines [16-23]. However, there are very few correlations available in the literature which model individual frictional components on a crank angle basis rather than on a cycle basis. Rezeka and Henein [17], developed a method to determine the instantaneous engine friction during firing. The method, known as the p-ω method, is based on the fact that the instantaneous cylinder gas forces and the instantaneous frictional forces, inertia and load forces cause the instantaneous variation in the flywheel angular velocity. They developed a set of correlations to calculate the instantaneous friction for each of the major frictional components which were classified under two categories; 1) Piston assembly friction, and 2) Crankcase assembly friction.

<u>Piston Assembly Friction</u> - Three components of the piston assembly friction are considered: 1) Ring Viscous Lubrication Friction (F_{RVL}), 2) Ring Mixed Lubrication (F_{RML}), and 3) Piston Skirt (F_{PS}):

$$F_{RVL} = a1[\mu V_p w_o (P_{gas}+P_e)]^{.5}(n_o+0.4n_c) D\ r\ T_k \quad (22)$$

$$F_{RML} = a_2 \pi D n_c w_c (P_{gas}+P_e)(1-\sin\theta) r\ T_k \quad (23)$$

$$F_{PS} = a_3(\mu V_D L_p r\ T_k/h_o) \quad (24)$$

<u>Crankcase Assembly Friction</u> - Crankcase friction include three major components; 1) Valve Train Friction (F_{VAL}), 2) Auxiliaries and Unloaded Bearing Friction (F_{AUB}), and 3) Loaded Bearing Friction (F_{LB}):

$$F^{VAL} = a_4\ G L_s r\ T_k / \sqrt{\omega} \quad (25)$$

$$F_{AUB} = a5\ \mu\ \omega \quad (26)$$

$$F_{LB} = a_6 \frac{\pi}{4} D^2\ r_c\ P_{gas} \cos\theta/\sqrt{w} \quad (27)$$

The above correlations were used to calculate the instantaneous friction torque (IFT) for each component. The total instantaneous friction at any crank angle is given by:

$$IFT = \Sigma\ IFT_i = a_i \times w_i \qquad [NM] \quad (28)$$

where, a_i denotes the empirical coefficients for the i_{th} friction components, and w_i denotes the functions given in Eqs.(22) through (27). The values of a_i and w_i are given in Table 1. Figure 3 shows the torques for the different instantaneous frictional components calculated using the correlations in Table 1. For this figure, the engine is running at 900 rpm, no load. The summation of the instantaneous values of all frictional components gives the instantaneous total friction shown in Figure 4.

BLOWBY GAS FLOW - The blowby model used in this study represents the flow path by a series of chambers (volumes) connected by square-edged orifices (ring gaps) as shown in Figure 5. The ring gaps are assummed to be the only openings for the gas to leak out. The mass flow between these volumes can be expressed in terms of the pressure ratio and the stagnation conditions. The formula is for one-dimensional, unsteady, compressible adiabatic flow through an orifice, with a constant discharge coefficient:

$$M_b = C_d\ A_e\ P_1 \sqrt{Z\ g_c / R_1\ T_1} \quad (29)$$

where,

$$Z = \frac{2k}{\gamma-1}\left[\left(\frac{P_2}{P_1}\right)^{2/\gamma} - \left(\frac{P_2}{P_1}\right)^{(\gamma+1)/\gamma}\right]$$

C_d is the discharge coefficient for a square-edged orifice (approximately equal to

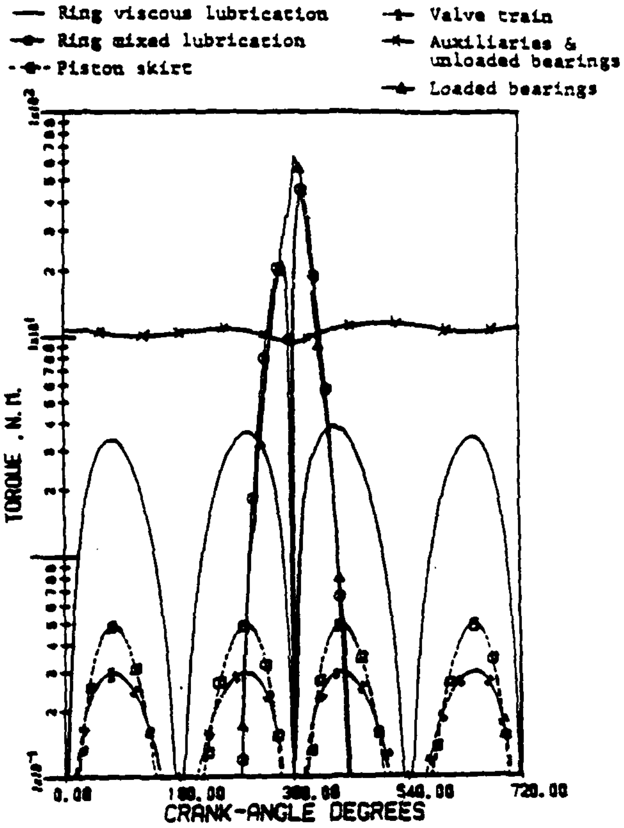

Figure 3 - Instantaneous Friction Components From Model Correlations (Ref.18) 900 rpm, No Load

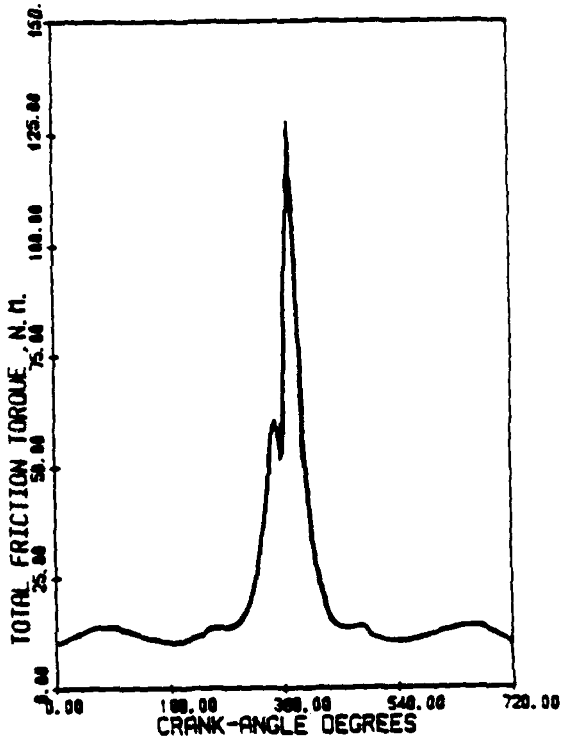

Figure 4 - Total Friction Torque (Ref.18) 900 rpm, No Load

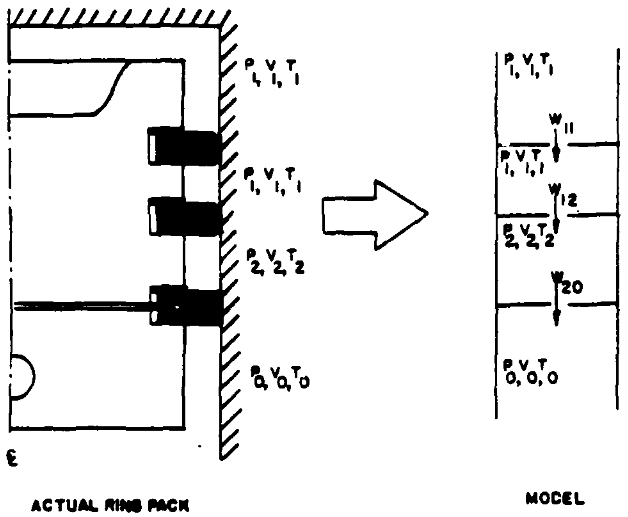

Figure 5 - Model for Blowby Gas Flow Past the Piston Rings

0.65). The mass flow (M_b) is found by examining each pair of adjacent volumes in turn. The mass and pressure changes within each volume are related by the perfect gas law:

$$dM_b = \frac{V_i}{R_i\, T_{wav}}\, dP_i \qquad (30)$$

where,

V_i = the crevice volume

T_{wav} = the average wall temperature.

Equations (29) and (30) can be numerically integrated to obtain the pressure history of each volume, and more importantly, the mass flow out of the main cylinder and into the crankcase (blowby).

ENGINE DYNAMICS - The model calculates the instantaneous angular velocity and acceleration of the engine's flywheel during cranking and starting. The instantaneous angular velocity of the flywheel depends on the moment of inertia of the moving parts, and on the instantaneous difference between the driving torques produced by the gas pressure and the starter motor (during cranking), and the resisting torques which are the load torque, the inertia torque, and the friction torque. Mathematically, this relationship can be expressed as:

$$T_{iner} = T_{start} + T_{gas} - T_{fric} - T_{load} \qquad (31)$$

where,

T_{iner} = the instantaneous inertia torque

T_{start} = the instantaneous starter motor torque

T_{gas} = the instantaneous gas pressure torque

T_{fric} = the instantaneous friction torque

T_{load} = the instantaneous load torque

The instantaneous inertia torque (T_{iner}) consists of two parts; 1) rotating inertia torque, and 2) reciprocating inertia torque. The rotating inertia torque, Trot, is calculated by;

$$Trot = I_e \frac{d\omega}{dt} \qquad (32)$$

where,

I_e = the moment of inertia calculated from the engine geometry and masses of the rotating parts (flywheel, crankshaft, and part of the connecting rod

$d\omega/dt$ = the instantaneous angular acceleration

$$= \frac{1}{2}\frac{d\omega^2}{d\theta}$$

and for small θ,

$$\frac{d\omega}{dt} = \frac{1}{2}\frac{\Delta\omega^2}{\Delta\theta} \qquad (33)$$

The reciprocating torque (T_{rec}) is calculated according to:

$$T_{rec} = rTk\ mr(\ Tk\, \omega^2 \frac{d\omega}{dt}\ )\ \frac{dTk}{d\theta}$$

$$= mr^2Tk\ (Tk \frac{d\omega}{dt} + \omega^2 \frac{dTk}{d\theta}\ ) \qquad (34)$$

where,

m = the mass of the reciprocating parts (piston assembly, part of the connecting rod, etc.)

r = the crank radius

ω = the angular velocity

Tk = the transformer ratio

$$= \frac{\sin\theta + r/l\ \sin\theta\ \cos\theta}{[\ 1 - (r/l\ \sin\theta)^2\ ]^{.5}} \qquad (35)$$

The output torque produced by the starter motor is a function of the input power (battery voltage and current), the load that it drives, and the mechanical efficiency of the starter. These determine the resulting starter speed. The instantaneous torque output of the starter motor is approximated by using an empirical relationship suggested by Poublon et al. [28] as:

$$T_{start} = C_s \exp(-K_s\ N\ ) \qquad (36)$$

where,

N = the instantaneous flywheel speed (in rev/min)

C_s, K_s = are empirical constants based on the starter characteristics.

The value of C_s and K_s are determined by plotting the natural log of the starter motor torque during cranking against the starter speed for a number of speeds. The resulting points are curve fitted using a least squares technique. Then, the $\ln(T_{start})$ is then converted back to its linear form and the constants are calculated. Figure 6 shows a plot of the starter torque calculated using Eq.(36).

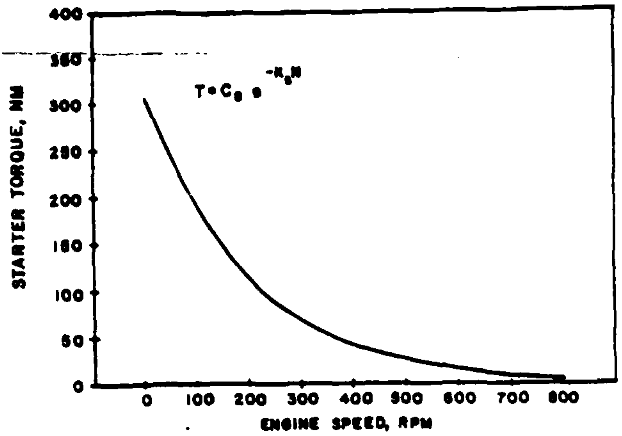

Figure 6 - Starter Motor Torque as a Function of Engine Speed

The instantaneous gas torque (T_{gas}) is computed at each crank angle from the gas pressure (P_{gas}), piston area (Ap_{is}), crank radius (r), and length of the connecting rod (l) according to:

$$T_{gas} = rTk\left(P_{gas}\, A_{pis} - m_{rec}\, g\, \sin\theta\right) \qquad (37)$$

where,

m_{rec} = the mass of the reciprocating piston assembly

Tk = the transformer ratio.

The instantaneous load torque (T_{load}) can be determined from the characteristics of the load. Figure 7 shows a plot of the instantaneous torque components during steady state motoring, calculated using Eqs.(31) through (37). Substituting Eqs.(32) and (34) into Eq. (31) and re-arranging the resulting expression, the angular acceleration of the engine can be calculated by:

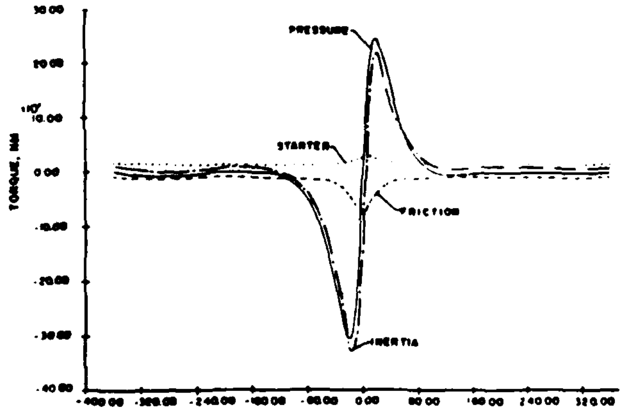

Figure 7 - Instantaneous Torque Components 1100 rpm, No Load

$$\frac{d\theta}{dt} = \frac{T_{start} + T_{gas} - T_{fric} - T_{load} - mr^2\omega^2 T_k \dfrac{dTk}{d\omega}}{mr^2\, Tk^2 + I_e} \qquad (38)$$

By substituting Eq.(38) into Eq.(33), and re-arranging the resulting expression, the instantaneous angular velocity of the flywheel at the next crank angle (time) step, can be approximated by;

$$\frac{d\omega}{dt} = \frac{\omega_{i+1}{}^2 - \omega_i{}^2}{2\ \Delta\theta}$$

or,

$$\omega_{i+1} = \left[2\ \Delta\theta\ \frac{d\omega}{dt} + \omega_i{}^2\right]^{.5} \qquad (39)$$

Figure 8 shows the instantaneous angular velocity and acceleration calculated from Eqs.(39) and (38) for a single cylinder diesel engine running at 1100 rpm, no load.

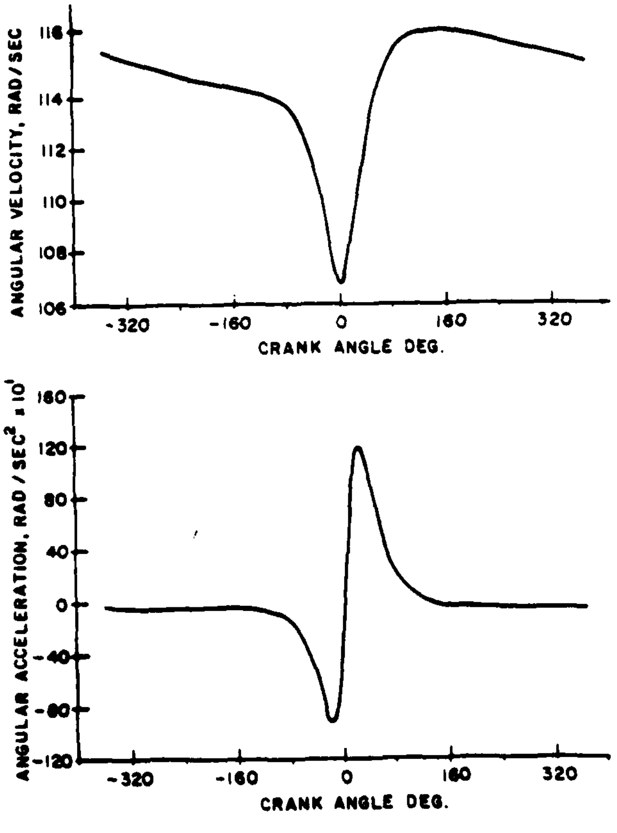

Figure 8 - Instantaneous Angular Velocity and Acceleration, 1100 rpm, No Load

METHOD OF SOLUTION

For transient operation, the differential equations for the three control volumes must be solved as an initial value problem since the conditions at the end of the cycle will not (necessarily) equal those at the beginning. The details of the solution are given in reference [11]. The starter motor torque is applied to the engine as driving function which produces torque imbalances in the system and changes in the system's operating conditions. These changes are computed from the time that the starter key is turned on, until the engine fires and accelerates to its idling speed, or until a specified time (number of cycles) has expired. The engine is assumed to have started when the engine speed reaches or exceeds a specified rpm. The calculation is then stopped, and the results are printed.

The predictor-corrector method used in the present study consists of the following formulas [40]:

Predicting equation:

$$Y_{i+1} = Y_i + h\, f'(X_i, Y_i) \qquad (40)$$

Correcting equation:

$$Y'_{i+1} = Y_i + h/2[f'(X_i, Y_i) + f'(X_{i+1}, Y_{i+1})] \qquad (41)$$

where,

Y_i = the value at the current step
Y_{i+1} = the predicted value at the next step
Y'_{i+1} = the corrected value at the next step
h = the step size.

EXPERIMENTAL APPARATUS AND PROCEDURES

The engine used to obtain experimental data for comparison with the model predictions was a F1L 210 DEUTZ MAG single cylinder, four-stroke, air-cooled, direct injection diesel engine. The engine's specifications are given the appendix. The engine was equipped with a starting motor and battery for starting the engine without a dynomometer, and for motoring the engine (i.e. cranking without combustion).

A series of starting tests were conducted with the engine warmed-up to idling temperatures. The inlet air temperature and pressure were 88 °F and 29.7 in Hg., respectively The oil temperature was 130 °F. Fuelling was .0142 mm per cycle (F/A = 0.02). Engine behavior was monitored from the instant the starter key was turned on, referred to as the starter-on point, to the time when the engine started and accelerated to reach its final idle speed of approximately 1100 rpm.

The cylinder gas pressure was measured using an AVL 12QP 300 CVK pressure transducer, flush mounted in the cylinder head. The transducer signal was fed into a Kistler model 504 E charge amplifier, and its output displayed on an oscilloscope. The crank angle marks used for referencing the pressure were measured and recorded simultaneously using a magnetic pick-up transducer mounted opposite to the 93-tooth ring gear on the engine's flywheel. A separate magnetic pick-up was used to indicate TDC.

The angular velocity of the flywheel was computed by measuring the time taken to move through a fixed angle of rotation. An electro-magnetic pick-up was installed in the flywheel housing opposite the teeth in such a way to produce a pulse signal to indicate the presence of a tooth on the flywheel ring gear. The instantaneous angular velocity at the flywheel end was calculated from:

$$\omega_f = \Delta\theta \,/\, t_k \qquad (42)$$

where,

$\Delta\theta$ = the angle between two successive gear teeth
= $2\pi \,/\, N_t$
N_t = the number of teeth
t_k = the time taken to move $\Delta\theta$
= $Y_k \,/\, f_{ck}$
Y_k = the number of clock counts during $\Delta\theta$
f_{ck} = the clock frequency.

Substituting the expressions for $\Delta\theta$ and t_k into Eq.(42) gives the following expression for the angular velocity:

$$\omega_f = 2\pi\, f_{ck} \,/\, Y_k\, N_t \qquad (43)$$

The power input to the starter motor was determined by measuring the battery voltage and the starter current while cranking the engine. The input power was then calculated by:

$$P_s = V_s \times I_s \qquad (44)$$

where,

P_s = the input power to drive the starter in watts
V_s = the batery voltage
I_s = the starter current.

COMPARISON BETWEEN EXPERIMENTAL AND MODEL RESULTS

Figure 9 shows a comparison of the analytical and experimental instantaneous angular velocity and cylinder pressure as a function of crank angle for the first 12 cycles during the starting process. Initially, the model predicts a slightly higher angular velocity than the experiment. The lower experimental angular velocity is probably due to mechanical losses in the starter which were not accounted for in the model. The starter off speed for this test was about 90 rad/sec (859 rpm). Once the starter torque was turned off in the model, the calculated angular velocity approached the measured angular velocity. By the time the engine had accelerated to its idle speed of about 120 rad/sec (1150 rpm), the angular velocities from the test and from the model agreed very closely.

In the first three firing cycles, the calculated peak pressures were significantly higher than the measured pressures. This may be partly due to the assumptions used in the

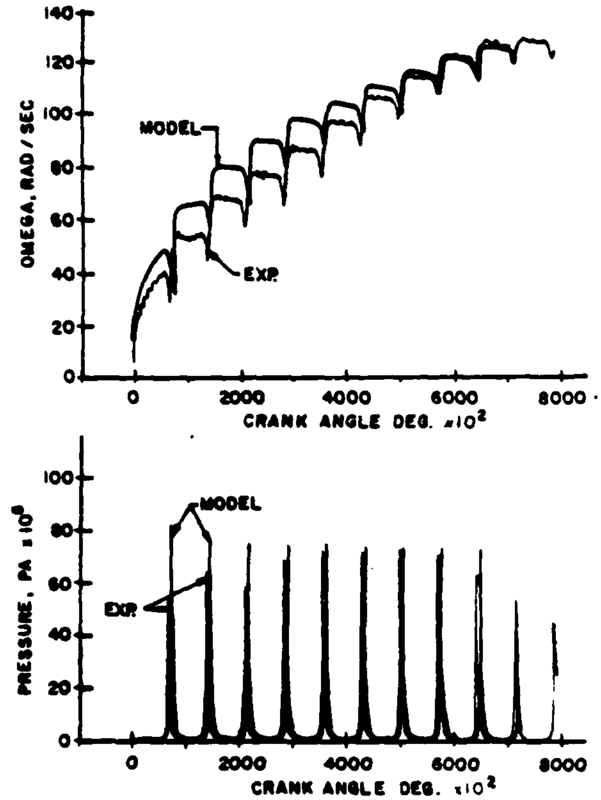

Figure 9 - Instantaneous Angular Velocity and Cylinder Pressure During Cranking and Starting from the Model and Experiment

combustion model. Once the model determines that conditions are favorable for ignition to occur; that is, the ignition delay is shorter than the available time, it assumes complete combustion of all the fuel injected. In the actual engine, however, this is not the case. Partial combustion, and sometimes no combustion (misfire) can occur, particularly under marginal starting conditions. Hence, the higher pressures predicted by the model may have resulted from the higher energy release from the additional fuel. The higher cylinder pressures would also account for the higher angular velocities.

There appears to be a phase shift in time (crank angle) between the two curves. This may be due to a possible error in measurement of TDC in the engine, or a slight difference in the starting crank angle used in the comparison.

In summary, the comparisons between the analytical and experimental results appears satisfactory for the starting conditions investigated. While there is some difference in the absolute values predicted by the model, the relative trends seem correct.

MODEL LIMITATIONS

The model is necessarily tailored quite extensively to the test engine, both in the physical constants describing the engine and to the dynamic and thermodynamic models used. The empirical basis for the combustion model, starter model, and valve flow coefficients limits usefulness of the results obtained from the simulation only to the test engine. However, the methodology used to develop the model can be applied to other engines with minumum difficulty.

Several areas in the model need further development. First of all, the effects of friction heating, and oil cooling on the cylinder walls during cranking and starting may be significant, and should be accounted for in the model. Secondly, improvement is needed in starter model to include load effects on the starter output during initial cranking. Also, the constants used in the starter model should be adjusted to account for friction in the starter. Thirdly, extension of the model for multi-cylinder engines would be useful in studying the effect of several cylinders on engine startability.

CONCLUSIONS

The comparisons between the analytical and experimental results generally show that the model satisfactorily describes the starting behavior of the test engine at room temperatures. However, cold room experiments definitely needed to validate model predictions for startability at low ambient temperatures.

The basic assumptions employed in the "filling & emptying" approach to cycle analysis can be extended to the low rpm range to study engine behavior during initial cranking and starting.

The inclusion of detailed calculations of instantaneous friction, blowby, and heat transfer coupled with engine dynamic calculations in a cycle simulation program provides an interesting framework in which to study the combined effects of changes in CR, ambient temperature, and fuel/air ratio, etc on engine startability.

NOMENCLATURE

Symbol	Description
A_{eff}	effective flow area
A_{pis}	area of piston
A_t	total surface area of combustion chamber
a1-a6	optimum coefficients for friction model
B_m	mode of burning factor
C_d	discharge coefficient
C_{d1}, C_{d2}	diffusion shape factors for combustion model
C_n	cetane number
C_p	specific heat
C_{p1}, C_{p2}	pre-mixed shape factors for combustion model
CR	compression ratio
C_s, Ks	Starter coefficients
D	diameter of cylinder
EA	activation energy
E_s	battery voltage
F_{AUB}	friction due to auxillaries & bearings

f_{ck}	clock frequency
F_{LB}	friction due to loaded bearings
FMEP	friction mean effective pressure
F_{PS}	friction due to piston skirt
F_{RML}	friction due to ring mixed lubrication
F_{RVL}	friction due to ring viscous lubrication
f_s	stoichiometric fuel/air ratio
F_{VAL}	friction due to valve train
G	number of valves per cylinder
g_c	gravitational constant
h	specific enthalpy
h_c	cylinder gas-to-wall heat transfer coefficient
h_f	enthalpy of formation
h_o	oil film thickness
h_s	crank angle step size
ID_a	ignition delay in degree
ID_s	ignition delay in seconds
I_e	moment of inertia of engine
IFT	instantaneous friction torque
I_s	starter current
L	length of connecting rod
L_p	length of piston skirt
L_s	valve spring load
M_a	mass of air
M_b	mass of blowby gas
M_d	mass of diffusion burned fuel
M_f	mass of fuel
M_i	mass in control volume i
M_p	mass of pre-mixed burned fuel
M_{rec}	mass of reciprocating parts
M_t	total mass of engine parts
M_u	mass of fuel unburned
N	engine speed, rpm
n_c	number of compression rings
n_o	number of oil rings
n_t	number of flywheel gear teeth
N_u	Nusselt number
P_e	elastic ring pressure forces
P_{gas}	pressure due to cylinder gases
P_s	power input to starter
Q	heat transfer rate
R	universal gas constant
r	crank throw radius (1/2 stroke)
r_c	radius of journal bearing
R_e	Reynolds number
R_g	gas constant
RPM	revolutions per minute
T_c	cylinder gas temperature
TDC	top dead center
T_{fric}	total friction torque
T_{iner}	torque due to inertia
t_k	time between successive flywheel gear teeth
T_k	transformer ratio
T_{load}	torque due to load
T_m	mean temperature
T_{rec}	torque due to reciprocating parts
T_{rot}	torque due to rotating parts
T_{start}	torque due to starter motor
T_w	cylinder wall temperature
T_{wav}	average cylinder wall temperature
u	specific internal energy
V_i	volume of control volume i
V_c	clearance volume
V_d	cylinder volume swept by piston
V_{gas}	velocity of the gas
V_p	piston velocity
V_s	Voltage input to Starter
w_c	width of compression ring
w_o	width of oil ring
Y'_{i+1}	corrected value at next step, i+1
Y_i	value at current step i
Y_{i+1}	predicted value at next step
y_k	number of clock counts per flywheel tooth
λ	ratio of r/L
ω	angular velocity
ω_f	angular velocity of flywheel
χ	density of inlet air
μ	dynamic viscosity
ν	kinematic viscosity
θ	crank angle in degrees
γ	ratio of specific heats (c_p/c_v)
Φ	equivalence ratio
Φ_{tr}	equivalence ratio of trapped gas

ACKNOWLEDGEMENTS

The authors acknowledge the program support by the U.S. Army Research Office, Research Triangle Park, and the U.S. Army Tank Automotive Command, Warren Michigan. The authors express their appreciation to Ford Motor Company for helpful discussions, and to the students in the Center for Automotive Research at Wayne State University for their assistance in the laboratory.

REFERENCES

1. R.S.Benson, "A Comprehensive Digital Computer Program to Simulate A Compression Ignition Engine Including Intake and Exhaust Systems", SAE Paper No. 710173, 1971.
2. N.Watson, "Transient Performance Simulation and Analysis of Turbocharged Diesel Engines", SAE Paper No. 810338, 1981.
3. G.L.Borman, "Mathematical Simulation of Internal Combustion Engine Processes and Performance Including Comparisons with Experiment", Ph.D. Thesis, Mechanical Engineering Dept., University of Wisconsin, 1964.
4. N. Watson and M. Marzouk, "A Non-Linear Digital Simulation of Turbocharged Diesel Engines Under Transient Conditions", SAE Paper No., 770123, 1977.
5. D. E. Browns, P. R. Cave, M.R.O. Hargreaves, F. J. Wallace, "Transient Characteristics of Turbo-charged Diesel Engines", Proc. I. Mech. Engr.,CP15, 1973.
6. R.S. Benson, J. D. Ledger, N. D. Whitehouse, and S. Walmsley, "Comparison of Experimental and Simulated Transient Responses of a Turbocharged Diesel Engine", SAE Paper No. 730666, 1973.
7. D.E. Winterbone and W.Y. Loo, "A Dynamic Simulation of a Two-Stroke Turbocharged Diesel Engine", SAE Paper No. 810337, 1981.
8. J. D. Ledger and W. Walmsey, "Computer Simulation of a Turbocharged Diesel Engine

"Operating Under Transient Load Conditions", SAE Paper 710177, 1971.

9. J. D. Ledger, R.S Benson, and N.D. Whitehouse, "Dynamic Modelling of a Turbocharged Diesel Engine", Proc. Inst. Mech. Engrs., CP15, 1973.

10. D.E. Bown, P.R. Cave, M.R.O Hargreaves, and F.J. Wallace, "Transient Characteristics of Turbocharged Diesel Engines", Proc. Inst. Mech. Engrs., CP15, 1973.

11. T.P. Gardner, "Optimization of Compression Ratio in Compression Ignition Engines", Ph.D Thesis, Mechanical Engineering Department, Wayne State University, Detroit, Michigan, 1987.

12. N. Watson and A. D. Pilley, "A Combustion Correlation for Diesel Engine Simulation", SAE Paper No. 80029, 1980.

13. R.B. Krieger and G. L. Borman, "The Computation of Apparent Heat Release for Internal Combustion Engines", ASME Paper No. 66WA/DGP-4, 1964.

14. W. J. D. Annand, "Heat Transfer in the Cylinders of Reciprocating Internal Combustion Engines",Proc. Inst. Mech. Engrs., Vol. 177, No. 36, 1963.

15. G.L. Malchow, S. C. Sorenson, and R. O. Buckius, "Heat Transfer in the Straight Section of an Exhaust Port of a Spark Ignition Engine", SAE Paper No. 790309, 1979.

16. R.E. Gish, J.D. McCullough, J.B. Retzloff, and H. T. Mueller, "Determination of True Engine Friction", SAE Paper No. 117, 1957.

17. S. F. Rezeka and N. A. Henein, "A New Approach to Evaluate Instantaneous Friction and its Components in Internal Combustion Engines", SAE Paper No. 840179, 1984.

18. S.F. Rezeka, "A Mathematical Model of Reciprocating Combustion Engine Dynamics for the Diagnosis of Deficient Energy Conversion", Ph.D Thesis, Mechanical Engineering Department, Wayne State University, Detroit, Michigan, 1984.

19. B. W. Millington and E. R. Hartles, "Frictional Losses in Diesel Engines", SAE Paper No. 680590, 1968.

20. I.N. Bishop, "Effect of Design Variables on Friction and Economy", SAE Paper No. 812A, 1964.

21. D.E. Winterbone, D. W. H. Tennant, "The Variation of Friction and Combustion Rates During Diesel Engine Transients", SAE Paper No. 810339, 1981.

22. S.K. Chen and P. F. Flynn, "*Development of a* Single Cylinder Compression Ignition Research Engine", SAE Paper No. 650733, 1965.

23. J.T. Kovach, E. A. Tsakiris, and L. T. Wong, "Engine Friction Reduction for Improved Fuel Economy", SAE Paper No. 820085, 1982.

24. T.W. Biddulph, W. T. Lyn, "Unaided Starting of Diesel Engines", Proc. Inst. Mech. Engrs., Vol. 181, 1966-67.

25. W.T. Lyn, "The Effects of Physical Factors on Ignition Delay", Proc. Inst. Mech. Engrs., Vol. 181, 1966-67.

26. A. Andree and S. J. Pachernegg, "Ignition Conditions in Diesel Engines", SAE Paper No. 690253, 1969.

27. W.E. Meyer and J.J. Decarolis, "Compression Temperatures in Diesel Engines Under Starting Conditions", SAE Trans., 1962, pp. 163-174.

28. M. Poublon and D.J. Patterson, "Instantaneous Crank Speed Variations as Related to Engine Starting", SAE Paper No. 850482.

29. M. Brunner and H. Ruf, "Contribution to the Problem of Starting and Operating Diesel Vehicles at Low Temperatures", Proc. Inst. Mech. Engrs., No. 5, 1959-60, pp. 124-137.

30. H.O. Hardenberg and F.W. Hase, "An Empirical Formula for Computing the Pressure Rise Delay of a Fuel From its Cetane Number and from Relevant Parameters of Direct-Injection Diesel Engines", SAE Paper No. 790493.

31. N.A. Henein, "Starting of Diesel Engines: Uncontrolled Fuel Injection Problems", SAE Paper No. 860253, 1986.

32. L.C. Lichty, "Internal Combustion Engines", McGraw-Hill Book Company, New York, pp.389-395, Copyright 1951.

33. H.K. Newhall and E.S. Starkman, "Thermodynamic Properties of Octane and Air for Engine Performance Calculations", SAE Paper No. 633G, 1963.

34. H.N. Powell, "Application of an Enthalpy-Fuel/Air Ratio Diagram to 'First Law' Combustion Problems", ASME Trans., 79, 5, 1957.

35. M. Marzouk, "Simulation of Turbocharged Diesel Engines Under Transient Conditions", Ph.D Thesis, University of London (Imperial College), 1976.

36. "JANAF Interim Thermodynamical Data Tables", Joint Army-Navy-Air Force Thermochemical Panel. ARPA Program USAF Contract Af 33(616)-6149, Thermal Laboratory Dow Chemical Corp., 1960.

37. S. Furahama, and T. Tada, "On the Flow of the Gas Through the Piston-Rings", JSME, Bulletin, Vol. 4, No. 16, 1961.

38. C.M. Gray and J.T. Gray, "A Study of Marginal Compression Ignition", SAE Paper No. 670948, 1967.

39. G.F. Hohenberg, "Advanced Approaches For Heat Transfer Calculations", SAE Paper No. 790825, 1979.

40. B. Carnahan, H.A. Luther, and J.O. Wilkes, "Applied Numerical Methods", John Wiley & Sons, Inc., New York, 1969, pp. 341-400.

41. R. Phatak, and T. Nakamura, "Cold Startability of Open-Chamber Direct-Injection Diesel Engines - Part I: Measurement Technique and Effects of Compression Ratio", SAE Paper No. 831335, 1983.

APPENDIX

Engine Specifications for Deutz FIL 210 MAG

Combustion System	D.I.
No. of Cylinders	1
Bore x Stroke (mm)	95 x 95
Displacement (cc)	673
Compression Ratio (nom.)	17:1
Clearance Volume (cc)	0.4208
Piston Skirt Length (mm)	66.5
Piston Skirt/Liner Clearance (mm)	0.031
Connecting Rod Length (mm)	160
Journal Bearing Diameter (mm)	95.19
No. of Compression Rings	2
Width of 1st Ring (mm)	2.54
Width of 2nd Ring (mm)	2.54
No. of Oil Rings	1
Width of Oil Ring (mm)	3.60
Volume Between Rings 1 & 2 (cc)	2.621
Area Between Rings 1 & 2 (cm$_2$)	0.0222
Volume Between Rings 2 & O (cc)	1.818
Area Between Ring 2 & O ( )	0.0222
Mass of Piston & Rings (kg)	1.18
Mass of Connecting Rod (kg)	0.65
Rotating Moment of Inertia (kg-m-s)	0.384
Area of Cylinder Head (cm2)	75.0
Area of Piston (cm2)	99.15
Area of Liner at TDC (cm2)	0.358
Injection Timing (Deg. BTDC)	23
Intake Valve Opens (Deg. BTDC)	21
Intake Valve Close (Deg. ABDC)	62
Exhaust Valve Opens (Deg. BBDC)	62
Exhaust Valve Close (Deg. ATDC)	21

Table 1

Coefficients of Correlation for Friction Components

	COMPONENT	a_i	w_i
PISTON ASSEMBLY	FRVL	23.00	$\mu V_p w_o (P_{gas} + P_e)^{0.5} (n_o+0.4n_c) D r TK$
	FRML	0.252	$\pi D n_c w_c (P_{gas} + P_e) (1 - \sin\theta) r TK$
	FPS	1.00	$\mu V_p D L_p r TK / h_o$
CRANKCASE ASSEMBLY	FVAL	0.26	$G L_s r TK / \sqrt{\omega}$
	FAUB	9.60	$\mu \omega$
	FLB	0.50	$\frac{\pi}{4} D^2 r_c P_{gas} \cos\theta / \sqrt{\omega}$

SECTION 6

CONCLUSIONS AND RECOMMENDATIONS

6.1 Conclusions

1. The basic function of the cetane scale is to rate the autoignition behavior of a fuel by matching its ignition delay to that of a blend of two primary reference fuels under specified conditions of inlet temperature, engine speed, coolant temperature, fuel-air-ratio, injection timing and injector opening pressure. The only engine variable is the compression ratio. The cetane scale was not intended to rate any other combustion, performance or emissions parameter.
2. Three intrinsic problems exist in the cetane rating of fuels.
    - a- Inability to rate low ignition quality fuels. The solution is to raise the inlet air temperature above the 150 F specified in the ASTM D-613 procedure.
    - b- Instability of the ignition delay meter in rating low ignition quality fuels. This has been found to be due to the cycle-to-cycle variation in the I.D. of these fuels with the meter trying to reflect what is actually occuring in the engine. No solution is known at this time to the problem of cycle-to-cycle variation in the I.D.
    - c- Inconformity of the CFR combustion system with actual diesel combustion systems. A possible solution is

to redesign the combustion system. Part of the problem may be solved for the existing system by optimizing the injection pressure such that the rating of the fuel is independent fo the needle opening pressure.

3. Three fuel/engine performance problems are examined:
   a- Invalidity of C.N. in correlating the I.D. for different fuels in different engines under all operating conditions. The I.D. should be correlated in terms of three basic parameters: mean temperature, mean pressure, and a global activation energy. The global activation energy can be correlated with the C.N.
   b- Inaccuracy of C.N. in rating the overall performance and emissions behavior of fuels in diesel engines. This correlation should be done in terms of I.D. and the combustion parameters which characterize the premixed and diffusion combustion regimes.
   c- Inability of C.N. in rating the cold startability of diesel engines on different fuels. Startability depends on the success of both the autoignition and the subsquent combustion reactions. Many parameters other than C.N. need to be included.

4- The C.N. alone cannot rate the cold startability of diesel engines on alternate fuels. Other fuel properties play a major role in the starting of engine. The most important property is fuel volatility. This conclusion is supported by steady state tests on the misfiring temperatures and ignition delay periods. Also it is supported by actual starting tests at low ambient temperatures in a cold room.

6.2 Recommendations

1- Study the cetane rating at inlet air temperatures higher than the 150 F specified by the ASTM D-613 procedure. Determine the most suitable temperature which allows a suitable size of electric heater to be used.

2- Investigate the phenomena of cycle-to-cycle variation in the autoignition process of fuels.

3- Investigate the effect of optimizing the needle opening pressure for each fuel on the cetane rating.

4- Develop correlations between the C.N. and the global activation energy for the preignition reactions for different fuels, to be used for correlating I.D. with C.N., temperature and pressure.

5- Develop correlations between I.D. and the parameters for the premixed and diffusion combustion and the fuel/engine performance parameters. Relate these parameters to C.N. by using C.N.-I.D. correlations.

6- Make a combustion failure analysis during engine starting on different fuels and ambient temperatures. This will identify the engine and fuel parameters, other than C.N., which affect engine startability.

7- Investigate the process of spray formation, autoignition and combustion at low ambient temperatures.

DATE

FILMED

4 8